to my dear father **Gerrit Volkers**

Lay-out

Linda Volkers

Cover design

Arend-Jan Smit

Print

Proefschriftmaken.nl, uitgeverij BOXPress

Copyright © Linda Volkers, Utrecht 2012

All right reserved. No part of this publication may be reproduced, stored, or transmitted in any form or by any means, without written permission of the author

An electrophysiological characterization of $K_v7.2$ and $Na_v1.1$ channel mutations in genetic epilepsy

Een elektrofysiologische karakterisering van $K_v7.2$ en $Na_v1.1$ ion kanaal mutaties bij genetisch bepaalde epilepsie

(met een samenvatting in het Nederlands)

PROEFSCHRIFT

ter verkrijging van de graad van doctor
aan de Universiteit Utrecht op gezag van de
rector magnificus, prof.dr. G.J. van der Zwaan,
ingevolge het besluit van het college voor promoties
in het openbaar te verdedigen op

dinsdag 27 november 2012 des middags te 2.30 uur

door

Linda Volkers

geboren op 2 juni 1979 te Coevorden

Promotor: Prof. dr. D. Lindhout

Co-promotoren: Dr. B.P.C. Koeleman
Dr. M.B. Rook

The studies described in this thesis were primarily performed at the Departments of Medical Genetics and Medical Physiology, University Medical Center Utrecht, The Netherlands. The studies were supported by ‘Ter Meulen Fund’, Royal Netherlands Academy of Arts and Sciences, The Netherlands Organization of Scientific Research and Development (ZonMW), and the National Epilepsy Fund of The Netherlands.

Contents

Chapter 1 **9**
General introduction

Chapter 2 **29**
Functional analysis of novel KCNQ2 mutations found in patients with Benign Familial Neonatal Convulsions

Chapter 3 **45**
Assembly and efficient membrane transport of monomeric K_v7.2 ion channels lacking the carboxy-terminal coiled-coil structures

Chapter 4 **59**
Na_v1.1 Dysfunction in Genetic Epilepsy with Febrile Seizures Plus or Dravet Syndrome

Chapter 5 **79**
Febrile temperatures unmask biophysical defects in Na_v1.1 epilepsy mutations supportive of seizure initiation

Chapter 6 **105**
General discussion

Chapter 7 **127**
Summary

Chapter 8 **133**
Samenvatting

Acknowledgements **138**
Curriculum vitae **141**

General introduction

1

Neuronal voltage gated sodium and potassium channels are transmembrane proteins responsible for rapid upstroke and repolarization of action potentials. Mutations in the genes encoding the neuronal sodium channel $Na_v1.1$ and potassium channel $K_v7.2$ have been linked to various forms of epilepsy. Mutations of $Na_v1.1$ are linked to Genetic Epilepsy with Febrile Seizures Plus (GEFS+) and Dravet syndrome (DS) and mutations of $K_v7.2$ are linked to Benign Familial Neonatal Epilepsy (BFNE). This general introduction will address the physiology and molecular biology of these ion channels, their role in maintaining a balanced excitatory and inhibitory network, and the relevance of these channels to the different epileptic syndromes.

Aim of the thesis

Careful clinical studies with indepth evaluation of phenotypes combined with extensive molecular genetic analysis are essential for disclosing the mechanism of epileptogenic mutations. However, these studies cannot provide a complete genotypephenotype correlation. Even though software prediction tools can calculate whether an undetermined variant is probably a pathogenic mutation or a naturally occurring variant, the functional consequences of a mutation are difficult to predict. Therefore functional studies are of vital importance for further clarification of a genotypephenotype correlation. However, one must take into account that the specific types of experimental techniques and functional assays used represent oversimplified disease models, which puts restrictions on the determination of the exact disease mechanism. Common techniques to characterize functional defects related to mutations in ion channels include heterologous invitro expression studies in Xenopus leavis oocytes and mammalian cell lines. This thesis aims to address the main research question: Is it possible to validate novel and undetermined variations found in patients diagnosed with a specific subtype of epilepsy and correlate the observed gating defects to the phenotypic seizure and developmental outcome using these simplified functional invitro assays?

Action potential

Most dynamic signaling events in excitable cells arise from the interplay between voltage gated ion channels. The classical example of controlled electrical signaling is the action potential, an electrical signal that propagates rapidly along the surface of a neuronal axon or a muscle cell in an all-or-none fashion (Reviewed by Bean B.P. 2007, Kandel et al. 2000). An action potential (Figure 1) is generated by the activation of sodium channels, causing a sodium influx that depolarizes the plasma membrane to a certain voltage threshold ($V_{treshold}$). This voltage threshold or action potential threshold is the minimal depolarization in a neuron that must be achieved for allornone firing to occur. The sodium influx causes a further membrane depolarization, which in turn rapidly activates more sodium channels. As membrane potentials peak, the sodium channels begin to inactivate in a time and voltage dependent manner. The repolarization phase

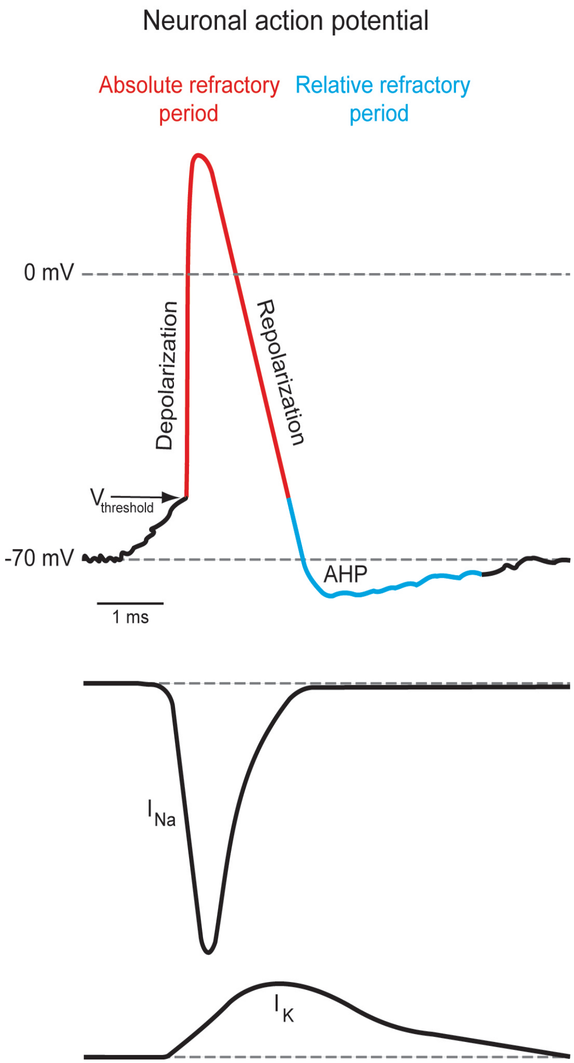
Neuronal action potential
Absolute refractory period
Relative refractory period
0 mV
Depolarization
Repolarization
Vthreshold
-70 mV
AHP
1 ms
INa
IK

Figure 1.

A schematic representation of an action potential and the involvement of sodium and potassium current. The resting membrane potential in a pyramidal neuron is typically in the range of -85 mV to -60 mV (Bean BP 2007). The voltage threshold ($V_{treshold}$) is the minimal depolarized voltage that must be achieved by the neuron for all or non firing to occur. The sodium influx cause a further membrane depolarization, which in turn activates more voltage gated sodium channels producing the rising phase of the action potential. Subsequently, the inactivation of sodium channels and the activation of various voltage gated potassium channels such as calcium dependent potassium channels and M-channels, cause the repolarization phase of the action potential. The repolarization is usually followed by an afterhyperpolarization (AHP) due to the inactivated sodium channels in combination with the slow deactivation of potassium channels. Sodium ion channels that fail to inactivate carry the persistent sodium current. The absolute refractory period in which sodium channels are either activated or inactivated is depicted in red, the relative refractory period in which sodium channels recover from inactivation in light aquamarine.

is generated in two ways: 1) the gradual inactivation of sodium ion channels and 2) the slow opening of potassium channels, which causes an efflux of potassium ions eventually support repolarization. In neurons, the repolarization typically causes an undershoot to more negative membrane potential, i.e. the afterhyperpolarization (AHP), due to the inactivation of voltage gated sodium channels in combination with the slow responsiveness of potassium channels. By the end of the hyperpolarization phase all potassium channels are closed.

Just after the neuron has generated an action potential, it is impossible to excite the cell, regardless of the strength of the stimuli. This period is called the absolute refractory period (Figure 1). The neuron cannot generate an action potential because the population of sodium ion channels is either activated or non-recovered from the inactivation state. The absolute refractory phase is followed by a relative refractory period, during which it is possible to generate an action potential by applying stimuli that are stronger in voltage than those normally required to reach threshold. This is because part of the sodium channel population is still inactive and part of the potassium channel population is still activated. The duration of the absolute and relative refractory periods lasts only a few milliseconds, which is important to notice, since this determines how fast neurons can fire action potentials.

Sodium ions are more concentrated extracellularly, while potassium ions are more concentrated intracellularly. This distribution is maintained by the active transport of ions conducted by the sodium/potassium pump (Liberman and Skulachev 1970). The sodium/potassium pump operates continuously to restore this unequal concentration by actively transporting sodium and potassium ions against their concentration gradients. It is important to notice that this simple scheme describes only a fraction of the voltage sensitive ion transport events that influence electrical signaling in an excitable cell.

Voltage gated potassium ion channels

Potassium channels play a prominent role in the repolarization phase and thereby in maintaining the membrane potential and recovering the cell from excitation. Potassium channel families are the most diverse group of ion channels with over 70 subunits discovered. Based on sequence homology, functional characteristics, and low and highresolution structural data, almost all potassium channels appear to exist as tetramers of identical (homomeric) or similar (heteromeric) subunits, each containing 26 helical transmembrane segments around a central conductive pore (Tempel et al. 1987, MacKinnon R 1991, MacKinnon et al. 1993, Schulteis et al. 1996, Doyle et al. 1998, Kuo et al. 2003). A typical potassium channel consists of four α-subunits with heteromeric assembly of subunits (Figure 2B and 2C), and coassembly with accessory units. Thus, cells have a broad repertoire of potassium channel complexes with various gating characteristics (Jenkinson D.H. 2006).

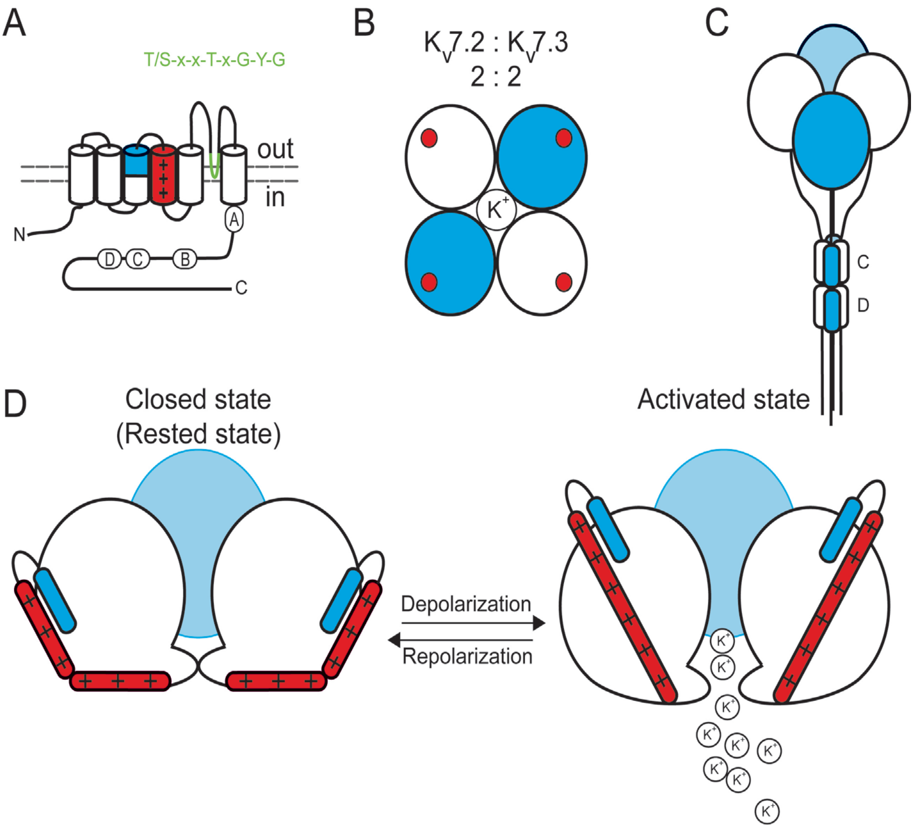

Figure 2.

A) Schematic topology of a 6 transmembrane segment potassium ion channel such as K_v7.2. The S4 voltage sensor is depicted in red, positively charged amino acids are indicated with plus signs. The C-terminal half of the S3 transmembrane is illustrated in aquamarine. The pore-loop with its potassium selectivity filter (green) is located between transmembrane domains S5 and S6. A typical feature of the K_v7.X family is their short intracellular N-terminus and very long C-terminus. The C-terminus harbors four coiled-coiled structures (A-D), which are necessary for proper assembly, modulation and gating of the channel. B) A typical tetrameric K_v7.2/K_v7.3 ion channel with a 2:2 α-subunit stoichiometry; the ion channel is shown from the extracellular environment. K_v7.2 is depicted in white, K_v7.3 in light aquamarine. The locations of the S4 voltage sensors are shown as red circles. C) Assembly of heteromeric K_v7.2/K_v7.3 α-subunits (K_v7.2 in white, K_v7.3 in aquamarine) is generally believed to occur via the intracellular coiled-coil structures C and D. For clarity, the C-terminal helices A and B are not shown. D) A medial cross section of the tetrameric channel depicted in figure B, showing the K_v7.2 α-subunits in white and the K_v7.3 α-subunit in light aquamarine. The voltage sensor paddle, which is formed by the outer part of S3 (aquamarine), the voltage sensor S4 (red) and the linker, undergoes a conformational change during membrane depolarization. This in turn causes the opening of the potassium channel and hence an efflux of potassium ions.

six transmembrane segments (Figure 2A). Additional channel diversity arises from alternative RNA splicing, Despite their diversity, voltage gated potassium channels share some general features, in terms of kinetics, selectivity and modulation. Potassium channels share a common potassium selectivity filter, characterized by the consensus sequence T/S-x-x-T-x-G-Y-G (Heginbotham et al. 1992; Figure 2A) and can be activated by changes in membrane voltage, pharmacological agents, phosphorylation, or intracellular Ca^{2+} (Miceli et al. 2008). Furthermore, six transmembrane segment voltage-gated potassium channels possess a S4 transmembrane segment consisting of several positively charged arginines and/or lysines that function as a voltage sensor that detects changes in the membrane voltage causing the channel to open or close. The C-terminal half of S3, S4 and their linker together form a helix-turn-helix motif termed the voltage sensing paddle (Figure 2D). Upon depolarization the paddle undergoes a conformational change, altering the gate at the intracellular side of the S6 inner helices, which causes the channel to open (Jiang et al. 2003, Long et al. 2007). Compared to other voltage-gated ion channels such as sodium or calcium channels, most potassium channels tend to activate slowly and are closed at highly negative potentials.

Potassium channels finetune their properties by permitting only one or a few combinations of a-subunits to interact. Specific assembly of tetramers also adds to the great diversity of channels, as functional heteromeres often have different electrophysiological characteristics than homomeres. In most cases it appears that specific potassium channel assembly is determined by interaction of intracellular domains in each asubunit, such as coiledcoil structures (Figure 2A and 2C) (Miceli et al. 2008).

Voltage gated sodium channels

Sodium ion channels are poreforming multimeric voltagegated ion channel that are highly selective for sodium ions. The voltagegated sodium channel consists of three glycoprotein subunits: a principle asubunit associated with two auxilliary β-subunits (β1-β4). The primary structure of the α–subunit consists of four homologous transmembrane domains (DI-DIV), each containing six transmembrane spanning segments (S1-S6) with a central pore region (figure 3A). The region between S5 and S6 of each domain is called the poreloop and forms the sodium selectivity pore. The primary role of voltagedependent sodium channels is the initiation and propagation of action potentials, making them critical determinants of neuronal excitability. The sodium channel family consists of nine members; $Na_v1.1$-$Na_v1.9$. In the central nervous system (CNS), the most abundant αsubunits are $Na_v1.1$, $Na_v1.2$, and $Na_v1.6$ (Catterall et al. 2005).

The voltage dependence of activation of the sodium channel derives from the outward movement of gating charges in response to voltage changes in the membrane. The fourth transmembrane segment (S4) in each of the four domains contains positively charged residues, arginines or lysines, which serve as a voltage sensor that underlies channel activation. The most recognized model of how voltage gated ion channels detect and respond to membrane depolarization is the sliding helix model (Catterall et al. 1986; Figure 3B). According to this model, the positively charged residues within the voltage sensors respond to changes in voltage across the membrane (Hille et al. 2001). A depolarization of the membrane causes an outward movement of the S4 voltage sensors along a spiral path, initiating a conformational change within the channel pore to shift it from a closed to an open state (Sands et al. 2005; Figure 3B). Subsequently the inactivation particle gains access to its binding site at the mouth of the inner pore. Inactivated channels

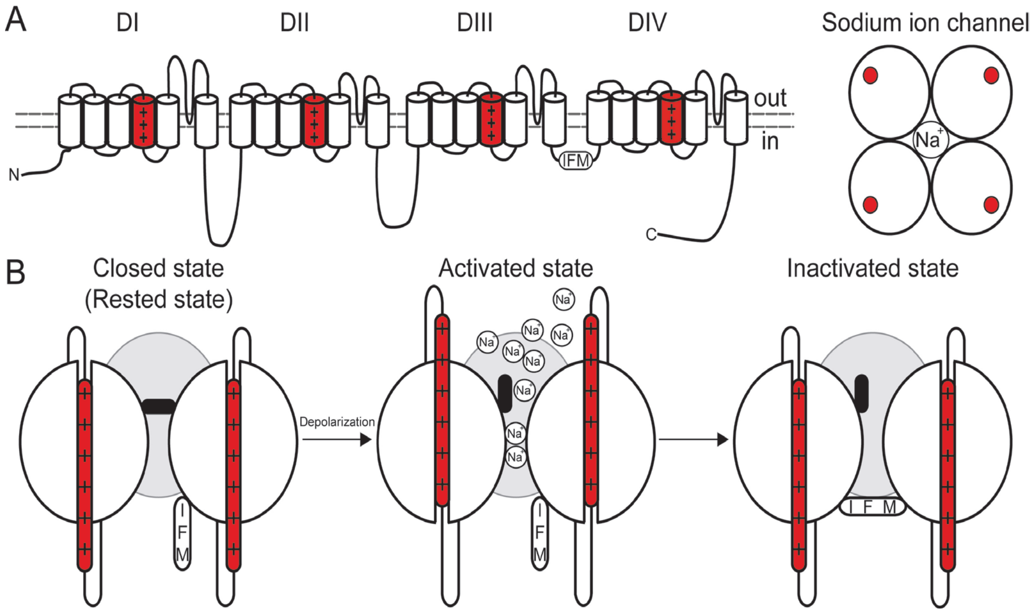

Figure 3.

A) Schematic topology of a sodium ion channel. The ion channel consist of four linked domains (DI-DIV) each containing six transmembrane segments (S1-S6) with a central pore selective for sodium ions. The four S4 voltage sensors are depicted in red and the positively charged amino acids as plus signs. The 'hinged lid' particle IFM that plays part in the inactivation is located in the intracellular loop between DIII and DIV of the channel. B) A simplistic view of the sliding helix model. The voltage sensors move outward upon membrane depolarization, creating a conformational change that shifts the channel from a closed to an open activated state causing an influx of sodium ions. The activation gate (or m-gate) is depicted as a thick black bar located in the pore-loop. Fast inactivation occurs rapidly after activation by closure of the channel via a hinged lid particle consisting of isoleucine, phenylalanine and methione (IFM) amino acids (or h-gate). Recovery from inactivation is a voltage and time dependent process and occurs by unplugging the pore-loop via the disconnection of the hinge lid particle at hyperpolarized membrane potential do not immediately recover from their inactivation state after hyperpolarization, but require also a certain amount of time to recover from it. Inactivation is a complex mechanism, which is characterized by several states divided into fast and slow components (Kahlig et al. 2006). The fast inactivation occurs briefly after channel opening, and blocks sodium ions permeating through the pore. At repolarizing potentials, channels remain in a refractory, inactivated state, inhibiting ion flux until their recovery at hyperpolarized resting membrane levels. Fast inactivation occurs via a 'hinged lid' mechanism. The hydrophobic triplet isoleucine, phenylalanine, methione (IFM) in the DIII-DIV intracellular loop are involved in inactivation gating (West et al. 1992; Figure 3A and 3B). In the inactivation state this triplet acts as a latch that docks within the intracellular pore through hydrophobic interactions with amino acids located in line with the mouth of the pore (West et al. 1992). In addition, the whole complex is stabilized by the proximal part of the C-terminus (Wu et al. 2005, Glaaser et al. 2006).

Slow inactivation occurs after depolarization for seconds or minutes. Slow inactivation plays an important role by contributing to the regulation of resting sodium channel availability (Ruff et al. 1988) and by aiding in slow activity-dependent changes in excitability such as spike frequency adaption or burst termination (Vilin et al. 2001). The molecular mechanisms of slow inactivation of voltage gated sodium channels are less understood and remain ill-defined in the literature (Ulbricht 2005). However, slow inactivation is likely a gating process independent from fast inactivation, because the slow inactivation mechanism is unaffected when fast inactivation is prevented by protease treatment, when specific antibodies block the movement of the inactivation gate, or when the IFM-motif is mutated (Rudy 1978, Vassilev et al. 1989, Featherstone et al. 1996, Vedantham et al. 1998). It has been shown that transposition of all four cardiac isoform poreloops into the human skeletal muscle isoform backbone conferred heart isoform-like slow inactivation properties on the chimeric construct, suggesting a role for the poreloops in slow inactivation (Balser et al. 1996, Vilin et al. 1999). Changes in flexibility of the poreloops may also affect slow inactivation (Benitah et al. 1999). Also the S5-S6 transmembrane segments are involved in the slow inactivation process by lining the inner pore of the channel (O'Reilly et al. 2001, Wang &Wang 1997).

Epilepsy

Brain regions like the neocortex and hippocampus consist of a neuronal interconnected network, which is functionally arranged into horizontal and vertical arrays or laminae of excitatory glutamatergic pyramidal and inhibitory GABAergic neurons. The pyramidal to pyramidal cell connectivity is expressed within as well as between laminae. Interposed between these pyramidal networks are a large variety of GABAergic inhibitory interneurons (Cossart et al. 2005). This pattern of connectivity places GABAergic neurons in the role of regulator of excitatory communication within and between laminae (Figure 4).

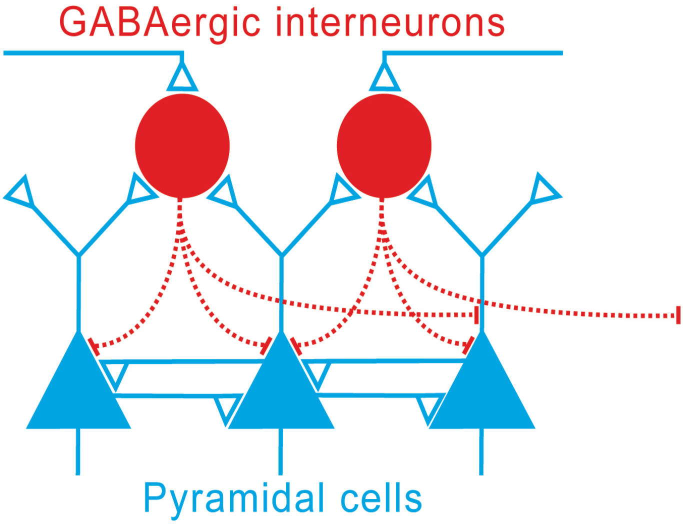

Figure 4.
Schematic overview of a cortical neuronal network. Excitatory pyramidal neurons and local GABAergic interneurons are highly interconnected through local axonal connections such that activity in pyramidal cells excites both other pyramidal cells as well as local inhibitory interneurons.

Epilepsy may be the result of an imbalance between excitatory and inhibitory influences, which cause excessive and hypersynchronous discharges in a large number of neurons. This synchronization is an essential feature of the generation and propagation of epileptic activity (reviewed by McCormick et al. 2001). Most epileptic seizures are due to discharges generated in cortical and hippocampal structures. The changes in neuronal excitability that underlie epileptogenesis not only induce abnormal activity in individual neurons but also recruit a population of hyperexcitable cells into highly synchronized activities that are propagated through normal or pathological connections.

Numerous electrophysiological studies have examined the cellular and network mechanism of seizure generation in the hippocampus with several experimental models of epilepsy in-vitro (reviewed by McNamara J.O. 1994). Seizure-like synchronous oscillation can readily be evoked in murine hippocampal slice preparations by altering the extracellular ionic environment or by blockage of ion channels, which indicates that either a reduction or increase in neuronal spike discharges in excitatory or inhibitory neurons can both lead to seizures. For example, epileptic seizures can be evoked with gaminobutyric acid (GABA) receptor antagonists that alter the balance between excitatory and inhibitory synaptic inputs (Isomura et al. 2008).

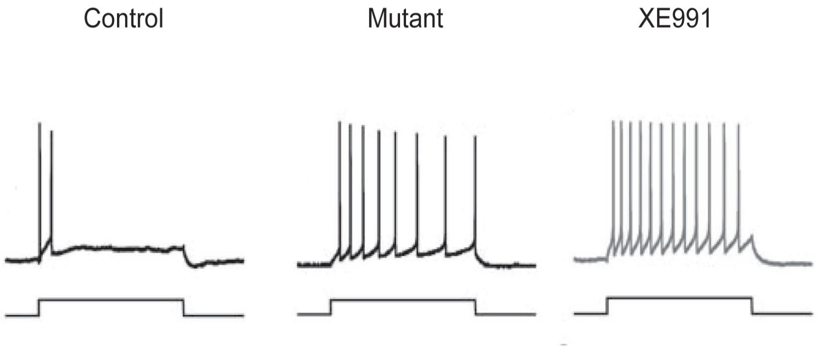

Figure 5.

Regulation of spike frequency in hippocampal pyramidal mouse neurons. Left panel: neurons from WT mice show strong suppression in spike-frequency due to the M-current produced by activated $K_v7.2/K_v7.3$ *heteromeric channels. Middel panel: pyramidal neurons from mice carrying a dominant negative* $K_v7.2$ *mutation produced more action potentials per pulse and showed a markedly weaker suppression in spike-frequency than controls. Right panel: blocking* $K_v7.2$ *with the M current blocker XE991 also greatly reduced adaptation and facilitated repetitive discharges. (Adapted from Peters et al. 2005).*

Ion channels can play a major role in epileptogenesis and the generation of the excessive and synchronous neuronal discharges that are characteristic of epilepsy. Most of the known mutations in epileptic syndromes are caused by mutations in voltage or ligand gated ion channels (Mantegazza et al. 2010), underlining the critical role ion channels play in normal physiology of the brain (reviewed by Reid et al. 2009). Genetically determined alterations of receptors such as GABA are also involved. More specific, around 20 genes encoding for ion channels and neurotransmitter receptors have been identified and linked to a variety of epilepsy syndromes (Mantegazza et al. 2010). In many cases, mutations in these proteins lead to a gainoffunction or loss of function in ion channels, which leads to a disturbance in the excitatory inhibitory brain network due to either insufficient or excessive compensatory mechanisms in response to a change in network activity (Reid et al. 2009, Gatto and Broadie et al. 2010). The impact of ion channels mutations on health may be minor to severe. In some cases, disease mutations affect the gating or conductance of a channel. More often, disease mutations cause defects in synthesis, folding or trafficking of channels to the cell surface or proper axonal or dendritic targets; the remaining channels function properly, but the overall excitability of the affected cell is changed (McArdle et al. 2008, Rusconi et al. 2007, Rusconi et al. 2009, Maljevic et al. 2011, Chung et al. 2006).

Different mutations may give rise to either recessive or dominant disease. In dominant channelopathies, one mutant channel gene is sufficient to disrupt normal function. A 50% reduction or less in protein function of the mutant is defined as haplo-insuffcient, while a dominant-negative effect occurs if more than 50% of normal function is disturbed or if the mutant protein interferes with the functionality of the WT protein. A recessive disorder is characterized by two affected alleles that are both necessary to cause a disease phenotype. However, since individuals with a heterozygous mutation also express a population of wildtype channels in the same cell, dominantly inherited channelopathies are often less severe than recessive forms (reviewed by Ashcroft FM 2006).

KCNQ2 mutations cause BFNE

K_v7 ($K_v7.1$-5) represents a family of voltage gated potassium ion channels predominantly expressed in the central nervous system and in heart. KCNQ2 and KCNQ3 encode for the potassium α-subunit $K_v7.2$ and $K_v7.3$, that produce a slow activating noninactivating neuronal M-current. The M-current has its name, because of the inhibition of the ion channels by activation of muscarinic acetylcholine receptors. Their biophysical properties, together with their specific protein subcellular localization, facilitate powerful control over the firing rate of a neuron. Because M-channels are inhibited by a neurotransmitter activated G protein coupled signaling pathway, the down regulation of the M-current by G protein signaling can in turn reduce conductance of the inhibitory M-current and thus potentiate membrane excitability. These opposing regulatory mechanisms are an important aspect of Mcurrent physiology (Hernandez et al. 2008).

The $K_v7.2$ channels form functional heteromeres with $K_v7.3$ (Figure 2B and 2C). Monomeric $K_v7.2$ and $K_v7.3$ channels produce small M currents, heteromeric potassium channels, preferably in a 2:2 subunit stoichiometry, yield a robust potassium current (Schwake et al. 2000, Stewart et al. 2012). The increased current is largely due to an increase in ion channel cell surface expression (Schwake et al 2000). Mutations in KCNQ2 and KCNQ3 are linked to a form of infant epilepsy termed Benign Familial Neonatal Epilepsy (BFNE), also known as Benign Familial Neonatal Convulsion (BFNC) or Seizures (BFNS). Seizures in BFNE typically start on the second or third day of life, and usually spontaneously remit within a few weeks.

Mutations in either KCNQ2 or KCNQ3 can cause a reduction in total maximal current when heterozygously expressed in a 1:1:2 ratio and/or are transported quite inefficiently to the cell surface or their proper axonal targets (Chung et al. 2006, see also CHAPTER 2 and CHAPTER 3). $K_v7.2$ and $K_v7.3$ are expressed in the CA1 and CA3 subfields and dentate gyrus (Rasmussen et al. 2007). Immunostaining primarily showed staining of these channels in excitatory pyramidal neurons, in the action initial segments (AIS), the location where action potentials are generated, and in the nodes of Ranvier where they colocalize with sodium ion channels (Devaux et al. 2004, Chung et al. 2006, Pan et al. 2006, Rasmussen et al. 2007). Activation of $K_v7.2/K_v7.3$ heteromeric channels during the initial stages of an action potential discharge serves to suppress later action potentials and shorten the duration and frequency of the spike train induced by sustained depolarization. Selective blockage of $K_v7.2$ by the antagonist linopirdine (XE991) or expression of a dominant negative $K_v7.2$ construct strongly enhances repetitive firing in murine hypocampal CA1 pyramidal neurons (Peña et al. 2006, Peters et al 2005, and Figure 5). The loss-of-function of $K_v7.2$ and $K_v7.3$ by haploinsufficiency is believed to be the major pathomechanism of BFNE and underlies the significance of these types of ion channels in controlling neuronal excitability via the Mcurrent.

SCN1A mutations are associated with GEFS+ and Dravet syndrome

Genetic Epilepsy with Febrile Seizures (GEFS+) is an autosomal dominant benign form of epilepsy in which patients have frequent febrile seizures early in childhood that persist beyond 6 years of age and are associated with generalized or partial epileptic seizures. Dravet syndrome (DS) or severe myoclonic epilepsy of infancy (SMEI) (Singh et al., 2001) is an intractable epilepsy syndrome, characterized by an onset of fever induced generalized tonic-clonic or hemiclonic seizures within the first year of life, followed by other seizure types including absence, atonic, and myoclonic seizures. DS subjects are usually refractory to treatment and are associated with intellectual disability. Also the psychomotor development in DS subjects is delayed and patients often experience mental decline and other neurological manifestations including ataxia. Mutations in voltage gated sodium channels (SCN1A and SCN2A), sodium channel auxiliary β1-subunit (SCN1B), and the GABA γ2 receptor (GABRG2) have been found in subjects diagnosed with GEFS+ or DS, with the majority of mutations found in the gene SCN1A; 10% of the mutations are found in GEFS+ patients and ~80% in DS (Lossin C 2009, Claes et al. 2009). Since only coding regions of the gene are sequenced, it is possible that in many of the patients negative for SCN1A mutations harbor mutations in regulatory regions of the gene outside of the coding sequence that could impair channel expression.

The gene SCN1A encodes for the a-subunit of the neuronal voltage gated sodium channel $Na_v1.1$, which is a glycosylated complex expressed in hippocampal, neocortex and cerebellar interneurons that are critical for GABAmediated neuronal inhibition. The majority of GEFS+ cases arise from heterozygous missense mutations inherited in a familial manner, while de novo frameshift, nonsense and splicesite mutations resulting in premature termination of $Na_v1.1$ proteins are common in DS. This suggests that GEFS+ is presumably caused by alterations in gating of the channel and hence alterations in GABA release, while non-functionality of $Na_v1.1$ channel resulting in reduced GABAergic inhibition causes DS. Scn1a knockout and knockin mouse models mimic the lossoffunction mutations found in most cases of this disease and correspond with the phenotype in DS subjects (Yu et al. 2006, Ogiwara et al. 2007). However, approximately one third of the reported DS mutations are missense mutations, complicating a straightforward genotype-phenotype correlation in DS subjects (see also CHAPTER 4 and CHAPTER 5 in this thesis).

Other mechanisms: auxilliary subunits

SCN1B encodes for the β1-ancillary subunit. Sodium channel bsubunits modulate the gating and surface expression of sodium ion channels (Patino GA and Isom LL 2010). SCN1B was the first gene to be identified to cause Genetic epilepsy with febrile seizures plus (GEFS+) (Wallace et al. 1998). The missense mutation C121W disrupts a highly conserved cysteine residue thought to be essential for maintaining the tertiary structure of the extracellular Immunoglobulinlike loop. Subsequent missense and inframe deletion mutations in this extracellular region found in subjects with similar phenotypes have been reported (Wallace et al. 2002, Audenaert et al. 2003, Scheffer et al. 2007, Orrico et al. 2009). Electrophysiological characterization of the β1 mutant coexpressed with voltage gated sodium channels showed that the C121W β1-subunit mutant causes a gainoffunction in sodium channel gating and kinetics (Wallace et al. 1998, Meadows et al. 2002). These findings imply the importance of the β1-subunit loop in normal neuronal functioning. Moreover, the significance of the β1 extracellular loop is highlighted by the finding of a homozygous recessive mutation in a Dravet syndrome patient that resulted in loss of cell surface expression (Patino et al. 2009).

Other mechanisms: receptors

Gammaaminobutyric acid (GABA) is the predominant inhibitory transmitter within the central nervous system and acts through three receptor classes: the ionotrophic $GABA_A$ and $GABA_C$ receptors and the metabotropic $GABA_B$ receptor. To date, all mutations related to epilepsy are found in $GABA_A$ receptors. The $GABA_A$ receptor is a transmitter-gated ion channel of the Cysloop family. $GABA_A$ receptors are pentameric proteins with a central chloride permeant pore that is formed from various combinations of proteins encoded by the α, β, γ, δ, ε and θ subunits. A variety of receptors can be formed by a combination of these subunits. The most common $GABA_A$ receptor in the brain is composed of two α-subunits, two β-subunits and one γ or δ receptor (Baumann et al. 2002). A missense mutation in the GABRG2 gene encoding the γ2-subunit, was first discovered in a French family diagnosed with GEFS+, with phenotypic heterozygosity ranging from mild febrile seizures to severe afebrile convulsions (Baulac et al. 2001). Functional studies in transfected mammalian cells showed loss of cell surface expression. Interestingly, transfected hippocampal neurons showed accelerated receptor deinactivation rates predicting a reduced duration of IPSP (Bianchi et al. 2002, Eugène et al. 2007); a defect that could not be observed in cultured cell lines. Moreover, a conditional knock-in mouse model with this GABRG2 mutation reduced seizure susceptibility when mutant proteins were suppressed during early development, suggesting that this mutation is a critical determinant of seizure susceptibility later on in life (Chiu et al. 2008).

Another missense mutation in the N-terminus of the γ2-subunit caused misfolding of the protein leading to ER retention and thus reduced surface expression of $GABA_A$ receptors in cortical pyramidal neurons of knockin mice (Tan et al. 2007). Interestingly, this model recapitulates absenceseizure not GEFS+ phenotypes and suggests that other factors such as modifier genes could influence the phenotypic outcome. Nevertheless, impaired neuronal inhibition may be a common etiology for epileptic syndromes.

Aim of this study

The aim of this study is to validate novel and undetermined variations in KCNQ2 and SCN1A found in patients diagnosed with a specific subtype of epilepsy and to correlate the observed gating defects to the phenotypic and developmental outcome using functional invitro assays.

Contents of this thesis

Chapter 2 describes a functional study of three novel BFNE mutations (V859X, T359K, P410fs12X) in the gene encoding the K_v7.2 potassium channel, where all three mutations cause an unprecedented reduction in Mcurrent, consistent with previous report that haploinsufficiency is the main defect causing BFNE. In addition, trafficking studies show that two mutants (V859X and T359K) are expressed at the cell surface of HEK293 cells and one of the mutants (P410fs12X) leads to channel retention outside the ER. Interestingly, P410fs12X is a truncation mutant that lacks an assembly domain necessary for tetramerization (see also Figure 2C). Tetramerization of aunits occurs in the ER, before the fully assembled ion channel gets transported to the cell surface. Therefore it is most likely that K_v7.2 α–units harbor a second assembly domain for proper tetramerization and cell surface expression. Chapter 3 describes a molecular functional study of two C-terminally truncated K_v7.2 mutants (P410X and L351X) that do not require their assemblydomain to form a tetrameric ion channel that can be expressed at the cell surface.

The most common target gene of epileptogenic mutations is the gene SCN1A, in which hundreds of different pathogenic mutations linked to epilepsy and a few mutations associated with familial hemiplegic migraine (FHM) have been discovered (Escayg et al. 2000, Claes et al. 2001, Kahlig et al. 2008). Chapter 4 describes the phenotypes of two GEFS+ patients (R859H) and six DS patients (R865G, R946C, and R946H). R859H was found in a small GEFS+ family; R865G, R946C and R946H were found in unrelated DS subjects. Since the functional consequences of these missense mutations in relation to GEFS+ and DS are difficult to predict, a functional study was conducted at room temperature in tsA201 cells of these four SCN1A mutations (R859H – GEFS+; R865G – DS; R946C – DS; R946H – DS) using the whole-cell patch clamp technique. Based on these findings it was still hard to establish a genotype-phenotype correlation between missense mutations in GEFS+ subjects harboring a R859H mutations and DS patients with an R865G mutation. Since a key feature of GEFS+ and DS is feverinduced seizures, a full characterization of the two previously tested SCN1A mutants (R859H – GEFS+; R865G – DS) was conducted at physiological and febrile temperatures using the same invitro assay. The results of this study are described in chapter 5.

References

Alabi AA, Bahamonde MI, Jung HJ, Kim JI, Swartz KJ. (2007) Portability of paddle motif function and pharmacology in voltage sensors. Nature 450:370376

Ashcroft FM. (2006) From molecule to malady. Nature 440:440447

Audenaert D, Claes L, Ceulemans B, Löfgren A, Van Broeckhoven C, De Jonghe P. (2003) A deletion in SCN1B is associated with febrile seizures and earlyonset absence epilepsy. Neurology 61:854856

Balser JR, Nuss HB, Chiamvimonvat N, PerezGarcia MT, Marban E, Tomaselli GF. (1996) External pore residue mediates slow inactivation in mu 1 rat skeletal muscle sodium channels. J Physiol. 494:431442

Baulac S, Huberfeld G, GourfinkelAn I, Mitropoulou G, Beranger A, Prud'homme JF, Baulac M, Brice A, Bruzzone R, LeGuern E. (2001) First genetic evidence GABA(A) receptor dysfunction in epilepsy: a mutation in the gamma2subunit gene. Nat Genet. 28:4648

Baumann SW, Baur R, Sigel E. (2002) Forced subunit assembly in alpha1beta2gamma2 GABAA receptors. Insight into the absolute arrangement. 277:4602046025

Bean BP. (2007) The action potential in mammalian central neurons. Nat. Rev. Neurosci. 8:451465

Benitah JP, Chen Z, Balser JR, Tomaselli GF, Marban E. (1999) Molecular dynamics of the sodium channel pore vary with gating: interactions between Psegment motions and inactivation. J Neurosci. 19:15771585

Bianchi MT, Macdonald RL. (2002) Slow phases of GABA(A) receptor desensitization: structural determinants and possible relevance for synaptic function. J Physiol 544:318

Catterall WA, Schmidt JW, Messner DJ, Feller DJ. (1986) Structure and biosynthesis of neuronal sodium channels. Ann N Y Acad Sci. 479:186:203

Catterall WA, Goldin AL, Waxman SG. (2005) International union of pharmacology. XLVII. Nomenclature and structurefunction relationship of voltage gated sodium channels. Pharmacol Rev. 57:397409

Cheng YH, Dale TJ, Romanos MA, Whitaker WR, Xie XM, Clare JJ. (2000) Cloning, distribution and functional analysis of the type III sodium channel from human brain. Eur. J. Neurosci. 12:4284:4289

Chiu C, Reid CA, Tan HO, Davies PJ, Single FN, Koukoulas I, Berkovic SF, Tan SS, Sprengel R, Jones MV, Petrou S. (2008) Developmental impact of familial GABAA receptor epilepsy mutation. Ann Neurol. 64:284293

Chung HJ, Jan YN, Jan LY. (2006) Polarized axonal surface expression of neuronal KCNQ channels is mediated by multiple signals in the KCNQ2 and KCNQ3 Cterminal domains. Proc Natl Acad Sci U.S.A. 103: 88708875

Claes L, Del Favero J, Ceulemans B, Lagae L, Van Broeckhoven C, De Jonghe P. (2001) De novo mutations in the sodiumchannel gene SCN1A cause severe myoclonic epilepsy of infancy. Am. J. Hum. Genet. 68:13271332

Claes LR, Deprez L, Suls A, Baets J, Smets K, Van Dyck T, Deconinck T, Jordanova A, De Jonghe P. (2009) The SCN1A variant database: a novel research and diagnostic tool. Hum. Mutat. 30:E904920

Cossart R, Bernard C, BenAri Y. (2005) Multiple facets of GABAergic neurons and synapses: multiple fates of GABA signalling in epilepsies. Trends Neurosci. 28:108115

Doyle DA, Morai Cabral J, Pfuetzner RA, Kuo A, Gulbis JM, Cohen SL, Chait BT, MacKinnon R. (1998) The structure of the potassium channel: molecular basis of K+ conduction and selectivity. Science 80:6977

Escayg A, MacDonald BT, Meisler MH, Baulac S, Huberfeld G, AnGourfinkel I, Brice A, Leguern E, Moulard B, Chaigne D, Buresi C, Malafosse A. (2000) Mutations of SCN1A encoding a neuronal sodium channel, in two families with GEFS+2. Nat. Genet. 24:362368

Eugène E, Depienne C, Baulac S, Baulac M, Fritschy JM, Le Guern E, Miles R, Poncer JC. (2007) GABA(A) receptor gamma 2 subunit mutations linked to human epileptic syndromes differentially affect phasic and tonic inhibition. J Neurosci. 27: 1410814116

Featherstone DE, Richmond JE, Ruben PC. (1996) Interaction between fast and slow inactivation in Skm1 sodium channels Biophys J. 71:30983109

Gatto CL and Broadie K. (2010) Genetic controls balancing excitatory and inhibitory synaptogenesis in neurodevelopmental disorder models. Front Synaptic Neurosci. 2:4

Glaaser, IW, Bankston JR, Liu H, Ttateyama M, Kass RS. (2006) A carboxylterminal hydrophobic interface is critical to sodium channe function. Relevance to inherited disorders. J Biol Chem. 281:2401524023

Heginbotham L, Abramson T, MacKinnon R. (1992) A functional connection between the pores of distantly related ion channels as revealed by mutant K+ channels. Science 258:11521155

Hernandez CC, Zaika O, Tolstykh GB, Shapiro MS. (2008) regulation of neural KCNQ channels: signaling pathways, structural motifs and functional implications. J Physiol. 586:18111821

Hille B. (2001) 3rd Ed. Ion channels of excitable membranes Sinauer Associates Inc., U.S.A.

Isom LL, Scheuer T, Brownstein AB, Ragsdale DS, Murphy BJ, Caterall WA. Coexpression of b1 and type IIA a subunits of sodium channels in a mammalian cell line. J. Biol. Chem. 270:33063312

Isomura Y, FujiwaraTsukamoto Y, Takada M. (2008) A network mechanism underlying hippocampal seizurlike synchronous oscillation. Neurosc Res. 61:227233

Jenkinson DH. (2006) Potassium channels – multiplicity and challenges. Br J. Pharmacol. 147 Suppl 1:S6371

Jiang Y, Lee A, Chen J, Ruta V, Cadene M, Chait BT, MacKinnon R. (2003) Xray structure of a voltagedependent K+ channel. Nature 423:3341

Kahlig KM, Misra SN, George AL Jr. (2006) Impaired inactivation gate stabilization predicts increased persistent current for an epilepsyassociated SCN1A mutation. J Neurosci. 26:1095810966

Kahlig KM, Rhodes TH, Pusch M, Freilinger T, PereiraMonteiro JM, Ferrari MD, van den Maagdenberg AM, Dichgans M, George Jr. AL. (2008) Divergent sodium channel defects in familial hemiplegic migraine. Proc. Natl. Acad. Sci. USA 105:97999804

Kandel ER, Schwartz JH, Jessell TM. (2000) 4th Ed. Principles of neuronal science. McGrawHill Companies Inc., U.S.A.

Krafte DS, Goldin AL, Auls VJ, Dunn RJ, Davidson N, Lester HA. (1990) Inactivation of clones sodium channels expressed in Xenopus oocytes. J. Gen. Physiol. 96:689706

Kuo MM, Saimi Y, Kung C. (2003) Gainoffunction mutations indicate that Escherichia coli Kch forms a functional K+ conduit in vivo. EMBO J. 22:40494058

Liberman EA and Skulachev VP. (1970) Conversion of biomembraneproduced energy into electric form. IV. General discussion. Biochem Biophys Acta. 216:3042

Long SB, Campbell EB, MacKinnon R. (2007) Atomic structure of a voltagedependent K+ channel in a lipid membranelike environment. Nature 450:376:382

Lossin C. (2009) A catalog of SCN1A variants. Brain Dev. 31:114130

MacKinnon R. (1991) Using mutagenesis to study potassium channel mechanisms. J Bioenerg Biomembr. 23:647:663

MacKinnon R, Aldrich RW, Lee SW. (1993) Functional stoichiometry of Shaker potassium channel inactivation. Science 262:757759

Maljevic S, Naros G, Yalcin Ö, Blazevic D, Loeffler H, Cağlayan H, Steinlein OK, Lerche H. (2011) Temperature and pharmacological rescue of a foldingdefective, dominantnegative KV 7.2 mutations associated with neonatal seizures. Hum Mut. 32:E22832293

Mantegazza M, Rusconi R, Scalmani P, Avanzini G, Franceschetti S. (2010) Epileptogenic ion channel mutations: From bedside to bench and, hopefully back again. Epilepsy Research 92:129

McArdle EJ, Kunic JD, George AL Jr. (2008) Novel SCN1A frameshift mutation with absence of truncated Nav1.1 protein in severe myoclonic epilepsy of infancy. Am J Med Genet. 146:2421:2423

McCormick DA, Contreras D. (2001) On the cellular and network bases of epileptic seizures. Annu. Rev. Physiol. 63:815:846

McNamara JO. (1994) Cellular and molecular basis of epilepsy. J. Neurosci. 14:34133425

Miceli F, Soldovieri MV, Martire M, Taglialatela M. (2008) Molecular pharmacology and therapeutic potential of neuronal Kv7modulating drugs. Curr Opin Pharmacol. 8:6574

O'Reilly JP, Wang SY, Wang GK. (2001) Residuespecific effects on slow inactivation at V787 in D2S6 of Na_v1.4 sodium channels. Biophys J 81:21002111

Orrico A, Galli L, Grosso S, Buoni S, Pianigiani R, Balestri P, Sorrentino V. (2009) Mutational analysis of the SCN1A, SCN1B and GABRG2 genes in 150 Italian patients with idiopathic childhood epilepsies. Clin Genet. 75:579581

Pan Z, Kao T, Horvatz Z, Lemos J, Sul JY, Cranstoun D, Bennett V, Scherer SS, Cooper EC. (2006) A common ankyrinGbased mechanism retains KCNQ and Nav channels at electrically active domains of the axon. J. Neurosci. 26:25992613

Patino GA, Claes LR, LopezSantiago LF, Slat EA, Dondeti RS, Chen C, O'Malley HA, Gray CB, Miyazaki H, Oyama F, De Jonghe P, Isom LL. (2009) A functional null mutation of SCN1B in a patient with Dravet syndrome. J Neurosci. 29:1076410778

Patino GA, Isom LL. (2010) Electrophysiology and beyond: Multiple roles of Na+ channel b subunits in development and disease. Neurosci Lett 486:5359

Peña F, AlavezPérez N. (2006) Epileptiform activity induced by pharmacologic reduction of Mcurrent in the developing hippocampus in vitro. Epilepsia 47:4754

Ogiwara I, Miyamoto H, Morita N, Atapour N, Mazaki E, Inoue I, Takeuchi T, Itohara S, Yanagawa Y, Obata K, Furuichi T, Hensch TK, Yamakawa K. (2007) Na(v)1.1 localizes to axons of parvalbuminpositive inhibitory interneurons: a circuit basis for epileptic seizures in mice carrying an Scn1a gene mutation. J. Neurosci. 27:5903:5914

Peters HC, Hu H, Pongs O, Storm JF, Isbrandt D. (2005) Conditional transgenic suppression of M channels in mouse brain reveals functions in neuronal excitability, resonance and behavior. Nat. Neurosci 8:5160

Qu Y, Curtis R, Lawson D, Gilbride K, Ge P, DiStifano PS, SilosSantiago I, Catterall WA, Scheuer T. (2001) Differential modulation of sodium channel gating and persistent sodium currents by the b1, b2 and b3 subunits. Mol. Cell. Neurosc. 18:570580

Rasmussen HB, FrøkjaerJensen C, Jensen C, Jensen HS, Jørgensen NK, Misonou H, Trimmer JS, Olesen SP, Schmitt N. (2007) Requirement of subunit coassembly and ankyrinG for Mchannel localization at the axon initial segment. J. Cell Sci. 120:953963

Reid CA, Berkovic SF, Petrou S. (2009) Mechanisms of human inherited epilepsies. Prog. Neurobiol. 87:4157

Rusconi R, Scalmani P, Cassulini RR, Giunti G, Gambardella A, Franceschetti S, Annesi G, Wanke E, Mantegazza M. (2007) Modulatory proteins can rescue a trafficking defective epileptogenic Nav1.1 Na+ channel mutant. J Neurosci. 27:1103711046

Rusconi R, Combi R, Cestèle S, Grioni D, Franceschetti S, Dalprà L, Mantegazza M. (2009) A rescuable folding defective Nav1.1 (SCN1A) sodium channel mutant causes GEFS+: common mechanism in Nav1.1 related epilepsies? Hum Mutat. 30:E747760

Rudy B. (1978) Slow inactivation of the sodium conductance in squid giant axons. J Physiol. 494:431442

Ruff RL, Simoncini L, Stuhmer W. (1988) Slow sodium channel inactivation in mammalian muscle: a possible role in regulating excitability. Muscle Nerve 11:502510

Rush AM, DibHajj SD, Liu S, Cummins TR, Black JA, Waxman SG. (2006) A single sodium channel mutation produced hyper or hypoexcitability in different types of neurons. Proc. Natl. Acad. Sci. USA 103:82458250

Sands Z, Grottesi A, Sansom MS. (2005) Voltagegated ion channels. Curr Biol. 15R4447

Scheffer IE, Harkin LA, Grinton BE, Dibbens LM, Turner SJ, Zielinski MA, Xu R, Jackson G, Adams J, Connellan M, Petrou S, Wellard RM, Briellmann RS, Wallace RH, Mulley JC, Berkovic SF. (2007) Temporal lobe epilepsy and GEFS+ phenotypes associated with SCN1B mutations. Brain 130:100109

Schulteis CT, Nagaya N, Papazian DM. (1996) Intersubunit interaction between amino and carboxylterminal cysteine residues in tetrameric shaker K+ channels. Biochemstry 35:1213312140

Schwake M, Pusch M, Kharkovets T, Jentsch TJ. (2000) Surface expression and single channel properties of KCNQ2/ KCNQ3, Mtype K+ channels involved in epilepsy. J Biol Chem 275:1334313348

Singh NA, Otto JF, Dahle EJ, Pappas C, Leslie JD, Vilaythong A, Noebels JL, White HS, Wilcox KS, Leppert MF. (2008) Mouse models of human KCNQ2 and KCNQ3 mutations for benign familial neonatal convulsions show seizures and neuronal plasticity without synapse reorganization. J. Physiol. 586:34053423

Stewart AP, GómezPasade JC, McGeorge J,Rouhani MJ, Villaroel A, MurrellLagnado RD, Edwardson JM. (2012) The Kv7.2/Kv7.3 heterotetramer assembles with a random subunit arrangement. J Biol Chem. doi:10.1074/jbc.M111.336511

Tan HO, Reid CA, Single FN, Davies PJ, Chiu C, Murphy S, Clarke AL, Dibbens L, Krestel H, Mulley JC, Jones MV, Seeburg PH, Sakmann B, Berkovic SF, Sprengel R, Petrou S. (2007) Reduced cortical inhibition in a mouse model of familial childhood absence epilepsy. Proc Natl Acad Sci U.S.A. 104:1753617541

Tempel BL, Papazian DM, Schwarz TL, Jan YN, Jan LY. (1987) Sequence of a probable potassium channel component encoded at Shaker locus of Drosophila. Science 237:770775

Ulbricht W. (2005) Sodium channel inactivation: molecular determinants and modulation. Physiol Rev. 85:1271:1301

Vasilev P, Scheuer T, Catterall WA. (1989) Inhibition of inactivation of single sodium channels by a sitedirected antibody. Proc Natl Acad Sci USA 86:8147:8151

Vedantham V, Cannon SC. (1998) Slow inactivation does not affect movement of the fast inactivation gate in voltagegated Na+ channels. J Gen Physiol. 11:8393

Vierbuchen T, Ostermeier A, Pang ZP, Kokubu Y, Südhof TC, Wernig M. (2010) Direct conversion of fibroblasts to functional neurons by defined factors. Nature 463:10351041

Vilin YY, Makita N, George AL, Ruben PC. (2001) Structural determinants of slow inactivation in human cardiac and skeletal muscle sodium channels. Biophys J. 77:13841393

Wallace RT, Wang DW, Singh R, Scheffer IE, George AL Jr, Phillips HA, Saar K, Reis A, Johnson EW, Sutherland GR, Berkovic SF, Mulley JC. (1998) Febrile seizures and generalized epilepsy associated with a mutation in the Na+channel beta1 subunit gene SCN1B. Nat Genet. 19:366370

Wallace RH, Scheffer IE, Parasivam G, Barnett S, Wallace GB, Sutherland GR, Berkovic SF, Mulley JC. (2002) Generalized epilepsy with febrile seizures plus: mutation of the sodium channel subunit SCN1B. Neurology 58:14261429

Wang SY, Wang GK. (1997) A mutation in segment IS6 alters slow inactivation of sodium channels. Biophys J. 72:16331640

West JW, Patton DE, Scheuer T, Wang Y, Goldin AL, Catterall WA. (1992) A cluser of hydrophobic amino acid residues required for fast Na+ channel inactivation. Proc Natl Acad Sci USA 89:1091010914

Yoo AS, Sun AX, Li L, Shcheglovitov A, Portmann T, Li Y, LeeMesser C, Dolmetsch RE, Tsien RW, Crabtree GR. (2011) MicroRNAmediated conversion of human fibroblasts to neurons. Nature 476:228231

Yu FH, Mantegazza M, Westenbroek RE, Robbins CA, Kalume F, Burton KA, Spain WJ, McKnight GS, Scheuer T, Catterall WA. (2006) Reduced sodium current in GABAergic interneurons in a mouse model of severe myoclonic epilepsy in infancy. Nat. Neurosci. 9:11421149

Functional analysis of novel KCNQ2 mutations found in patients with Benign Familial Neonatal Convulsions

Linda Volkers, Martin B. Rook, Joost H.G. Das, Nienke E. Verbeek,
W. Antoinette Groenewegen, Marjan J.A. van Kempen,
Dick Lindhout, Bobby P.C. Koeleman

2

Neurosci Lett. 2009; 462:24-29

This article refers to supplementary information, which can be found at http://www.sciencedirect.com/

Abstract

Benign Familial Neonatal Convulsions (BFNC) is a rare epilepsy disorder with an autosomal dominant inheritance. It is linked to mutations in the potassium channel genes KCNQ2 and KCNQ3. These encode for Kv7.2 and Kv7.3 potassium ion channels, which produce an M-current that regulates the potential firing action in neurons through modulation of the membrane potential. We report on the biophysical and biochemical properties of V589X, T359K and P410fs12X mutant-KCNQ2 ion channels that were detected in three BFNC families.

Mutant KCNQ2 cDNAs were co-expressed with WT-KCNQ2 and KCNQ3 cDNAs in HEK293 cells to mimic heterozygous expression of the KCNQ2 mutations in BFNC patients. The resulting potassium currents were measured using patch-clamp techniques and showed an approximately 75% reduction in current and a depolarized shift in the voltage dependence of activation. Furthermore, the time-constant of activation of M-currents in cells expressing T359K and P410fs12X was slower compared to cells expressing only wild-type proteins. Immunofluorescent labeling of HEK293 cells stably expressing GFP-tagged KCNQ2-WT or mutant α-subunits indicated cell surface expression of WT, V589X and T359K mutants, suggesting a loss-of-function, while P410fs12X was predominantly retained in the ER and sub-cellular compartments outside the ER suggesting an effectively haplo-insufficient effect.

Introduction

KCNQ (KCNQ1-5) represent a family of voltage-gated potassium channel genes predominantly expressed in the central nervous system (CNS) and in heart [1]. KCNQ2 and KCNQ3 encode for a-subunits of the voltage-gated Kv7.2 and Kv7.3 channels that produce a neuronal M-current, a slow activating non-inactivating potassium current important in the modulation of the resting membrane potential. This limits the repetitive firing of many neurons [2]. KCNQ2 and KCNQ3 α-subunits can form functional homomeric potassium ion channels, however, a typical wild-type M-current is produced by heteromeric tetramerization of these α-subunits [2]. Monomeric KCNQ2 or KCNQ3 ion channels produce small M-currents, but M-channels composed of both α-subunits yield more robust potassium currents. This is largely due to an increase in functional M-channels at the cell membrane [3].

Mutations in the KCNQ2 and KCNQ3 gene are found in families affected by Benign Familial Neonatal Convulsions (BFNC). BFNC is an autosomal-dominant inherited epilepsy syndrome characterized by seizure onset in the neonatal period and, in general, a spontaneous remission within a few months. Most BFNC-related mutations are deletions, missense, frame-shift and nonsense mutations in KCNQ2, with some missense mutations in KCNQ3; many of these are located in the carboxy-terminus of these ion channels.
Previous functional studies of KCNQ2 mutations overexpressed as homomeric α-subunits showed loss-of-function defects. However, when co-expressed with either wild type (WT)-KCNQ2 or KCNQ3 α-subunits, a small reduction in total M-current was observed [4,5]. Functional analysis of C-terminal BFNC-related KCNQ2 mutations, expressed in a heterozygous manner, showed only a ~25% reduction in total M-current, which could either be caused by accelerated protein degradation or possible trafficking defects due to a loss of calmodulin binding to the mutated channels [4,6]. Since M-currents activate near the threshold levels of action potential firing, this moderate reduction in K^+-current is hypothesized to be sufficient to trigger epileptic seizures in neonates [5].

Only a small number of studies have reported the functional characterization of KCNQ2 mutations co-expressed with WT-KCNQ2 and KCNQ3 α-subunits in a heterozygous manner as found in patients [5]. We investigated the functional properties of three C-terminal KCNQ2 mutations, V589X, T359K and P410fs12X, in a heterologous cell expression system (Figure 1B inset). We examined the electrophysiological characteristics of the three KCNQ2 mutations by co-expressing mutant KCNQ2, WT KCNQ2 and WT KCNQ3 in a 1:1:2 ratio. Since the C-terminus of KCNQ2 ion channels contains motifs necessary for correct targeting of the channel to the cell surface, we also investigated the trafficking behavior of WT KCNQ2 monomeres and all three KCNQ2 mutations.

Material and Methods

The KCNQ2 V589X mutation was detected in a family with neonatal convulsions [7]. The T359K mutation was detected in a mother and daughter who both suffered from neonatal convulsions, although the mother also had one generalized seizure during childhood and one as an adult. The daughter showed a moderate developmental delay at age 4 years. The P410fs12X mutation was found in a mother and her two children, all had neonatal convulsions. This mother and some of her relatives also had hemiplegic migraine. The P410fs12X mutation did not co-segregate with this phenotype.

Human Embryonic Kidney 293 (HEK293) cells were maintained in Dulbecco's Modified Eagle's Medium (DMEM, Biowhittaker) supplemented with 10% fetal bovine serum (Lonza), penicillin 100 U/ml (Lonza), streptomycin 100 U/ml (Lonza) and 2 mM L-glutamine (Lonza). Mutations in KCNQ2 were made using the QuickChange kit (Stratagene) and verified by sequencing.

For functional analysis of WT channels, cells were transiently transfected with a total of 4 µg pXOOM/KCNQ2 and pXOON/KCNQ3 in a 1:1 ratio using Lipofectamine2000 (Invitrogen). Heterozygous expression and analysis of mutant ion channels was achieved by transfecting in total 4 µg of mutant, KCNQ2 and KCNQ3 cDNAs in a 1:1:2 ratio. Homomeric ion channels were analyzed by transfecting either 2 µg of KCNQ2 or KCNQ3 constructs. As a control, electrophysiological experiments were performed on untransfected cells and cells transfected with 2 µg empty pXOOM vector. In all experiments a GFP construct was co-transfected and used as a reporter to identify successfully transfected cells.

For fluorescence microscopy, the KCNQ2 and mutant coding region from the pXOOM/KCNQ2 construct was excised with HindIII/BamHI and subcloned in-frame in the pEGFP-C1 fusion vector (Clontech Laboratories). The pEGFP/KCNQ2 and pEGFP/KCNQ2 mutants were subsequently transfected in HEK293 cells and grown under geneticin G-418 sulfate (Gibco) selection to generate stable polyclonal cell lines.

For indirect immunofluorescence and localization studies, HEK293 cells stably expressing pEGFP/KCNQ2 or one of the pEGFP/KCNQ2 mutants were grown on laminin-coated glass coverslips. After 24 hours, cells were rinsed twice with cold PBS, fixed with 4% paraformaldehyde for 20 minutes at 4ºC and quenched for 5 minutes with 10 mM NH_4CL. Membranes were permeabilized using 0.2% (v/v) Triton X-100 in PBS. Non-specific binding was blocked with blocking buffer [3% (w/v) BSA in PBS] for 1 hour at room temperature. Immunolabeling was performed in blocking buffer for 1 hour using either mouse anti-Calnexin or rabbit anti-Flotillin 1 antibodies (Sigma-Aldrich). Cells were rinsed three times with 0.2% (v/v) Triton X-100 in PBS and incubated with Texas-Red conjugated anti-mouse or anti-rabbit antibodies for 1 hour at room temperature. Cells were rinsed five times in PBS and coverslips were mounted in vectashield. Confocal laser scanning microscopy was performed using a Nikon RCM 8000 microscope equipped with a 60x oil immersion objective. For image acquisition and analysis, we used the EZ 2000 software package (Coord Version 2.4.17, Nikon, Europe BV).

For electrophysiological analysis, cells were bathed in modified Tyrode's solution containing 125 mM NaCl, 5.4 mM KCl, 1.8 mM $CaCl_2$, 1mM $MgCl_2$, 6 mM Glucose, 6 mM HEPES (pH 7.4). Transfected HEK293 cells marked by GFP expression were selected using an inverted fluorescence microscope (Nikon diaphot TMF). Currents were measured at room temperature 2 days after transfection using the whole-cell voltage clamp configuration with an Axopatch 200B amplifier (Axon Instrument, Inc). Patch pipettes had a resistance of 3-4 MΩ when filled with a pipette solution containing 125 mM K-gluconate, 10 mM KCl, 5 mM HEPES, 5 mM EGTA, 2 mM $MgCl_2$, 0.6 mM $CaCl_2$, 4 mM Na_2ATP (pH 7.2). For measurements of the voltage dependence of activation, cells were clamped by applying 3 s conditioning voltage pulses to potentials between -100 mV and + 30 mV in 10 mV increments from a holding potential of -80 mV. A subsequent 500 ms test potential at -40 mV was used to evoke tail currents, which were used to determine the voltage dependence of activation by plotting tail current amplitudes against the range of conditional voltages. Patch-pipette series resistance was 80-90% compensated. Whole cell currents were low-pass-filtered at 2.5 kHz using the four-pole Bessel filter in the clamp amplifier and digitized at 5 kHz. Data acquisition and analysis were performed using custom-made software.

Steady-state activation data were fitted to the Boltzmann function: $y = I_{max}/(1+\exp((1/k)-(V-V½)))$, where V is the variable conditioning potential, V½ the voltage of half maximal activation, k the slope, and Imax the normalized maximal amplitude of the Boltzmann current. The time-constant of activation ($\tau_{activation}$) was obtained by fitting a single exponential $A_{(t)} = A_0 \exp(-t/\tau_{activation})$ to the rate of activation, where t is time in ms and τ is time constant of activation, through the elicited recordings obtained in the -30 mV to +30 mV membrane potential range. Data is presented as mean ± SEM. The compared data sets were subjected to an ANOVA Bonferroni or Kruskal-Wallis test. We considered a value of $P<0.05$ as significant.

Results

To investigate the functional consequences of V589X, T359K and P410fs12X KCNQ2 mutations, we analyzed the electrophysiological properties of the human WT and mutant KCNQ2/3 heteromeric channels transiently expressed in HEK293 cells. Figure 1A shows representative current recordings of cells transfected with WT and mutant ion channels. In agreement with previous reports [2,3,5], expression of KCNQ2 or KCNQ3 monomeric channels gave rise to small M-currents, while cells co-expressing WT KCNQ2/3 (ratio 2:2) channels showed substantially larger M-currents (Figure 1B).

Compared to cells expressing WT KCNQ2/3 ion channels, we observed a large reduction in peak M-current density in cells co-expressing KCNQ2 mutant channels, (71 ± 7% for V589X, 85 ± 3% for T359K and 74 ± 6% for P410fs12X) as shown in Figure 1A, 1B and Table 1. The differences in current densities were statistically significant ($P<0.05$). Cells expressing exclusively V589X, T359K, or P410fs12X mutated ion channels showed very small currents comparable with background currents (data not shown). The latter experiment suggests a complete loss-of-function of all three monomeric mutant KCNQ2 α-subunits, the effect of which, when present in a KCNQ2/3 heteromere could be similar to haplo-insufficiency for KCNQ2. To test this hypothesis, we analyzed current densities in HEK293 cells expressing WT-KCNQ2/3 in a 1:2 ratio. Maximal current amplitude showed a substantial decrease in total K^+-current (81 ± 6%, n=8) quite comparable with the heterozygously expressed mutant ion channels, which suggests that these mutations in KCNQ2 result in a substantial fraction of nonfunctional heteromeric ion channels (Figure 1B and Table 1).

Table 1. Biophysical parameters of KCNQ2/3 WT and mutant ion channels

	V½ [mV]	*k*	*Current density [pA/pF]*
WT Q2/Q3 (ratio 2:2)	-28.4 ± 1.9	6.1 ± 0.3	793 ± 150
V589X + Q2 + Q3 (ratio 1:1:2)	-21.4 ± 0.8	7.5 ± 0.4*	229 ± 141‡
T359K + Q2 + Q3 (ratio 1:1:2)	-22.2 ± 2.2	7.5 ± 0.4*	121 ± 23‡
P410fs12X + Q2 + Q3 (ratio 1:1:2)	-23.9 ± 0.8	7.4 ± 0.3*	205 ± 44‡
Q2 + Q3 (ratio 1:2)	-20.7 ± 1.9	7.4 ± 0.4*	154 ± 51‡
Q2	-17.9 ± 1.9	8.5 ± 0.5	124 ± 33
Q3	-37.3 ± 1.3	5.2 ± 0.2	51 ± 6
Mock (EV)			17 ± 3
Untransfected			20 ± 4

*Significant differences are indicated as follows: ‡ $P<0.05$, ANOVA; * $P<0.05$, Kruskal-Walllis.*

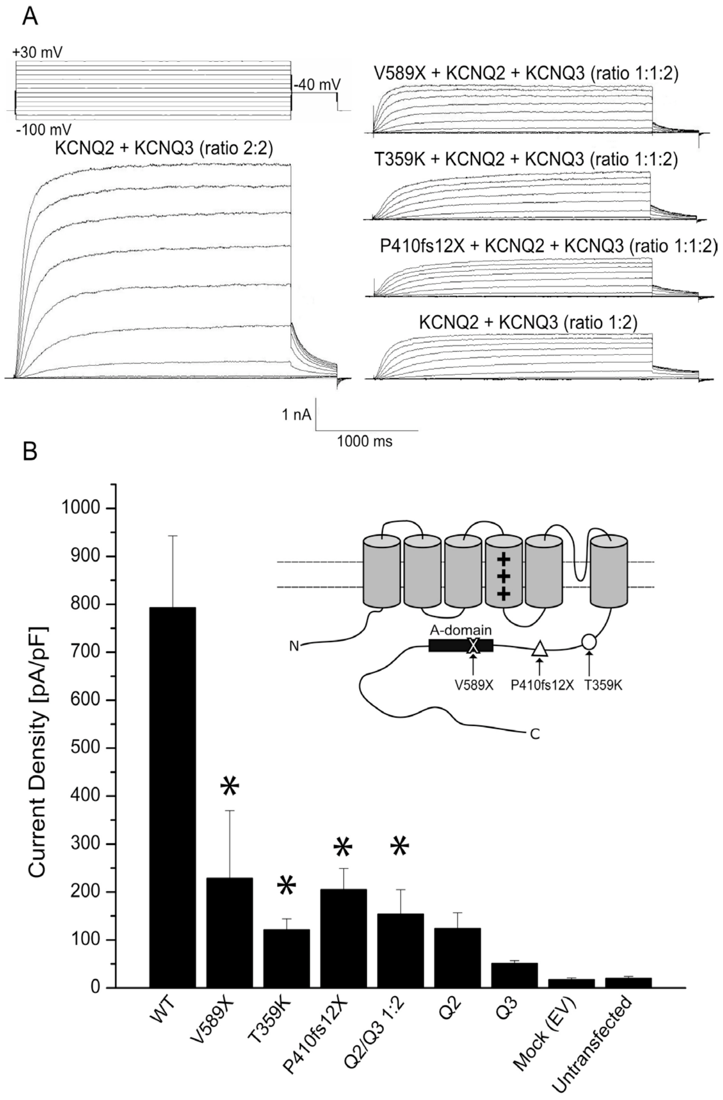

Figure 1.

*Reduction of M-current caused by expression of heteromeric KCNQ2/3 channels harboring V589X, T359K, and P410fs12X BFNC mutations in KCNQ2. A) Current recordings from HEK293 cells transiently transfected with WT KCNQ2/3 (ratio 2:2), V589X, T359K, or P410fs12X with KCNQ2 and KCNQ3 (ratio1:1:2), and KCNQ2/3 (ratio 1:2). Amplitude and time scale are 1 nA and 1000 ms, respectively. B) Maximum current amplitudes at +30mV, normalized to cell capacitance to obtain current densities. * Indicates significant difference of P<0.05 compared to WT. Mock (empty pXOOM vector) and untransfected cells showed negligible background currents <50 pA/pF. The values of the current densities are provided in table 1. Inset) Schematic overview of the KCNQ2 α-subunit; the position of the V589X, T359K and P410fs12X BFNC mutations are shown.*

Next, we constructed activation curves from tail current recordings at -40mV (Figure 1A). Channel populations harboring either one of the mutant α-subunits trend towards activation at more positive membrane potentials (Figure 2A and Table 1). The slope of the I-V relationship of all three mutants was significantly shallower compared to WT. In other words, the three heteromeric mutant ion channels require stronger depolarizations to acquire the same open channel probability as WT-KCNQ2/3 ion channels.

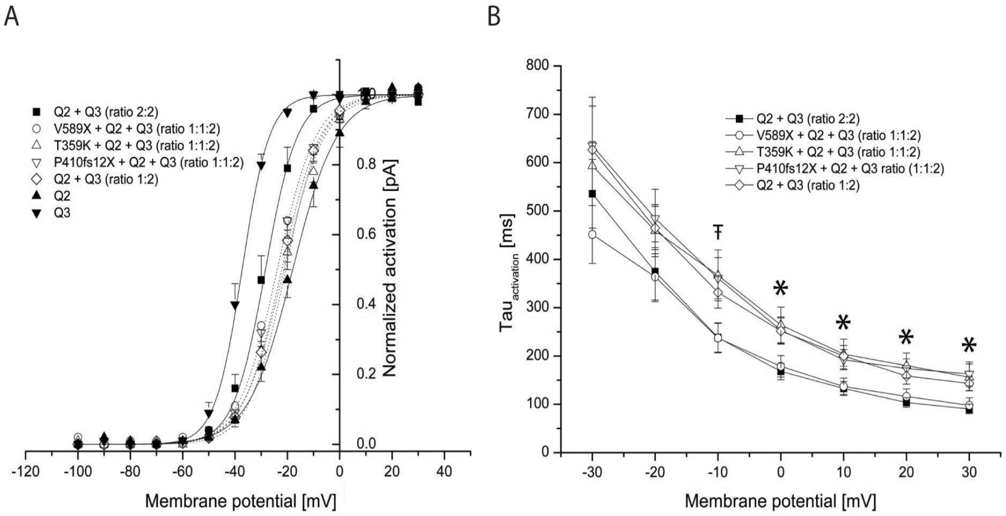

Figure 2.

*The voltage dependence and time-constants of activation of WT and BFNC mutated channels expressed in a heterozygous manner. A) Voltage dependence of activation of heterozygously expressed WT and mutated KCNQ2 ion channels was determined by tail current analysis. Activation-curves were constructed by normalizing tail current amplitudes to the maximal tail-currents and plotted against the membrane potential during the conditioning voltage clamp steps. Slope factors of V589X (7.5 ± 0.4; n=6), T359K (7.5 ± 0.4; n=8), P410fs12X (7.4 ± 0.3; n=7), and KCNQ2/3 (ratio1:2) (7.4 ± 0.4; n=8) were significantly different from WT-KCNQ2/3 (6.1 ± 0.3; n=8) (P<0.05). V½ values were not significantly different from WT-KCNQ2/3. The biophysical parameters of the voltage dependence of activation are provided in table S1. B) Time-constants of activation were obtained by fitting a single exponential through the rising phase of currents obtained by -30 mV to +30mV voltage steps. * indicates a significant difference (P<0.05) for the time-constants of activation for T359K or P410fs12X heterozygously expressed α-subunits, and 'haplo-insufficient' KCNQ2+KCNQ3 (ratio1:2) mutant channels compared to WT channels. Ŧ indicates a significant (P<0.05) slowing in speed of activation for channels harboring T359K and P410fs12X α-subunits compared to WT channels. V589X mutants are comparable to WT data. Fit parameters are provided in Table 2.*

The time-constant of activation was determined by fitting the rising phase of currents elicited by voltage steps between -30mV to +30mV to a single exponential equation. The activation time of WT channels became faster at more positive potentials (Figure 2B and Table 2). Channels containing the V589X a-subunit showed a time-constant of activation that is comparable to WT ion channels. Cells over-expressing T359K, P410fs12X or KCNQ2/3 (ratio1:2; ‘haplo-insufficient’) channels in a heteromeric manner had a significantly larger time-constant of activation. In neurons, M-channels become fully activated at a 0 mV to +30 mV range. Compared to WT channels, the reduced current amplitude in combination with the slower rate of activation of channels containing T359K and P410fs12X α-subunits probably have an additive effect on the loss-of-function in M-current activation during repetitive action potential firing.

Table 2. Speed of activation parameters of KCNQ2/3 WT and mutant ion channels

Membrane potential [mV]	***Q2 + Q3 (ratio 2:2)***	***V589X + Q2 + Q3 (ratio 1:1:2)***	***T359K + Q2 + Q3 (ratio 1:1:2)***	***P410fs12X + Q2 + Q3 (ratio 1:1:2)***	***Q2 + Q3 (ratio 1:2)***
-30	536 ± 71	452 ± 60	593 ± 50	635 ± 100	465 ± 44
-20	374 ± 62	364 ± 48	459 ± 54	485 ± 60	332 ± 33
-10	238 ± 30	237 ± 30	367 ± 53*	361 ± 42*	252 ± 27*
0	168 ± 17	179 ± 22	264 ± 37*	253 ± 28*	200 ± 22*
10	133 ± 14	137 ± 17	204 ± 31*	192 ± 21*	159 ± 17*
20	104 ± 10	116 ± 15	180 ± 26*	174 ± 20*	143 ± 15*
30	90 ± 10	98 ± 16	156 ± 28*	163 ± 25*	465 ± 44
	(n=8)	(n=7)	(n=8)	(n=8)	(n=9)

*Values are presented as mean ± SEM in milliseconds. Significant differences are indicated as follows: * P<0.05, ANOVA.*

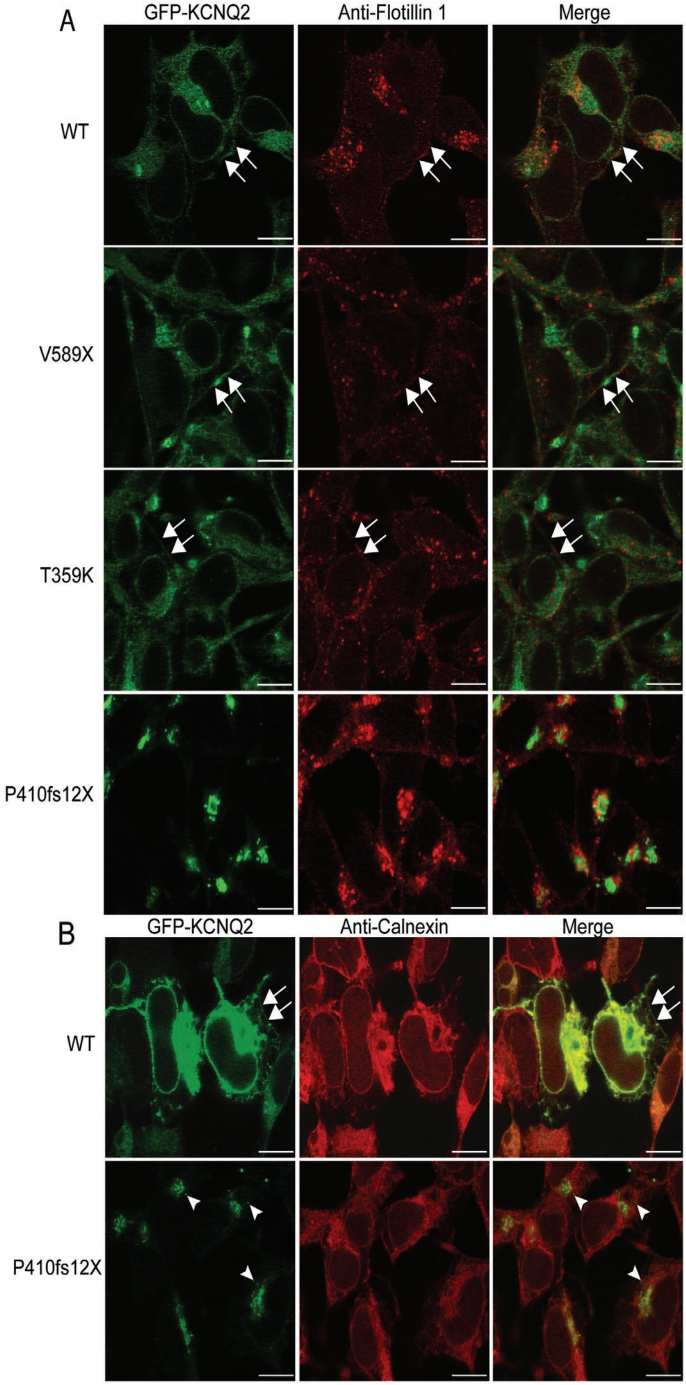
A
GFP-KCNQ2
Anti-Flotillin 1
Merge
WT
V589X
T359K
P410fs12X
B
GFP-KCNQ2
Anti-Calnexin
Merge
WT
P410fs12X

Previously, Soldovieri et al. reported a biophysical and biochemical characterization of two KCNQ2 C-terminal frameshift mutations and showed that these mutations lead to a reduction in current due to impairment in trafficking of these channels [4]. To explore the trafficking behavior of the three C-terminally mutated KCNQ2 ion channels, we generated polyclonal stable cell lines expressing GFP-tagged homomeric KCNQ2 or mutant channels and performed immunofluorescent confocal microscopy. Figure 3A clearly shows co-localization of WT GFP-KCNQ2 potassium channels with the plasma membrane marker anti-Flotillin (arrows). Interestingly, the V589X and T359K mutants were expressed at the cell surface, while P410fs12X was completely absent at the cell surface and concentrated in intracellular compartments.

The P410fs12X mutant produces a KCNQ2 ion channel protein that lacks the Assembly-domain (A-domain) (inset Figure 1B). As reported by several groups, assembly of potassium ion channels occurs in the Endoplasmatic Reticulum (ER) before transport to the cell membrane takes place. Improper or abolished tetramerization of these ion channel α-subunits will lead to ER retention [8]. We performed immunofluorescence on WT and P410fs12X mutant GFP-tagged KCNQ2 channels in combination with the ER-marker anti-Calnexin. Even though WT ion channels showed protein accumulation in the ER, still a substantial proportion of the ion channels was expressed at the cell surface (Figure 3B arrows). The P410fs12X mutant, however, was absent at the cell membrane, but co-localized with the ER marker and interestingly, also with some intracellular compartments outside the ER (arrowheads). These results strongly indicate that the P410fs12X mutant protein is trafficking-defective, which leads to retainment in the ER and in cytosolic vesicles possibly related to the degradation pathway.

Figure 3.

Distribution of WT and mutated KCNQ2 channel proteins in HEK293 cells. A) Confocal images of GFP-tagged WT, V589X, T359K, or P410fs12X proteins. Cell surface was labeled by the plasma-membrane marker anti-Flotillin (red signal). B) WT-KCNQ2 or P410fs12X cells were labeled with the ER marker anti-Calnexin (red signal). WT KCNQ2 ion channels were expressed at the cell surface of HEK293 cells (indicated by arrows). P410fs12X (green) was trapped in the ER (red) as shown by the merge (yellow) and in some intracellular vesicle (arrowheads). Scale bar: 20 µm.

Discussion

We have described the functional characterization of V589X, T359K, and P410fs12X KCNQ2 mutations found in patients diagnosed with BFNC. Homozygous expression of each KCNQ2 gene mutation resulted in a complete loss of potassium current. Expression of GFP-tagged variants of these mutants indicated that T359K and V589X proteins reach the plasma membrane, but that P410fs12X proteins are retained in ER and other intracellular compartments.

Heterozygously expressed mutant KCNQ2 cDNAs caused a 70–85% reduction in M-current compared to WT-KCNQ2/3 heteromeres. This reduction in M-current suggests a dominant-negative effect by the mutants. However, co-expression of KCNQ2 and KCNQ3 also augments plasma membrane expression of KCNQ2 and KCNQ3 ion channels, resulting in a substantial increase in M-current [2,3,5]. Therefore, if mutated KCNQ2 a-subunits are defective (T359K and V589X) or absent in the plasma membrane (P410fs12X), not only the function of the resulting KCNQ2/3 channels is impaired, but overall expression of channel proteins should also be substantially reduced. Our finding that “haplo-insufficient” co-expression of WT-KCNQ2 with WT-KCNQ3 (ratio 1:2) also results in ~80% reduction in M-current corroborates this notion. Interestingly, heteromeric channels harboring a mutated KCNQ2 a-subunit or channels formed by haplo-insufficiency, exhibited similar depolarized shifts and shallower slopes in voltage dependence of activation. This suggests that a reduction of functional KCNQ2 a-subunits caused by the mutations has a common mechanism. However, T359K, P410fs12X and KCNQ2/3 (ratio 1:2) mutant ion channels exhibited an increased time-constant of activation, suggesting a more complex effect of these mutants on heteromeric M-channel function.

We studied the electrophysiological and biochemical properties of the WT and mutated KCNQ2 ion channels in a non-neuronal cell line. Although the V589X and T359K mutants are expressed at the cell surface in HEK293 cells, the trafficking behavior of the mutated ion channels in neurons remains unknown. Notably, KCNQ2 harbors several domains and motifs in its C-terminus that are crucial in correct targeting of the channel to the axon and cause an enrichment of cell surface expression at the axon initial segment (AIS) [9].

The generation, duration and propagation of neuronal action potentials depend primarily on the AIS and axon, since voltage gated Na^+ and K^+ ion channels, including KCNQ2/3 channels, are enriched in these regions. The targeting of KCNQ2 and KCNQ3 channels to the AIS is mediated by Ankyrin-G binding to a conserved motif present in the C-termini of both a-subunits [9,10]. Mice lacking Ankyrin-G show diffused distribution of voltage gated Na^+ and KCNQ2/3 channels in Purkinje neurons [10,11]. The V589X mutation results in a KCNQ2 α-subunit that lacks the Ankyrin-G binding motif, which probably leads to dispersion of these mutated potassium ion channels over the soma. Apart from the loss-of-function caused by the mutation, this would then lead to a substantial reduction in M-current at the AIS.

KCNQ2 expression increases from late fetal life to early infancy in different regions of the developing brain [12]. Previous immunohistochemical studies have shown a widespread expression of KCNQ2 in the hippocampus that in time gradually changes into a predominantly axonal pattern [13]. Recently Chung et al. have shown that several previously reported C-terminal KCNQ2 mutations, which cause channel activation defects and reduction in currents [4], also lead to a reduced axonal surface expression. The T359K mutation is a substitution of a neutral threonine to a positively charged lysine, which could possibly lead to a change in folding of the C-terminus, thereby masking some of the motifs present in this C-tail necessary for correct axonal targeting of this KCNQ2 channel. Since, axonal mistargeting of KCNQ2 ion channels could contribute to hyperexcitability in neonatal neurons leading to seizures in neonates, further research to determine where V589X and T359K mutant KCNQ2 channels locate in neurons is warranted.

The trafficking defective P410fs12X mutation shows accumulation in the ER. Interestingly, we also detected vesicle-shaped structures outside the ER (Figure 3B). Soldovieri et al. have shown that certain frame-shift mutations can lead to accelerated protein degradation [4]. Therefore, it is tempting to speculate that the vesicles outside the ER are early or late endosomes which target the mutated P410fs12X proteins to the degradation pathway. The Western blot shown in figure S2 supports this notion.

Giant Depolarizing Potentials (GDPs) are a form of spontaneous neuronal activity that is essential for establishing a neuronal network in the premature brain and require GABA excitatory receptor activity [14,15]. Both maturation of the M-current through up-regulation of KCNQ2/3 ion channels [12,16], and expression of NKCC1 and KCC2 chloride ion transporters, which change pre-mature excitatory GABAergic responses into inhibitory reactions [17,18], cause the disappearance of GDPs in humans after birth. In principle, the ~75% reduction in M-current we measured for heterozygously expressed V589X, T359K, and P410fs12X mutant ion channels (Figure 1B) could lead to a reduced dampening of GDPs in neonates after birth and subsequently cause the age-dependent BFNC phenotype.

In conclusion, we have functionally characterized three BFNC mutations that all show very similar electrophysiological aberrations, although these are due to different biochemical defects. The V589X and T359K mutations are reminiscent of loss-of-function defects, while the P410fs12X mutation causes virtually complete impairment in trafficking to the cell surface.

References

1. T.J. Jentsch, Neuronal KCNQ potassium channels: physiology and role in disease, Nat. Rev. Neurosci. 1 (2000) pp. 21-30
2. H.-S. Wang, Z. Pan, W. Shi, B.S. Brown, R.S. Wymore, I.S. Cohen, J.E. Dixon, and D. McKinnon, KCNQ2 and KCNQ3 Potassium channel subunits: molecular correlates of the M-channel, Science 282 (1998) pp. 1890-1893
3. M. Schwake, M. Pusch, T. Kharkovets, and T.J. Jentsch, Surface expression and single channel properties of KCNQ2/KCNQ3, M-type K^+ channels involved in epilepsy, J. Biol. Chem. 275 (2000) pp. 13343-13348
4. M.V. Soldovieri, P.Castaldo, L. Iodice, F. Miceli, V. Barrese, G. Bellini, E. Miraglia del Giudice, A. Pascotto, S. Bonatti, L. Annunziato, and M. Taglialatela, Decreased subunit stability as a novel mechanism for potassium current impairment by a KCNQ2 C terminus mutation causing benign familial neonatal convulsions, J. Biol. Chem. 281 (2006) pp. 418-428
5. B.C. Schroeder, C. Kubisch, V. Stein and T.J. Jentsch, Moderate loss of function of cyclic-AMP-modulated KCNQ2/KCNQ3 K^+ channels causes epilepsy, Nature. 396 (1998) pp. 687-690
6. A. Etxeberria, P. Aivar, J. A. Rodriguez-Alfaro, A. Alaimo, P. Villace, J. C. Gomez-Posada, P. Areso, and A. Villarroel, Calmodulin regulates the trafficking of KCNQ2 potassium channels, FASEB J. 22 (2008) pp. 1135-1143.
7. G.-J. de Haan, D. Pinto, D. Carton, A. Bader, J. Witte, E. Peters, G. van Erp, W. Vandereyken, E. Boezeman, M.C. Wapenaar, P. Boon, D. Halley, B.P.C. Koeleman, and D. Lindhout, A novel splicing mutation in KCNQ2 in a multigenerational family with BFNC followed for 25 years, Epilepsia 47 (2006) pp. 851-859
8. D.F Steele, J. Eldstrom, and D. Fedida, Mechanisms of cardiac potassium channel trafficking, J. Physiol. 582 (2007) pp.17-26.
9. H.J. Chung, Y.N. Jan, and L.Y. Jan, Polarized axonal surface expression of neuronal KCNQ channels is mediated by multiple signals in the KCNQ2 and KCNQ3 C-terminal domains, Proc. Natl. Acad. Sci. U S A. 103 (2006) pp. 8870-8875
10. Z. Pan, T. Kao, Z. Horvath, J. Lemos, J.-Y. Sul, S.D. Cranstoun, V. Bennett, S.S. Scherer, and E.C. Cooper, A common Ankyrin-G-based mechanism retains KCNQ and NaV channels at electrically active domains of the axon, J. Neurosci. 26 (2006) pp. 2599-2613
11. D. Zhou, A. Lambert, P.L. Malen, S. Carpenter, L.M. Boland, and V. Bennett, AnkyrinG is required for clustering of voltage-gated Na channels at axon initial segments and for normal action potential firing, J. Cell. Biol. 143 (1998) pp.1295-1304
12. T. Kanaumi, S. Takashima, H. Iwasaki, M. Itoh, A. Mitsudome, and S. Hirose, Developmental changes in KCNQ2 and KCNQ3 expression in human brain: possible contribution to the age-dependent etiology of benign familial neonatal convulsions. Brain Dev. 30 (2008) pp. 362-369
13. Y. G. Weber, J.Geiger, K. Kämpchen, B. Landwehrmeyer, C. Sommer and H. Lerche, Immunohistochemical analysis of KCNQ2 potassium channels in adult and developing mouse brain, Brain Res. 1077 (2006) pp. 1-6
14. Y. Ben-Ari, Excitatory actions of gaba during development: the nature of the nurture, Nature Reviews Neuroscience 3 (2002) pp.728-739
15. R. Khazipov, M. Esclapez, O. Caillard, C. Bernard, I. Khalilov, R. Tyzio, J. Hirsch, V. Dzhala, B. Berger, and Y. Ben-Ari, Early development of neuronal activity in the primate hippocampus in utero, J. Neurosc. 21 (2001) pp. 9770-9781
16. V.F. Safiulina, P. Zacchi, M. Taglialatela, Y. Yaari and E. Cherubini, Low expression of Kv7/M channels facilitates intrinsic and network bursting in the developing rat hippocampus, J. Physiol. 586 (2008) pp. 5437-5453
17. V.I. Dzhala, D.M. Talos, D.A. Sdrulla, A.C. Brumback, G.C. Mathews, Timothy A Benke, E. Delpire, F.E. Jensen, and K.J Staley, NKCC1 transporter facilitates seizures in the developing brain, Nature Medicine 11 (2005) pp. 1205-1213
18. C. Rivera, J.V., J.A. Payne, E. Ruusuvuori, H. Lahtinen, K. Lamsa, U. Pirvola, M. Saarma and K. Kaila, The K^+/Cl^- co-transporter KCC2 renders GABA hyperpolarizing during neuronal maturation, Nature 397 (1999) pp. 251-255

Assembly and efficient membrane transport of monomeric $K_v7.2$ ion channels lacking the carboxy-terminal coiled-coil structures

Linda Volkers, Joost H.G. Das, Marjan J.A. van Kempen, Dick Lindhout,
Bobby P.C. Koeleman*, Martin B. Rook*

* these authors contributed equally

3

In preparation

Abstract

The carboxy-terminus of K_v7.2 ion channels harbors multiple domains and motifs that are considered to be necessary for gating, assembly and trafficking of potassium ion channels. Here we show that Dhelix B/C/D Kv7.2 mutants can still form tetramers and are incorporated at the plasma membrane of HEK293 cells. These results suggests that helix C and D are not essential for channel assembly and that another yet unknown assembly domain must exist in K_v7.2 that is crucial for the formation of monomeric K_v7 ion channels.

Introduction

K_v7 ($K_v7.1$-5) represents a family of voltage gated potassium ion channels predominantly expressed in the central nervous system and in heart [1]. KCNQ2 encodes for the a-subunit $K_v7.2$ that produces a slow activating and non-inactivating neuronal M-current. The M-current is important in the modulation of the resting membrane potential and dampens repetitive firing in many neurons [2]. Monomeric $K_v7.2$ and $K_v7.3$ channels produce small M-currents, but heteromeric potassium channels yield robust currents, which is largely due to increased cell surface expression [3].

$K_v7.2$ harbors several domains and motifs in its C-terminus crucial for channel gating, assembly and correct targeting of the channel to the plasma membrane [4-8] (Figure 1). Secondary structure analysis of this region predicts four a-helices (A, B, C, and D). Helices A and B contain Calmodulin (CaM) binding sites whereas the coiled-coil structures C and D are involved in multimerization and sub-unit specific heteromerization [9,10]. As reported by several groups, assembly of potassium ion channels occurs in the Endoplasmatic Reticulum (ER) before transport to the cell membrane takes place. Improper or abolished tetramerization of these ion channel α-subunits leads to ER retention [11-13].

Previously we reported on the biophysical and cell biological properties of three $K_v7.2$ mutations (V589X, P410fs12X, T359K) [14]. We showed that the P410fs12X frame-shift mutation, which codes for a presumably trafficking defective potassium channel lacking the helices C and D for proper tetramerization, was predominantly retained in sub-cellular compartments outside the ER. Here, we demonstrate that this mutant is retained in the Golgi apparatus. Furthermore, we show that truncated $K_v7.2$ proteins, lacking the tetramerization domain, can still form monomeric channels that are incorporated in the plasma membrane.

Material and methods

Constructs and cell lines

Wildtype (WT) pEGFP/KCNQ2, mutant pEGFP/P410fs12X, pEGFP/P410X, pEGFP/L351X constructs and stably transfected polyclonal cell lines were generated and cultured as previously described [14]. HeLa cells were transiently transfected with WT and mutant constructs using Lipofectamine (Invitrogen, Carlsbad, CA, U.S.A.).

Immunofluorescence

Polyclonal cell lines were grown on poly-L-lysin-coated Fluorodishes (World Precision Instruments, Sarasota, FL, U.S.A). Immmunofluorescence experiments were performed as previously described [14].

Biotinylation pull-down assay

Polyclonal cell lines were washed five times with cold PBS on ice and incubated with sulfo-NHS-SS-Biotin (Thermo Scientific, Rockford, IL, U.S.A.) for 1 hour at 4°C. The reaction was quenched with 100 mM glycine and lysed with Gentle Lysis Buffer (GLB) (75 mM NaCl, 50 mM Tris-HCl (pH 7.4), 1% (v/v) NP-40, 10% glycerol, 2 mM PMSF, 1 µg/ml aprotinin, 1 µg/ml leupeptin). Scraped cells were incubated on ice for 30 minutes and clarified by 16,000 X g centrifugation for 10 min at 4°C. Protein concentration was quantified using a Bichinchoninic Acid protein assay and 150 mg of lysates per sample were incubated with Streptavidin agarose beads (Thermo Scientific, Rockford, IL, U.S.A.) and tumbled overnight at 4°C. Beads were washed three times with GLB. Proteins were eluted from the beads with Leammli sample buffer, separated by NuPAGE 4-12% Bis-Tris gel (Invitrogen, Carlsbad, CA, U.S.A.), transferred to a polyvinylidene difluoride membrane, blocked in 2% milk and 1% BSA, incubated with anti-GFP (Santa Cruz Biotechnology, Santa Cruz, CA, U.S.A.) and dog anti-mouse HRP secondary antibody (Jackson ImmunoResearch Europe Ltd., Suffolk, UK), and detected via chemiluminescence (Santa Cruz Biotechnology, Santa Cruz, CA, U.S.A.). Cells surface expression was calculated using ImageJ 1.45 software and normalized to the total amount of protein expression.

Native gel electrophoresis

Polyclonal cell lines were washed twice with ice-cold PBS. Cells were scraped and lysed in Native Page Lysis Buffer (75 mM NaCl, 50 mM Tris-HCl (pH 7.4), 1% (v/v) NP-40, 10% glycerol, 2 mM PMSF, 1 µg/ml aprotinin, 1 µg/ml leupeptin, 1X NativePAGE Sample Buffer (Invitrogen, Carlsbad, CA, U.S.A.), 0.5% digitonin) and incubated on ice for 10 minutes. Collected samples were clarified by centrifugation at 16,000 X g for 20 min at 4°C. 30 mg of lysates per sample was loaded onto a NativePAGE 3-12% Bis-Tris gel (Invitrogen, Carlsbad, CA, U.S.A.). Prior to electrophoresis, NativePAGE G-250 solution was added to a final concentration of 0.6%. Protein quantification and detection is described in section biotinlylation pull down assay.

Results

In a previous study we found that the frame-shift mutant P410fs12X, which lacks helices C and D for proper assembly of $K_v7.2$ α-subunits (Figure 1), was retained in subcellular compartments outside the ER [14]. Interestingly, immature potassium a-subunits lacking their assembly domain, are normally trafficking-defective and retained in the ER [13].

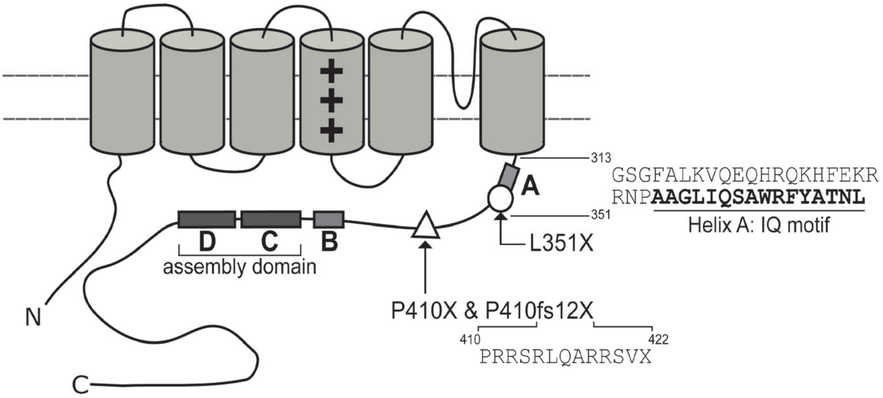
+
+
+
313
GSGFALKVQEQHRQKHFEKR
A
RNP**AAGLIQSAWRFYATNL**
351
Helix A: IQ motif
L351X
D
C
B
assembly domain
N
P410X & P410fs12X
410
422
PRRSRLQARRSVX
C

Figure 1.

Schematic representation of the Kv7.2 α-subunit. The position of L3511X, P410X and P410fs12X C terminal mutations are shown as well as the location of helices A and B and the coiled coil tetramerization domain that is comprised of helices C and D. The frame shift consensus sequences of P410fs12X (amino acids 410-421) together with the amino acid sequence starting from the beginning of the C-tail at 313 till position 351 are shown. Part of the consensus residues of helix A, including the IQ motif, are depicted in bold.

To further examine the subcellular localization of P410fs12X, we performed immunostaining of the Golgi apparatus in polyclonal cells expressing wildtype (WT) or P410fs12X proteins. The vast majority of WT $K_v7.2$ channels were located outside the Golgi, while the frame-shift mutant was retained in the Golgi apparatus (Figure 2).

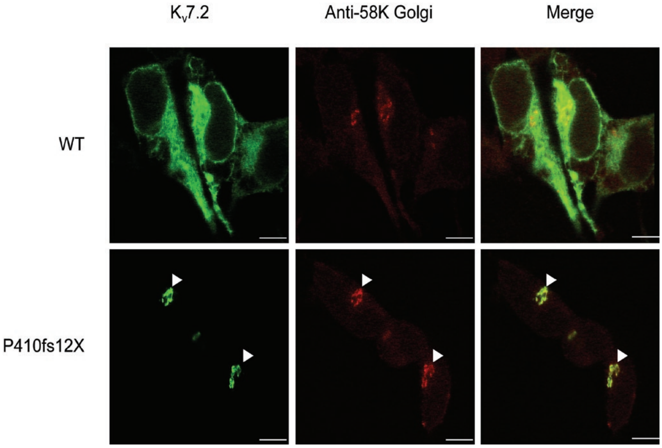

Figure 2.

P410fs12X mutants are retained in the Golgi apparatus. Confocal images of GFP tagged WT and P410fs12X proteins. The Golgi apparatus was labeled by mouse anti-p58 antibody (Sigma Aldrich St. Louis, MO, U.S.A.; red signal). The majority of Kv7.2 WT channels was expressed outside the Golgi, while P410fs12X (green) was trapped in the Golgi (red) as shown by the merge (yellow); see arrowheads. Scale bar: 20 µm.

The frame-shift sequence of P410fs12X may influence the folding of the C-terminus of K_v7.2, thereby masking unknown signals such as Golgi export signals or PKC phosphorylation sites that are necessary to transport proteins from the Golgi to the plasma membrane [15]. Nevertheless, this finding could indicate that apart from the known coiled-coil tetramerization helices C and D an alternative assembly domain within K_v7.2 a-subunit may exist. To investigate this hypothesis and to overcome the potential influence of the frame-shift tail of P410fs12X, we generated a P410X C-terminally nonsense truncated mutant that lacks helices B, C and D (Figure 1). To examine whether K_v7.2 WT and P410X truncated monomeric proteins were expressed at the cell surface, we stained cell membranes of polyclonal stably transfected cells expressing WT K_v7.2 and P410X with anti-Flotillin-1. Although, the vast majority of WT and P410X proteins showed accumulation inside the cell, still a substantial proportion of proteins were expressed at the cell surface (Figure 3A). To determine whether this cell surface trafficking feature of P410X is present in other nonsense mutants that lack helices B, C and D, we generated the L351X mutant that consist of a membrane proximal region of only ~40 amino acids (Figure 1). Immunofluorescent experiments with HEK293 cells stably expressing L351X showed plasma membrane expression of the deletion mutant (Figure 3A) indicating that helices C and D are not necessary for K_v7.2 expression at the cell surface.

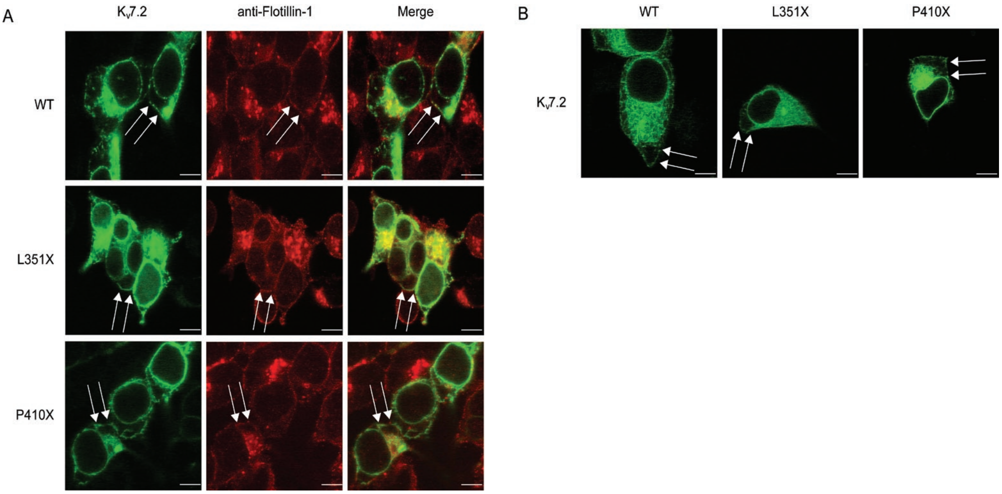

Figure 3.

P410X and L351X are expressed at the cell surface. A) Confocal images of GFP tagged WT, P410X and L351X proteins. The cell surface was labeled by the plasma-membrane marker anti-Flotillin 1 (red signal). Cell surface expression for both WT and truncation mutants is indicated with white arrows. B) WT and truncation mutants were transiently expressed in HeLa cells. Cell surface expression of the channels is indicated with white arrows. Scale bar A) and B): 20 µm

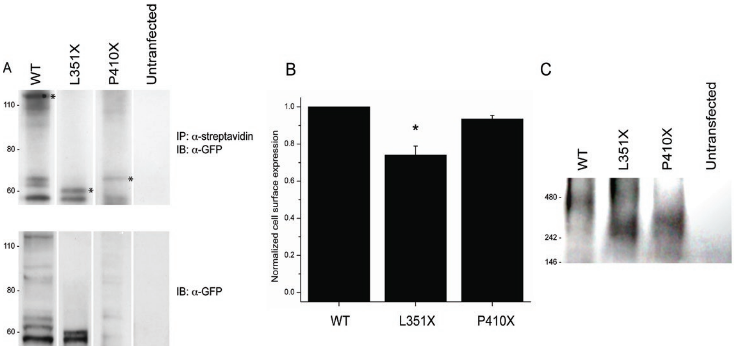

Figure 4.

*Kv7.2 WT and mutants form tetramers and are incorporated into the surface plasmamembrane. A) Upper panel: biotinylation pull down assay of HEK293 cells stably expressing WT, P410X and L351X clearly shows that these ion channel proteins are incorporated into the cell surface membrane. Lower panel: western blot probed with anti GFP antibody showing WT, P410X and L351X protein levels and some aspecific binding. Sample shown are composite from the same blot from different lanes. * indicate the WT or deletion mutant proteins (WT $K_v7.2$ ~124 kDa; L351X ~66 kDa; P410X ~73 kDa) . The Novex Sharp Prestained Protein Standard (Invitrogen, Carlsbad, CA, U.S.A.) was used as a molecular weight marker. B) Normalized cell surface expression of WT and truncation mutants. Cell surface expression was normalized to the total protein expression (n = 3; * indicates P<0.05, unpaired Student's t test). C) Native blot of WT, L351X and P410X showing tetrameric Kv7.2 proteins at the correct molecular weight (WT $K_v7.2$ ~496 kDa; L351X ~264 kDa; P410X ~292 kDa). The NativeMark Unstained Protein Standard (Invitrogen, Carlsbad, CA, U.S.A.) was used as a molecular weight marker.*

To determine whether the cell surface expression was not due to an in-vitro background artifact of the HEK293 cell line, we transiently overexpressed WT, P410X, and L351X in HeLa cells. WT as well as the two truncated mutants showed a similar expression pattern comparable to our previous finding in HEK293 cells (Figure 3B arrows). Next, we tested whether these deletion mutants were incorporated in the plasma membrane by performing a biotinylation pull-down assay. WT and P410X channels showed similar normalized cell surface expression. The L351X exhibited a significant decrease in cell surface expression, though this deletion mutant is still robustly expressed at the plasma membrane (Figure 4A and 4B). Furthermore, we performed a native blot experiment to confirm that the C-terminally truncated mutants could tetramerize to form monomeric α-subunits (Figure 4C). These results indicate that K_v7.2 mutants that lack the coiled-coil structures C and D can still form monomeric potassium ion channels that are expressed at the cell surface. Moreover, our data suggests the presence of an alternative assembly domain within Kv7.2 α-subunits.

Discussion

The C-terminus of K_v7 a-subunits is highly conserved among KCNQ family members and harbors several helical domains (helices A-D) for proper channel functioning (Figure 1), including tetramerization and trafficking to the cell surface. It has been reported that K_v7 channels bearing helices B, C and D deletions, including those that are a consequence of certain disease mutations, fail to assemble into functional channels that are trafficking-defective [3,16,17]. Our successful expression of helix C and D deleted $K_v7.2$ mutants P410X and L351X contradict with previous findings [4] that these domains are strictly required for tetramerization and trafficking. The discrepancies between our study and previous ones could for instance be caused by differences in mutants that were used. More specifically, in our study almost the entire C-terminus is missing, while previous studies that substantiated the role of helix C and D in α-subunit tetramerization, focused mainly on potassium currents carried by K_v7 C-termini chimeras [4,5,10]. Indeed, mutations that delete or disrupt helix C, suppressed cell surface expression and potassium currents of $K_v7.2$ and $K_v7.3$ channels [10], but still permitted tetramerization of isolated assembly domain (helices C and D) protein fragments harboring a missense mutation in helix C [18]. Conversely, deletion or disruption of the coiled-coil structure of helix D allows for tetramerization or dimerization, respectively [18,19]. Surprisingly, the a-subunits with a disrupted helix D formed channels that produce currents similar to WT $K_v7.2$ [10]. In addition, co-expression of $K_v7.3$ and $K_v7.2$ mutants that lack the entire assembly domain resulted in a suppressed M-current [16,20,21]. This suggests that these mutants can interact with the WT K_v7 α-subunits in the absence of an assembly domain by using additional unidentified binding regions other than the coiled-coiled structures helices C and D. Also, the use of different in-vitro assays could contribute to the observed differences between various studies as a trafficking defective $K_v7.2$ mutant expressed in Xenopus oocytes showed cell surface expression in Chinese Hamster Ovary cells albeit the expression was reduced compared to WT proteins [22]. This indicates that oocytes could lack particular chaperone proteins that play an important role in the trafficking process of ion channels. In addition, the uniformly distributed CD4 receptor, fused with either helices A and B (amino acids 323-500) or helices C and D (amino acids 501-579) of the $K_v7.2$ C-terminus, resulted in preferentially targeting the fusion proteins to the axonal plasma membrane of primary hippocampal rat neurons [6]. Furthermore, two truncated $K_v7.2$ proteins, Q323X (lacks helices B, C, and D) and Y534X (lacks helix D) mutants, impaired $K_v7.3$ axonal and somatodendritic surface expression, suggesting that the coiled coil structure of helix D is necessary for the formation and polarization of heteromeric K_v7 channels.

In conclusion, neither mutated Kv7.2 channels with a deletion or disruption of the assembly domain [10,19] nor the two D-helices B/C/D mutants in our study yielded potassium currents (data not shown), but did tetramerize and were expressed at the plasma membrane. This data in combination with previous findings suggest that the coiled-coil structures are apparently less important in channel tetramerization, but are important for channel function. Moreover, our results indicate that there is an alternative assembly domain in $K_v7.2$ present for the formation of monomeric K_v7 ion channels.

REFERENCES

1. Soldovieri, M.V., Miceli, F., and Taglialatela, M. (2011). Driving with no brakes: molecular pathophysiology of Kv7 potassium channels. Physiology 26, 365-376.
2. Brown, D.A., and Passmore, G.M. (2009). Neuronal KCNQ (Kv) channels. Br. J. Pharmacol. 156, 1185-1195.
3. Schwake, M., Pusch, M., Kharkovets, T., and Jentsch, T.J. (2000). Surface expression and single channel properties of KCNQ2/KCNQ3, M-type K+ channels involved in epilepsy. J. Biol. Chem. 275, 13343-13348.
4. Maljevic, S., Lerche, C., Seebohm, G., Alekov, A.K., Busch, A.E., and Lerche, H. (2003). C-terminal interaction of KCNQ2 and KCNQ3 K+ channels. J. Physiol. 548, 353-360.
5. Schwake, M., Jentsch, T.J., and Friedrich, T. (2003). A carboxy-terminal domain determines the subunit specificity of KCNQ K+ channel assembly. EMBO Rep., 4 (2003), pp. 76-81.
6. Chung, H.J., Jan, Y.N., and Jan, L.Y. (2006) Polarized axonal surface expression of neuronal KCNQ channels is mediated by multiple signals in the KCNQ2 and KCNQ3 C-terminal domains. Proc. Natl. Acad. Sci. U S A. 103, 8870-8875.
7. Howard, R.J., Clark, K.A., Holton, J.M., and Minor D.L. Jr. (2007). Structural insight into KCNQ2 (Kv7) channel assembly and channelopathy. Neuron, 53, 663-675.
8. Etxeberria, A., Aivar, P., Rodiquez-Alfaro, J.A., Alaimo, A., Villacé, P., Gómez-Posada, J.C., Areso, P., and Villarroel, A. (2008). Calmodulin regulates the trafficking of KCNQ2 potassium channels. FASEB J. 22, 1135-1143.
9. Yus-Nájera, E., Santana-Castro I., and Villaroel, A. (2007). The identification and characterization of a noncontinuous Calmodulin-binding site in noninactivating voltage-dependent KCNQ Potassium channels. J. Biol. Chem. 277, 28545-28553.
10. Schwake, M., Athanasiadu, D., Beimgraben, C., Blanz, J., Beck, C., Jentsch, T.J., Saftig, P., and Friedrich, T. (2006). Structural determinants of M-type KCNQ (K_v7) K+ channel assembly. J. Neurosc. 26, 3757-3766.
11. Steele, D.F., Eldstrom, J., and Fedida, D. (2007). Mechanisms of cardiac potassium channel trafficking. J. Physiol. 582, 17-26.
12. Alaimo, A., Gómez-Posada, J.C., Aivar, P., Etxeberría, A., Rodriguez-Alfaro, J.A., Areso, P., and Villarroel, A. (2009). Calmodulin activation limits the rate of KCNQ2 K+ channel exit from the endoplasmic reticulum. J. Biol. Chem. 284, 20668-20675.
13. Jensen, C.S., Rasmussen, H.B., and Misonou, H. (2011). Neuronal trafficking of voltage-gated potassium channels. Mol. Cell. Neurosci. 48, 288-297.
14. Volkers, L., Rook, M.B., Das, J.H.G., Verbeek, N.E., Groenewegen, W.A., van Kempen, M.J.A., Lindhout, D., and Koeleman, B.P.C. (2009). Functional analysis of novel KCNQ2 mutations found in patients with Benign Familial Neonatal Convulsions. Neurosc. Lett. 462, 24-29.
15. Sallese, M., Pulvirenti, T., Luini, A. (2006). the physiology of membrane transport and endomembrane-based signaling. EMBO J. 25:2663-2673.
16. Schmitt, N., Schwarz, M., Peretz, A., Abitbol, A., Attali, B., Pongs, O., (2000). A recessive C-terminal Jervell and Lange-Nielsen mutation of the KCNQ1 channel impairs subunit assembly. EMBO J. 19, 332-340.
17. Biervert, C., Schroeder, B.C., Kubisch, C., Berkovic, S.F., Propping, P., Jentsch, T.J., Steinlein, O.K. (1998). A potassium channel mutation in neonatal human epilepsy. Science 279, 403-406.
18. Wehling, C., Beimgraben, C., Gelhaus, C., Friedrich, T., Saftig, P., Grotzinger, J., and Schwake, T. (2007). Self-assembly of the isolated KCNQ2 subunit interaction domain. FEBS lett. 581, 1594-1598.
19. Kanki, H., Kupershmidt, S., Yang, T., Wells, S., and Roden, D.M. (2004). A structural requirement for processing the cardiac K+ channel KCNQ1. J. Biol. Chem. 279, 33976-33983.
20. Smith, J.S., Iannotti, C.A., Dargis, P., Christian, E.P., and Aiyar, J. (2001). Differential expression of KCNQ2 splice variant: Implications to M current function during neuronal development. J. Neurosc. 21, 1096-1103.
21. Ghosh, A., Nunziato, D.A., and Pitt, G.S. (2006). KCNQ1 assembly and function is blocked by Long-QT syndrome mutations that disrupt interaction with Calmodulin. Circ. Res. 98, 1048-1054.
22. Maljevic, S., Naros, G., Yalçin, Ö., Blazevic, D., Loeffler, H., Çağlayan, H., Steinlein, O.K., Lerche, H. (2011). Temperature and pharmacological rescue of a folding-defective, dominant-negative K_v7.2 mutation associated with neonatal seizures. Hum. Mutat. 32, E2283-2297.

4

Na_v1.1 Dysfunction in Genetic Epilepsy with Febrile Seizures Plus or Dravet Syndrome

Linda Volkers, Kristopher M. Kahlig*, Nienke E. Verbeek* Joost H.G. Das,
Marjan J.A. van Kempen, Hans Stroink, Paul Augustijn,
Onno van Nieuwenhuizen, Dick Lindhout, Alfred L. George Jr.,
Bobby P.C. Koeleman§, Martin B. Rook§

*,§ these authors contributed equally

Eur J Neurosci. 2011; 34:1268-1275

Abstract

Relatively few SCN1A mutations associated with genetic epilepsy with febrile seizures plus (GEFS+) and Dravet syndrome (DS) have been functionally characterized. In contrast to GEFS+, many mutations detected in DS patients are predicted to have complete loss-of-function. However, functional consequences are not immediately apparent for DS missense mutations. Therefore, we performed biophysical analysis of three SCN1A missense mutations (R865G, R946C, and R946H) we detected in six patients with DS. Furthermore, we compared the functionality of the R865G DS mutation with that of a R859H mutation detected in a GEFS+ patient; both mutations reside in the same voltage sensor domain of $Na_v1.1$. The four mutations were co-expressed with β1 and β2-subunits in tsA201 cells and characterized using the whole-cell patch clamp technique.

The two DS mutations, R946C and R946H, were non-functional. However, the novel voltage sensor mutants R859H (GEFS+) and R865G (DS) produced sodium current densities comparable to wild-type channels. Both mutants had negative shifts in the voltage dependence of activation, slower recovery from inactivation, and increased persistent current. Only the GEFS+ mutant exhibited a loss-of-function in voltage dependent channel availability.

Our results suggest that the R859H mutation causes GEFS+ by a mixture of biophysical defects in $Na_v1.1$ gating. Interestingly, while loss of $Na_v1.1$ function is common in DS, the R865G mutation may cause DS by overall gain-of-function defects.

Introduction

Genetic Epilepsy with Febrile Seizures (GEFS+) is a benign form of epilepsy in which patients have frequent febrile seizures early in childhood and later might develop epilepsy with afebrile seizures. Dravet syndrome (DS) or severe myoclonic epilepsy of infancy (SMEI) (Singh et al., 2001) is an intractable epilepsy syndrome, characterized by an onset of fever induced generalized tonic-clonic or hemiclonic seizures within the first year of life, followed by other seizure types, slowing of development and mental disability in the majority of subjects. Absence of some of these features has also been described in what some call borderline SMEI (Fukuma et al., 2004). Voltage gated sodium channels are glycosylated complexes that are usually associated with one or two auxiliary β-subunits. Mutations in SCN1A (encoding the α-subunit $Na_V1.1$) and SCN1B (encoding the b1 subunit) have been linked to both GEFS+ and DS (Escayg et al., 2000, Wallace et al., 1998, Claes et al., 2001, Patino et al., 2009), with the majority of mutations found in SCN1A (Lossin, 2009). The majority of GEFS+ cases arise from missense mutations, which are distributed throughout the coding region. Functional analysis of some SCN1A missense mutations found in GEFS+ subjects exhibit a variety of biophysical defects that have been generalized as causing either gain-of-function or loss-of-function gating defects (Spampanato et al., 2001, Lossin et al., 2002, Lossin et al., 2003, Spampanato et al., 2003, Spampanato et al., 2004, Barela et al., 2006).

In DS, approximately half of the mutations are nonsense or frameshift alleles resulting in premature translation termination in SCN1A, which suggests that DS results from a complete loss-of-function of the mutant allele (Lossin, 2009). This hypothesis is supported by evidence from Scn1a knockout mice (Yu et al., 2006, Ogiwara et al., 2007) and SCN1A-gene deletions in DS patients (Suls et al., 2006). However, approximately one third of the reported DS mutations are missense alleles. Functional studies demonstrated that a high proportion of missense mutations lead to non-functional sodium channels (Ohmori et al., 2006). Nevertheless, a few studies have shown that some missense mutations produce functional channels and can either exhibit gain-of-function properties such as increased persistent current or loss-of-function effects such as decreased channel availability (Rhodes et al., 2004, Ohmori et al., 2006). The aim of this study was to investigate the electrophysiological properties of one GEFS+ and three DS associated missense mutations.

Material and methods

Molecular SCN1A analysis

Genomic DNA was isolated from blood lymphocytes according to standard DNA isolation procedures. Genomic DNA was amplified by PCR and subsequently the entire coding region, including flanking regions of the exons, was analyzed by sequence analysis using automated sequence facilities (ABI3730, Applied Biosystems, Foster City, CA, USA). Sequence traces were analyzed using Mutation Surveyor software (SoftGenetics, LLC State College, PA, USA) using AB093548.1 as a reference.

Constructs

The SCN1A plasmid, which encodes the human neonatal Na$_v$1.1 ion channel, was previously described (Lossin et al., 2002). Mutations R859H or R865G were introduced by QuikChange site-directed mutagenesis (Stratagene, Cedar Creek, TX, U.S.A.) according to the manufacturer's protocol using the following primer pairs: sense 5' GGAAGGATTATCTGTTCTCCATTCATTTCGATTGCTGCGAG 3' and anti-sense 5' CTCGCAGCAATCGAAATGAATGGAGAACAGATAATCCTTCC 3' (exchange c.G2576A to obtain p.R859H), sense 5' GTTCATTTCGATTGCTGGGAGTTTTCAAGTTGGC 3' and anti-sense 5' GCCAACTTGAAAACTCCCAGCAATCGAAATGAAC 3' (exchange c.C2593G to obtain p.R865G), sense 5' CTTCCTGATTGTGTTCTGCGTGCTGTGTGGGG 3' and anti-sense 5' CCCCACACAGCACGCAGAACACAATCAGGAAG 3' (exchange c.C2836T to obtain p.R946C) and sense 5' CTTCCTGATTGTGTTCCACGTGCTGTGTGGGGAG 3' and anti-sense 5' CTCCCCACACAGCACGTGGAACACAATCAGGAAG 3' (exchange c.G2837A to obtain p.R946H). All constructs were verified by sequencing

Cell culture and transfections

Human derived tsA201 cells were cultured in Dulbecco's Modified Eagle Medium supplemented with 10% FBS, penicillin 100 U/ml, streptomycin 100 μg/ml and 0,05% L-glutamine in a humidified incubator at 37ºC with 5% CO_2. Culture media and supplements were obtained from Biowhittaker, Vervier, Belgium. Transient transfections were performed with Lipofectamine (Invitrogen, Carlsbad, CA, U.S.A.) using in total 6 µg of Na_v1.1, b1 and b2 pDNAs in a ratio of 10:1:1, as previously described by Lossin et al., 2002. Cells were incubated with CD8 positive beads (Invitrogen, Oslo, Norway) to identify β1 expressing cells, cells expressing β2 were identified with epifluorescence. Cells that expressed both β-subunits were used for electrophysiological recording experiments. All experiments were performed 48 to 72 hours after transfection. For electrophysiological measurements at least two different clones of either WT or mutant constructs were evaluated.

Electrophysiology

Prior to patching, cells were incubated for at least 1 hour in cell culture medium containing 140 mM NMDG, 4 mM KCl, 1 mM $CaCl_2$, 1 mM $MgCl_2$, 14.3 mM Na_2HCO_3, 15.1 mM HEPES, 17.5 mM Glucose, 1X Amino Acids (Gibco, Paisley, UK), 1x Non Essential Amino Acids (NEAA) (Gibco, Paisley, UK) (pH 7.35) supplemented with 10% FCS (Biowhittaker, Vervier, Belgium), penicillin 100 U/ml (Biowhittaker, Vervier, Belgium), streptomycin 100 U/ml (Biowhittaker, Vervier, Belgium) and 2 mM L-glutamine (Biowhittaker, Vervier, Belgium) in a humidified atmosphere at 37 ºC, 5% CO_2. For patch experiments, cells were bathed in modified Tyrode's solution containing 140 mM NaCl, 5.4 mM KCl, 1.8 mM $CaCl_2$, 1mM $MgCl_2$, 6 mM Glucose, 6 mM HEPES (pH adjusted to 7.4 with NaOH). Sodium currents were measured at room temperature (20-22ºC) using the whole-cell voltage clamp configuration with an Axopatch 200B amplifier (Axon Instruments, Union City, CA, U.S.A.). Patch electrodes were pulled from borosilicate glass capillaries and fire polished. Pipettes were fabricated with a micro-pipet puller (Sutter Instruments, Novato, CA, U.S.A.) and had a resistance of 1.5-2.2 MΩ when filled with the following intracellular solution: 10 mM NaF, 110mM CsF, 20 mM CsCl 2mM EGTA, 10 mM HEPES (pH 7.35). Cells were allowed to stabilize for 10 minutes after the whole cell configuration was established. Cells that had a sodium current of <-600pA were excluded from analyses to avoid contamination by endogenous currents. Cells expressing sodium current >-6000pA where excluded from analyses to avoid recordings with poor voltage control. Cell capacitance and pipette series resistance were compensated for 90%. Leak currents were subtracted using a P/4 procedure. Currents were acquired with a low-pass filter of 10 kHz and digitized at 100 kHz. For analysis, the recorded currents were low-pass filtered at 5 kHz. The voltage clamp protocols were generated using pCLAMP9.2 (Axon Instruments, Union

City, CA, U.S.A.). Steady state of activation and channel availability where determined by fitting the data with a single Boltzmann $y = I_{max} / (1+\exp((1/k)*(V-V½)))$, where V is the variable conditioning potential, V½ the voltage of half maximal activation, k the slope, and I_{max} the normalized maximal amplitude of the Boltzmann current. The recovery from inactivation was analyzed by fitting the data with a double exponential function $I/I_{max} = A_{fast} * (1-\exp(-t/\tau_{fast})) + A_{slow} * (1-\exp(-t/\tau_{slow})) + C$, where τ_{fast} and τ_{slow} denote a fast and a slow time constant, A_{fast} and A_{slow} represent the two fractional amplitudes and C the level of non-inactivating sodium current. Speed of inactivation was evaluated by fitting the decay phase of the sodium current with a double exponential function $I/I_{max} = A_{fast} * \exp(-t/\tau_{fast}) + A_{slow} * \exp(-t/\tau_{slow}) + C$, where the parameters are defined as above. Persistent sodium current was measured in the final 10 ms of a 100 ms depolarizing pulse to -20mV, -10 mV and 0 mV and determined by subtracting background current measured in the presence of 10 mM tetrodotoxin (Alomone, Jerusalem, Israel) from tetrodotoxin-free records. Data analysis was performed using Excel 2008 (Microsoft, Seattle, WA, U.S.A.) and Origin Pro 8.0 (Microcal, Northhampton MA, U.S.A.), and Kaleidagraph 4.0 (Synergy Software, Reading, PA, USA) software. Values are expressed as means ± SEM. Statistical comparison was done using an unpaired Student's t-test, a $P<0.05$ value was considered significant.

Results

Clinical Phenotypes

The novel R859H mutation was detected in a girl diagnosed with GEFS+ and a paternal history of (a) febrile seizures (Table 1). Her febrile convulsions, generalized tonic-clonic seizures (GTCS), started at the age of 13 months after a Diphtheria/Tetanus/whole cell Pertussis/inactivated poliovirus (DTwcP-IPV) and Haemophilus influenzae type b (Hib) vaccination and were recurrent and often prolonged. After the age of 3.5 years she also experienced afebrile GTCS and an isolated complex partial seizure (CPS). Electroencephalography (EEG) demonstrated bilateral occipital-temporal spike-wave complexes and a few predominantly left-sided isolated occipital spike-waves. The patient responded well to valproate (VPA). Her last seizure was reported at age 5.5 years and EEG analysis at the age of 6 years did not show epileptiform activity. She had normal development except for some features of attention deficit hyperactivity disorder (ADHD). Her father experienced approximately ten febrile seizures between age 1 and 6 years. In the next 9 years, he experienced approximately five afebrile seizures. He received VPA from age 11 years until he was 17 years old. The family history of first-degree relatives was negative for febrile or afebrile seizures.

The novel R865G mutation was detected in a boy who had right-sided hemiconvulsions with postictal hemiparesis since the age of 9 months (Table 1). He also experienced myoclonic jerks and CPS. His EEGs showed a near normal background pattern with isolated sharps and sharp waves in both hemispheres. He was diagnosed with DS. Magnetic resonance brain imaging was normal. At the age of 60 months, he was deemed to have a severe developmental delay with a developmental age of 29 months. After addition of levetiracetam (LEV) to VPA and lamotrigine (LTG) at the age of 6.5 years he is seizure free till to date. His family history was negative for febrile convulsions and epilepsy. His parents are consanguineous. DNA analysis of the parents was not available.

The R946C mutation was previously found in subjects with DS, but not functionally characterized. We also detected this mutation in a girl diagnosed with DS. She experienced her first seizure at age 10 months, after a vaccination against DTwcP-IPV and Hib. The majority of her seizures were fever provoked GTCS. VPA monotherapy controlled her seizure frequency to twice a year. She showed ataxia and a moderate developmental delay. Her IQ was 60 at the age of 5.5 years (Table 1).

The R946H mutation was previously described in five patients with DS and one subject with partial epilepsy with antecedent febrile seizures (Fukuma et al., 2004, Berkovic et al., 2006, Harkin et al., 2007, Depienne et al., 2009, Liao et al., 2010). Functional analysis of this mutation showed complete loss-of-function of the mutant allele (Liao et al., 2010). We also detected the R946H mutation in three unrelated subjects diagnosed with DS (Table 1).

The first case is an adult male who had GTCS, initially provoked by DTwcP-IPV vaccination followed by fever, in his first year of life. Subsequently, he developed myoclonias and complex partial seizures. He experienced monthly seizures while receiving a combination of VPA and topiramate (TPM), and exhibited a moderate developmental delay.

The second case is a boy who had his first seizure after a DTwcP-IPV and Hib vaccination at age 4 months (Table 1). Initially the clonic component of the seizures (focal/hemiconvulsions) did not involve all limbs. Later on he developed GTCS, often occurring in clusters and provoked by fever. At age 1.5 years a developmental delay became evident. His interictal EEG was normal until age 3 years rapidly followed by diffusely disturbed EEGs later in life. After replacement of the combination of VPA and LTG by VPA and TPM, seizure frequency was reduced.

The third patient is a girl who experienced her first GTCS at age 10 months, and subsequently developed myoclonias, atypical absences and myoclonic-astatic seizures previously described by Verbeek et al., 2011. Her EEG at the age of 3 years showed multifocal (poly)spike-wave complexes. VPA, LEV and clonazepam (CLZ) administration reduced seizures to two per month. She also showed developmental delay, with a developmental age of 18 months at the age of 2.5 years (Table 1). Her deceased father had been diagnosed with DS with a milder phenotype (Verbeek et al., 2011). Unfortunately, DNA of the father and the paternal grandparents was not available for analysis.

Table 1. Clinical features of patients with a SCN1A mutation.

SCN1A mutation	Gender	Age study	Seizure onset	Seizure types	AEDs	Response to AED	Development	Ataxia	Epilepsy classification	Inheritance
R859H	F	8.5 yrs	13 months	GTCS, CPS	Currently no AEDs	Seizure free	Normal	No	GEFS+	Paternal
R859H	M	29 yrs	1 yrs	GTCS	Currently no AEDs	Seizure free	Normal	No	GEFS+	ND
R865G	M	9.5 yrs	9 months	H, Mc, CPS	VPA, LTG, LEV	Seizure free	Severely delayed	No	Dravet	ND
R946C	F	5.5 yrs	10 months	GTCS	VPA	Intractable	Moderately delayed	Yes	Dravet	de novo
R946H	M	24 yrs	<1 yrs	GTCS, Mc, CPS	VPA, TPM	Intractable	Delayed	Unknown	Dravet	ND
R946H	M	4.5 yrs	4 months	GTCS, H	VPA, TPM	Intractable	Delayed	Unknown	Dravet	ND
R946H	F	3 yrs	10 months	GTCS, Mc, A, MAs	VPA, LEV, CLZ	Intractable	Delayed	Unknown	Dravet	ND

A= Atypical absences; AED = Anti-epileptic drugs; CLZ=Clonazepam; GTCS= Generalized tonic-clonic seizures; H=Hemiconvulsions; LEV= Levetiracetam; LTG=Lamotrigine; MAs=Myoclonic-Astatic seizures; Mc=Myoclonias; ND= Not determined; TPM=Topiramate; VPA=Valproate

R946C and R946H channels are non-functional

The two missense mutations, R946C and R946H, are located in the Na_v1.1 domain II pore-loop (Figure 1A). When co-expressed with the β1 and β2-subunits, neither mutant channel produced measurable sodium currents. Our findings for R946H are in agreement with recent observations made by Liao et al. 2010. The observation that R946C also leads to a complete loss of ion channel function, suggests that R946 is a residue critical for Na_v1.1 function.

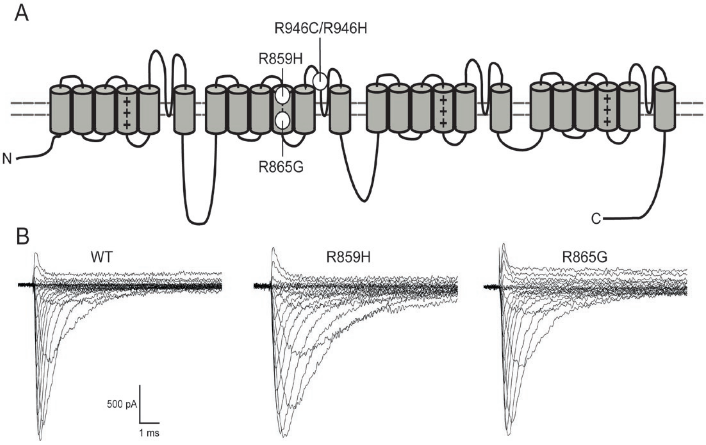

Figure 1.

Mutation location and representative WT and mutant Nav1.1 whole cell currents. A) Schematic representation of the Nav1.1 channel. The S4 voltage sensors are marked with plus signs (+). The locations of the mutations are as depicted. B) Assembled sodium currents elicited by increasingly depolarizing pulses. Representative sodium currents recorded from tsA201 cells expressing WT, R859H or R865G ion channels in combination with β1 and β2 subunits. Currents were activated by depolarizing voltage steps ranging from -80 mV to +90 mV in increments of 5 mV. Both mutants produced functional sodium currents, which were similar in amplitude as WT currents (Student's t test, WT n=13; R859H n=12, P=0.89; R865G n=10, P=0.97). See Methods and inset figure 2B for pulse protocol. Values presented are

Table 2. Biophysical parameters of Na_v1.1 WT and mutant ion channels

	Voltage dependence of activation				***Voltage dependence of inactivation***				***Recovery from fast inactivation***				
	V½ [mV]	***k***	***n***		***V½ [mV]***	***k***	***n***		***τ_{fast} [ms]***	***A_{fast} [%]***	***τ_{slow} [ms]***	***A_{slow} [%]***	***n***
Na_v1.1 WT	-23.1±1.1	7.3±0.3	13		-62.3±0.9	6.1±0.3	8		2.3±0.2	77±3	130±11	25±2	5
R859H	-27.1±0.6†	6.7±0.2	12		-68.1±0.7†	6.9±0.3	6		3.3±0.3*	76±1	191±25*	22±2	7
R865G	-31.2±1.1††	7.1±0.3	10		-60.1±0.9	5.9±0.1	10		2.9±0.3	71±5	207±12*	29±4	9

*Values presented are mean ± s.e.m.. Values significantly different from Na_v1.1 WT are indicated as follows *P<0.05; †P<0.001; ††P<0.0001*

R859H and R865G exhibit gating defects

The two novel SCN1A mutations located in the voltage sensing S4 segment of domain II, R859H and R865G, both produced functional sodium channels and were further examined (Figure 1B). Compared to wild-type (WT) channels, R859H and R865G exhibit similar peak current densities (R859H t_{23}=0.14, P=0.89; R865G t_{21}=0.03, P=0.97; Figure 2A). Voltage dependence of activation was altered for both mutant channels. Half maximal voltage (V½) for activation was shifted towards more hyperpolarized potentials (R859H -4 mV, n=12; R865G -8.1 mV, n=10; Table 2) compared to WT channels (R859H t_{23}=3.21, P=0.004; R865G t_{21}=5.27 P<0.0001; Figure 2B and Table 2), resulting in a gain-of-function for both mutants albeit more prominent for R865G. The V½ of inactivation was shifted towards more negative values for the R859H mutant channels (-5.8 mV, n=6), while the R865G mutant was comparable to WT channels (R859H t_{12}=4.94 P=0.0003; R865G t_{16}=-1.81 P=0.09; Figure 2C and Table 2). This loss-of-function gating defect for R859H suggests a reduction in channel availability at potentials more negative than -40 mV. To investigate the recovery from inactivation, we applied a 500 ms depolarizing pre-pulse to inactivate all ion channels, followed by a -120 mV step of increasing durations (1 ms to 3000 ms) to allow the channels to recover from inactivation and followed by a depolarizing test pulse. The fractional recovery from inactivation with time was calculated by dividing the maximum peak current elicited by the pre-pulse by the peak currents obtained at the various time points. The data was fit with a double exponential to obtain a fast (τ_{fast}) and a slow (τ_{slow}) recovery from inactivation constant. Both mutant channels exhibited a comparable slowing in the recovery from fast inactivation (Figure 2D) indicated by a larger time constant (τ_{slow}) of recovery (R859H t_{10}=-2.81 P=0.02; R865G t_{12}=-5.16 P=0.0002; Table 2).

Figure 3 illustrates the time to peak activation and the speed of inactivation for WT, R859H and R865G channels. We observed a significant delay in time to peak currents for R859H over the -30 mV to +5 mV voltage range, indicating a slowing in speed of activation of this mutant channel (Figure 3A). To quantify the speed of sodium channel inactivation for WT, R859H, and R865G channels, the decay in current traces during test pulses in the voltage range -30 mV to +30 mV were fitted with a double exponential to obtain fast and slow inactivation rate constants. The inactivation time constants were plotted against the test potentials (Figure 3B). Rate constants corresponding to the fast component of inactivation were significantly larger in the voltage range of -20 mV to +10 mV for R859H, but not for R865G (Figure 3B). The rate constant representing the slower component of inactivation for both mutations was significantly larger at many test potentials (Figure 3B). These findings suggest impaired fast inactivation for both mutants.

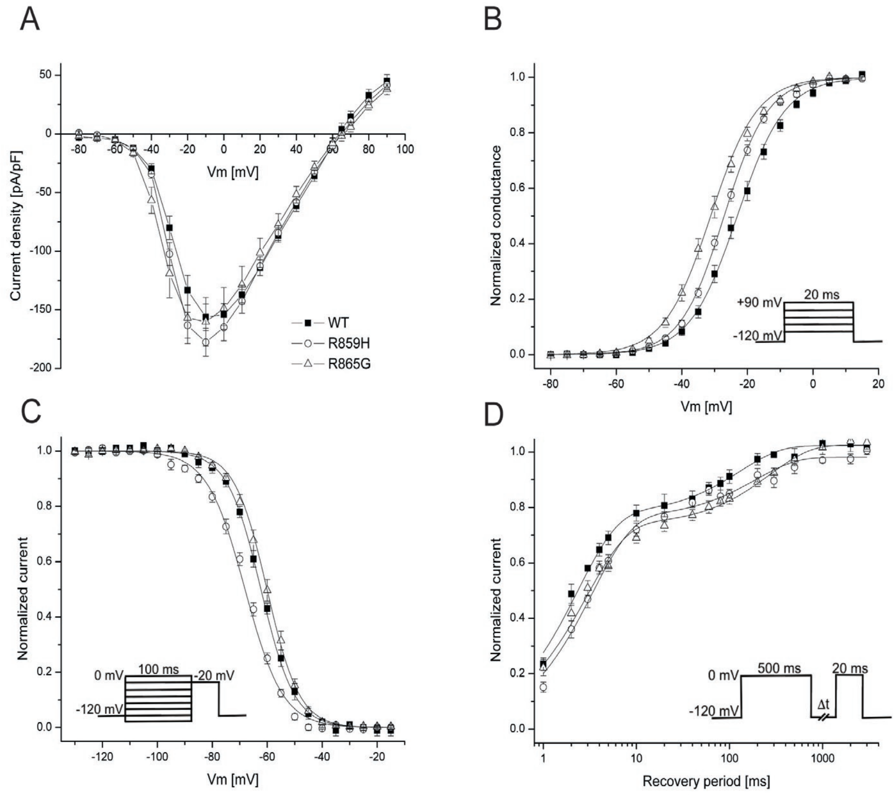

Figure 2.

SCN1A mutations alter gating of Nav1.1 channels. A) Current-voltage relationships for Nav1.1 WT, R859H and R865G. Whole cell currents were normalized to cell capacitance and plotted against the test potentials. WT and mutant channels produce comparable peak current densities. B) Voltage dependence of activation was determined by measuring peak currents during variable test pulses from a holding potential of 120 mV. The currents were divided by the electrochemical driving force and normalized to the maximum peak current to obtain the normalized sodium conductance. Both mutants exhibited a negative shift in the voltage dependence of activation, resulting in a gain of function of activation (Student's t-test, WT n=13; R859H n=12, P=0.004; R865G n=10, P<0.0001). C) Voltage dependence of inactivation (voltage dependence of channel availability) was measured using a two-step pulse protocol (inset) by applying inactivating pre-pulses from 140 mV to 10mV in 5 mV steps. Currents at the 20 mV test pulse were normalized to the peak current amplitude at the beginning of each pre pulse and plotted against the pre-pulse potential. The voltage dependence of inactivation of R859H channels showed a hyperpolarized shift, causing a loss of channel availability at potentials more negative than 40 mV (Student's t test, WT n=8; R859H n=6, P=0.0003). D) Recovery from fast inactivation was acquired by applying a 500 ms inactivating pre-pulse to the cell followed by a 120 mV step for variable time durations (1 ms to 3000 ms) to allow channel recovery then a 20 ms test pulse to 0 mV. Fractional recovery was calculated by dividing the maximum peak current of the pre-pulse by the maximum current amplitude of the corresponding conditioning pulse. The data were fit with a double exponential function. Both mutants showed a slower recovery from inactivation compared to WT (Student's t test, WT n=5; R859H, n=7, P=0.02; R865G, n=9, P=0.0002).

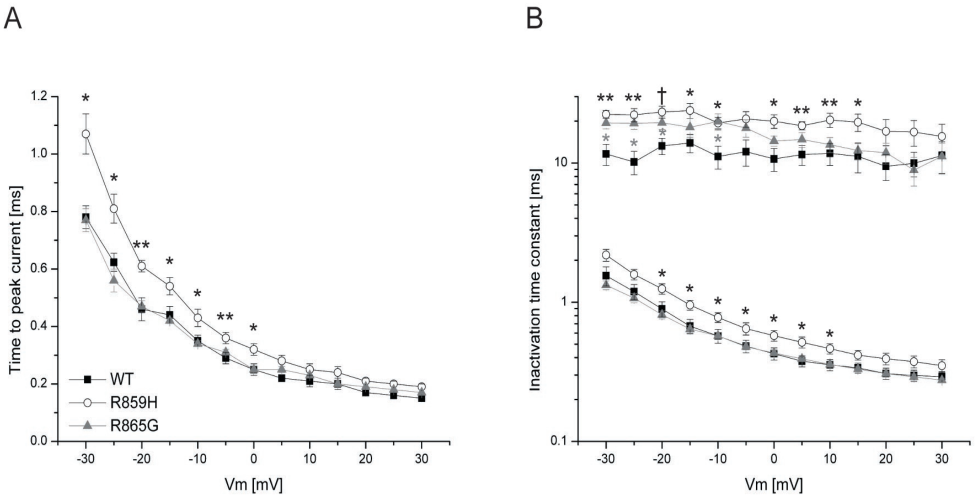

Figure 3.

*Mutant channels exhibit time dependent gating defects. A) Time to peak current was analyzed from 30 mV to +30 mV. R859H exhibits a significantly delayed activation time in the voltage range 30 mV to 5 mV compared to Nav1.1 WT (Student's t test, WT n=13; R859H n=12, *P<0.05). B) Inactivation rate constants (current decay after peak INa) were obtained by fitting the inactivating sodium current with a double exponential to obtain two rate constants; fast and slow component. R859H showed an overall slowing in the speed of inactivation, while the R865G only showed an increase in a slow inactivation rate constant (Student's t test, *P<0.05; **P<0.005; †P=0.00095; WT n=13; R859H n=12; R865G n=10).*

Abnormal elevated persistent current can be generated by incomplete sodium channel inactivation during membrane depolarization and may facilitate repetitive action potential firing in neurons (Stafstrom, 2007). Previously certain Na$_v$1.1 mutations associated with GEFS+ and DS were demonstrated to exhibit an increased persistent current (Lossin et al., 2002, Rhodes et al., 2004, Ohmori et al., 2006). To analyze persistent current for R859H and R865G channels, we recorded sodium currents by applying 100 ms depolarizing pulses (from -120 mV to -20 mV, -10 mV, and 0 mV) in the absence or presence of TTX and digitally subtracted the currents. Persistent current was determined at the final 10 ms of the 100 ms depolarizing pulse and normalized to peak sodium currents. Both mutants exhibited a significantly increased persistent current compared to Na$_v$1.1 WT channels (Figure 4); (-20 mV: R859H t_8=-2.51, P=0.04, n=5; R865G t_9=-5.29 P=0.0005, n=6; -10 mV: R859H t_8=-3.41 P=0.009, n=5; R865G t_9=-5.95 P=0.0002, n=6; 0 mV: R859H t_8=-2.27 P=0.02, n=5; R865G t_9=-5.66 P=0.0003, n=6).

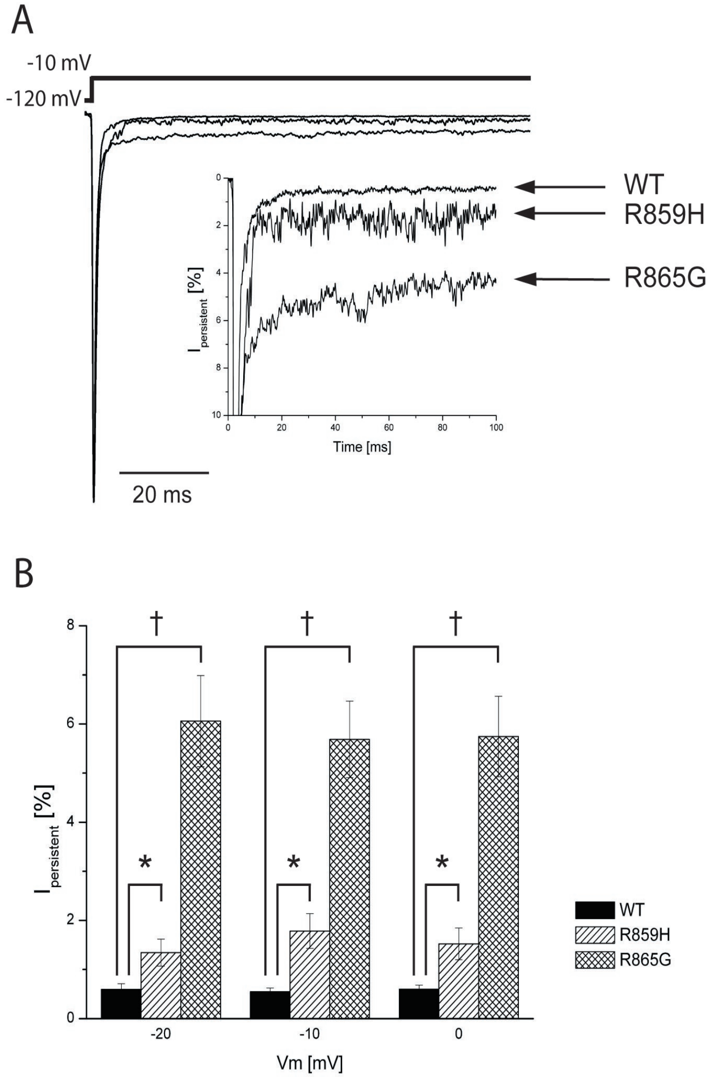

Figure 4. *Persistent current is increased in mutant channels. A) Typical sodium current elicited by a long 10 mV depolarizing pulse. Persistent current was determined by a 100 ms depolarizing pulse from 120 mV to voltages -20 mV, -10 mV and 0 mV. TTX sensitive current recordings were obtained by digital subtraction of sodium currents before and after TTX treatment. Persistent current was analyzed in the last 10 ms of the pulse and normalized to the peak sodium currents. Inset shows an expanded y axis scaled to highlight the increased persistent current of R859H and R865G channels compared to WT. B) The magnitude of persistent current as percentage of peak current amplitude plotted against the voltage steps. Both R859H and R865G mutants show a significant increase in persistent current at all test potentials, which suggest a destabilized inactivation gate that may lead to an increased hyperexcitability in neurons (Student's t- test, *P<0.05, †P<0.001; WT n=5; R859H n=5; R865G n=6)*

Discussion

SCN1A mutations are linked to a spectrum of epileptic phenotypes, ranging in severity from GEFS+ to DS. For GEFS+ only missense mutations have been reported leading to a wide array of biophysical gating defects. DS is often caused by mutations that are predicted to cause a truncated protein leading to a complete loss-of-function of the sodium ion channel. However, there are also several reports of missense mutations in patients with DS some of which have been shown to produce functional ion-channels in vitro (Rhodes et al., 2004, Ohmori et al., 2006).

We have studied four mutations in the SCN1A gene (R859H, R865G, R946C, R946H). Both R946C and R946H are associated with the Dravet phenotype and are mutations in the pore loop region of the SCN1A gene. A few pore-loop mutations (R393H, H939Q, R946H, C959R and T1709I) have been functionally characterized and all mutations produced non-functional channels (Rhodes et al., 2004, Ohmori et al., 2006, Liao et al., 2010). Our study also showed the pore-loop mutations (R946C and R946H) to be non-functional. Whether all pore-loop mutations are non-functional will require additional studies, but this finding is concordant with the general loss-of-function hypothesis of DS and supported by $Scn1a^{+/-}$ mice that show that a reduction in sodium current in GABAergic inhibitory interneurons is sufficient to cause DS (Catterall et al., 2010, Yu et al., 2006, Ogiwara et al., 2007).

Cells expressing the DIIS4 voltage sensor mutants R859H or R865G produced functional channels. We have shown that although both mutants produced sodium currents that were comparable to WT currents, we also found various gating defects. For the GEFS+ mutant R859H we found a reduction in voltage dependent steady state channel availability and a delayed recovery from fast inactivation. However, this mutant also displayed an increased persistent current and slower inactivation rate constant, which may predispose a neuron to increased sodium conductance upon membrane depolarization. These data indicate that the mutant causes GEFS+ (including CPS) by mixed biophysical gating defects. Notably, effects differ from a previously reported GEFS+ mutant R859C that showed smaller sodium peak currents, a depolarizing shift in the voltage dependence of activation, and a slower recovery from slow inactivation (Barela et al., 2006). These discrepancies in results may be explained by the difference in amino-acid substitution or differences in the experimental procedures such as the use of a Xenopus oocyte expression system instead of cultured human cells, expression of a mutated a-subunit in the absence of one of the b-subunits versus a mutated a-subunit expressed with both b1 and b2-subunits, and a species dependent modification of the rat versus human $Na_v1.1$ channel. The DS mutant R865G showed predominantly gain-of-function defects, including a hyperpolarized shift in the voltage dependence of activation and a large increase in persistent current. Interestingly, the hyperpolarizing shift in the voltage dependence of activation observed for the R865G mutant in combination with the unaltered voltage dependence of inactivation indicates an increase in window current (Figure 4). The increased persistent current in both mutant channels is caused by an incomplete inactivation of the mutant channel, which leads to a proportion of channels to either remain open or to reopen (Kahlig et al., 2006, Stafstrom, 2007). Previous studies of several SCN1A mutants associated with GEFS+ and DS (Lossin et al., 2002, Rhodes et al., 2004, Ohmori et al., 2006) showed increased persistent current which may be a contributing factor to the complex epileptic phenotypes. However, the gain-of-function defects in the DS mutant R865G do not support the general loss-of-function hypothesis of DS (Catterall et al., 2010), but the neuronal effects of these biophysical effects are not known.

It is not possible to extrapolate the gating defects of $Na_v1.1$ mutants to a neuronal network. In addition, the embryonic and postnatal development of the brain of subjects with SCN1A mutations in combination with the genetic background is difficult to determine. In this setting it seems feasible that any disturbance in excitation and inhibition in a neuronal network may lead to an epileptic outcome, including DS. There are reports of truncation mutations in SCN1A that lead to febrile seizures or GEFS+ instead of DS (Gennaro et al., 2003, Yu et al., 2010), indicating that the genetic background can play a role in the outcome of the disease. Such differences in severity of epileptic phenotypes have also been observed in $Scn1a^{+/-}$ mouse model strains (Yu et al., 2006).

In this study further circumstantial evidence is provided that non-functional channels as well as R865G mutant channels that show a variety of biophysical gating defects, can all cause DS. On the other hand, it can not be ruled out that mutant $Na_v1.1$ channels expressed in neurons behave differently than in our heterologous expression system, since tsA201 cells may lack key subunits of the ion channel macromolecular complexes. In neurons, defects in directing mutant $Na_v1.1$ proteins to the appropriate plasma membrane sites, e.g. soma or axon initial segment, might result in loss-of-function effects that can not be studied in tsA201 cells. Such distinct trafficking defects have been reported for sodium and potassium ion channel mutants (Mohler et al., 2004, Chung et al., 2006). In addition, fever-induced seizures are common in GEFS+ and DS subjects, and GEFS+ and DS mouse models showed increased seizure susceptibility at elevated body temperatures (Martin et al., 2010, Oakley et al., 2009). Future studies at physiological and febrile temperatures are warranted and could unmask important temperature-dependent gating effects.

References

Barela AJ, Waddy SP, Lickfett JG, Hunter J, Anido A, Helmers SL, Goldin AL, Escayg A (2006) An epilepsy mutation in the sodium channel SCN1A that decreases channel excitability. J Neurosci. 26:2714-2723

Berkovic SF, Harkin L, McMahon JM, Pelekanos JT, Zuberi SM, Wirrel EC, Gill DS, Iona X, Mulley JC, Scheffer IE (2006) De-novo mutations of the sodium channel gene SCN1A in alleged vaccine encephalopathy: a retrospective study. Lancet Neurol. 5:488-492

Catterall WA, Kalume F, Oakley JC (2010) $Na_v1.1$ channels and epilepsy. J. Physiol. 588:1849-1859

Chung HJ, Jan YN, Jan LY (2006) Polarized axonal surface expression of neuronal KCNQ channels is mediated by multiple signals in the KCNQ2 and KCNQ3 C-terminal domains. Proc Natl Acad Sci U S A. 103:8870-8875

Claes L, Del-Favore J, Ceulemans B, Lagae L, Van Broeckhoven C, De Jonghe P (2001) De novo mutations in the sodium-channel gene SCN1A cause severe myoclonic epilepsy of infancy. Am J Hum Genet. 68:1327-1332

Depienne C, Trouillard O, Saint-Martin C, Gourfinkel-An I, Bouteiller D, Carpentier W, Keren B, Albert B, Gautier A, Baulac S, Arzimanoglou A, Cazeneuve W, Nabbout R, LeGeurn E (2009) Spectrum of SCN1A gene mutations associated with DS: analysis of 333 patients. J Med Genet. 46:183-191

Escayg A, MacDonald BT, Meisler MH, Baulac S, Huberfeld G, An-Gourfinkel I, Brice A, LeGuern E, Moulard B, Chaigne D, Buresi C Malafosse A (2000) Mutation in SCN1A, encoding a neuronal sodium channel, in two families with GEFS+2. Nature 24:343-345

Fukuma G, Oguni H, Shirasaka Y, Watanabe K, Miyajima T, Yasumoto S, Ohfu M, Inoue T, Watanachai A, Kira R, Matsuo M, Muranaka H, Sofue F, Zhang B, Kaneko S, Mitsudome A, Hirose S (2004) Mutations of neuronal voltage-gated Na+ channel alpha 1 subunit gene SCN1A in core severe myoclonic epilepsy in infancy (SMEI) and in borderline SMEI (SMEB) Epilepsia 45:140-148

Gennaro E, Veggiotti P, Malacarne M, Madia F, Cecconi M, Cardinali S, Cassetti A, Cecconi I, Bertini E, Bianchi A, Gobbi G, Zara F (2003) Familial severe myoclonic epilepsy of infancy: truncation of Nav1.1 and genetic heterogeneity. Epileptic Disord. 5:21-25

Harkin LA, McMahon JM, Iona X, Dibbens L, Pelekanos JT, Zuberi SM, Sadleir LG, Andermann E, Gill D, Farrell K, Connolly M, Stanley T, Harbord M, Andermann F, Wang J, Batish SD, Jones JG, Seltzer WK, Gardner A, Infantile Epileptic Encephalopathy Referral Consortium, Sutherland G, Berkovic SF, Mulley JC, Scheffer IE (2007) The spectrum of SCN1A-related infantile epileptic encephalopathies. Brain 130:843-852

Kahlig KM, Misra SN, George AL Jr (2006) Impaired inactivation gate stabilization predicts increased persistent current for an epilepsy-associated SCN1A mutation. J Neurosci. 26:10958-10966

Liao WP, Shi YW, Long YS, Zeng Y, Li T, Yu MJ, Su T, Deng P, Lei ZG, Xu SJ, Deng WY, Liu XR, Sun WW, Yi YH, Xu ZC, Duan S (2010) Partial epilepsy with antecedent febrile seizures and seizure aggravation by antiepileptic drugs: Associated with loss of function of $Na_v1.1$. Epilepsia 19:443-445

Lossin C, Wang DW, Rhodes TH, Vanoye CG, George AL Jr (2002) Molecular basis of an inherited epilepsy. Neuron 34:877-884

Lossin C, Rhodes TH, Desai RR, Vanoye CG, Wang D, Carniciu S, Devinsky O, George AL Jr (2003) Epilepsy-associated dysfunction in the voltage-gated neuronal sodium channel SCN1A. J Neurosci. 23:11289-11295

Lossin C (2009) A catalog of SCN1A variants. Brain. Dev. 31:114-130

Martin MS, Dutt K, Papale LA, Dubé CM, Dutton SB, de Haan G, Shankar A, Tufik S, Meisler MH, Baram TZ, Goldin AL, Escayg A (2010) Altered function of the SCN1A voltage-gated sodium channel leads to gamma-aminobutyric acid-ergic (GABA-ergic) interneuron abnormalities. J Biol Chem. 285:9823-9834

Mohler PJ, Rivolta I, Napolitano C, LeMaillet G, Lambert S, Priori SG, Bennet V (2004) Nav1.5 E1053K mutation causing Brugada syndrome blocks binding to ankyrin-G and expression of Nav1.5 on the surface of cardiomyocytes. Proc Natl Acad Sci U S A. 101:17533-17538

Oakley JC, Kalume F, Yu FH, Scheuer T, Catterall WA (2009) Temperature- and age-dependent seizures in a mouse model of severe myoclonic epilepsy in infancy. Proc Natl Acad Sci U S A. 106:3994-3999

Ogiwara I, Miyamoto H, Morita N, Atapour N, Mazaki E, Inoue I, Takeuchi T, Itohara S, Yanagawa Y, Obata K, Furuichi T, Hensch TK, Yamakawa K (2007) Nav1.1 localized to axons of parvalbumin-positive inhibitory interneurons: a circuit basis for epileptic seizures in mice carrying an Scn1a gene mutation. J Neurosci. 27: 5903-5914

Ohmori I, Kahlig KM, Rhodes TH, Wang DW, George AL Jr (2006) Nonfunctional SCN1A is common in severe myoclonic epilepsy of infancy. Epilepsia 47:1636-1642

Patino GA, Claes LR, Lopez-Santiago LF, Slat EA, Dondeti RS, Chen C, O'Malley HA, Gray CB, Miyazaki H, Nukina N, Oyama F, De Jonghe P, Isom LL (2009) A functional null mutation of SCN1B in a patient with DS. J Neurosci. 29:10764-10778

Rhodes TH, Lossin C, Vanoye CG, Wang DW, George AL Jr (2004) Noninactivating voltage-gated sodium channels in severe myoclonic epilepsy of infancy. Proc Natl Acad Sci U S A. 101:11147-11152

Singh R, Andermann E, Whitehouse WP, Harvey AS, Keene DL, Seni MH, Crossland KM, Andermann F, Berkovic SF, Scheffer IE (2001) Severe myclonic epilepsy of infancy: extended spectrum of GEFS+? Epilepsia 42:837-844

Spampanato J, Escayg A, Meisler MH, Goldin AL (2001) Functional effect of two voltage-gated sodium channel mutations that cause generalized epilepsy with febrile seizures plus type 2. J Neurosci. 21:7481-7490

Spampanato J, Esacyg A, Meisler MH, Goldin AL (2003) Generalized epilepsy with febrile seizures plus type 2 mutations W1204R alters voltage-dependent gating of Na_v1.1 sodium channels. Neuroscience 116:37-48

Spampanato J, Kearney JA, de Haan G, McEwen DP, Escayg A, Aradi I, MacDonald BT, Levin SI, Soltesz I, Benna P, Montalenti E, Isom LL, Goldin AL, Meisler MH (2004) A novel epilepsy mutation in the sodium channel SCN1A identifies a cytoplasmic domain for beta subunit interaction. J Neurosci. 24:10022-10034

Stafstrom CE (2007) Persistent sodium current and its role in epilepsy. Epilepsy Curr. 7:15-22

Suls A, Claeys KG, Goossens D, Harding B, Van Luijk R, Scheers S, Deprez L, Audenaert D, Van Dyck T, Beeckmans S, Smouts I Ceulemans B, Lagae L, Buyse G, Barisic N, Misson JP, Wauters J, Del-Favero J, De Jonghe P, Claes LR (2006) Microdeletions involving the SCN1A gene may be common in SCN1A-mutation-negative SMEI patients. Hum Mutat. 27:914-920

Verbeek NE, van Kempen M, Gunning WB, Renier WO, Westland B, Lindhout D, Brilstra EH (2011) Adults with a history of possible Dravet syndrome: an illustration of the importance of analysis of the SCN1A gene. Epilepsia 52:e23-e25 doi: 10.1111/j.1528-1167.2011.02982.x.

Wallace RH, Wang DW, Singh R, Scheffer IE, George AL Jr, Philips HA, Saar K, Reis A, Johnson EW, Sutherland GR, Berkovic SF, Mulley JC (1998) Febrile seizures and generalized epilepsy associated with a mutation in the Na+ channel beta1 subunit SCN1B. Nat Genet. 19:366:37

Yu FH, Mantegazza M, Westenbroek RE, Robbins CA, Kalume F, Burton KA, Spain WJ, McKnight GS, Scheuer T, Catterall WA (2006) Reduced sodium current in GABAergic interneurons in a mouse model of severe myoclonic epilepsy in infancy. Nat Neurosci. 9:1142-1149

Yu MJ, Shi YW, Gao MM, Liu XR, Chen L, Long YS, Yi YH, Liao WP (2010) Milder phenotype with SCN1A truncation mutation other than SMEI. Seizure 19:443-445

Febrile temperatures unmask biophysical defects in Na$_v$1.1 epilepsy mutations supportive of seizure initiation

Linda Volkers, Kristopher M. Kahlig, Joost H.G. Das, Marjan J.A. van Kempen,
Dick Lindhout, Bobby P.C. Koeleman*, Martin B. Rook*

* contributed equally

5

Submitted

Abstract

Genetic Epilepsy with Febrile Seizures Plus (GEFS+) is an early onset febrile epileptic syndrome with therapeutic responsive (a)febrile seizures continuing later in life. Dravet syndrome (DS) or Severe Myoclonic Epilepsy of Infancy (SMEI) has a complex phenotype including febrile generalized or hemiclonic convulsions before the age of one, followed by intractable myoclonic, complex partial or absence seizures. Both diseases can result from mutations in the $Na_v1.1$ sodium channel and initially seizures are typically triggered by fever. We previously characterized two $Na_v1.1$ mutants - R859H (GEFS+) and R865G (DS) - at room temperature, and reported a mixture of biophysical gating defects which could not easily predict the phenotype presentation as either GEFS+ or DS. In this study, we extend the characterization of $Na_v1.1$ wild-type, R859H and R865G channels to physiological (37ºC) and febrile (40ºC) temperatures. At physiological temperature, a variety of biophysical defects were detected in both mutants, including a hyperpolarised shift in the voltage dependence of activation and a delayed recovery from fast and slow inactivation. Interestingly, at 40ºC we also detected additional gating defects for both R859H and R865G mutants. The GEFS+ mutant R859H showed a loss-of-function in the voltage dependence of inactivation and an increased channel use-dependency at 40ºC with no reduction in peak current density. The DS mutant R865G exhibited reduced peak sodium currents, enhanced entry into slow inactivation and increased use-dependency at 40ºC. Our results suggest that fever-induced temperatures exacerbate the gating defects of R859H or R865G mutants and may predispose mutation carriers to febrile seizures.

Introduction

Genetic Epilepsy with Febrile Seizures Plus (GEFS+) is an autosomal dominant disorder in which subjects have febrile seizures early in childhood with increased risk for febrile and afebrile seizures later on in life. Fortunately, most patients have spontaneously remitting epilepsy and a normal development (Deprez et al., 2009). Dravet syndrome (DS) is an intractable epilepsy type with poor prognosis, characterized by fever induced generalized tonic-clonic seizures during the first year of life. Phenotypic progression for DS patients includes complex seizure phenotypes with impairment of psychomotor development, including ataxia and mental disabilities (Deprez et al., 2009). Even though the outcome of these two different epilepsy syndromes differs dramatically, both are associated with the neuronal $Na_v1.1$ ion channel SCN1A (Escayg et al., 2000; Claes et al., 2003; Claes et al., 2009; Lossin, 2009).

GEFS+ patients harbour predominantly missense mutations, while in DS patients missense, truncation, frameshift, or deletion/duplication mutations have been reported that arise de novo. To date, more than 600 SCN1A mutations are associated with a spectrum of epileptic phenotypes, and a few of these missense mutations have been functionally characterized at room temperature to gain insight into the pathophysiology of GEFS+ and DS (Spampanato et al., 2001; Lossin et al., 2002; Lossin et al., 2003; Spampanato et al., 2003; Rhodes et al., 2004; Spampanato et al., 2004; Rhodes et al., 2005; Ohmori et al., 2006). When investigated at room temperature, GEFS+ mutant channels exhibit gain-of-function or loss-of-function gating defects while complete loss of ion channel function is common in DS patients (Yu et al. 2006; Ogiwara et al. 2007; Catterall et al., 2010).

Fever-induced seizures are common in GEFS+ and DS subjects and mouse models (Oakley et al., 2009; Martin et al., 2010) and are typically the first reported symptom. However, no study has investigated the role of elevated temperature in the development of gating defects in these mutant channels. Previous functional studies on several other mutated ion channels associated with temperature-induced disorders have already shown that gating of these ion channels changes at elevated temperatures (Dumaine et al., 1999; Han et al., 2007; Amin et al., 2008; Carle et al., 2009; Samani et al., 2009). We have previously characterized GEFS+ (R859H) and DS (R865G) SCN1A mutant channels at room temperature. The R859H mutant showed mixed biophysical gating defects; the R865G mutant showed overall gain-of-function gating defects that could not explain the disease severity of the DS subject (Volkers et al., 2011). Since GEFS+ and DS share fever-associated seizures, we sought to investigate the temperature dependent gating of the $Na_v1.1$ WT, R859H and R865G sodium ion channels. We hypothesized that the R859H (GEFS+) and R865G (DS) mutations differentially affect the sodium channel function in a temperature dependent manner. To test this hypothesis, we characterized the biophysical properties of WT and mutant ion channels at 37ºC and 40ºC.

Material and methods

Cell culture and transfection

Human derived tsA201 cells were cultured in Dulbecco's Modified Eagle Medium (DMEM) supplemented with 10% FBS, penicillin 100 U/ml, streptomycin 100 μg/ml and 0,05% L-glutamine in a humidified incubator at 37ºC with 5% CO_2. All culture media and supplements were obtained from Biowithakker, Vervier, Belgium. Transient transfections were performed with Lipofectamine (Invitrogen, Carlsbad, CA, U.S.A.) using in total 6 µg of Nav1.1, β1 and β2 pDNAs in a ratio of 10:1:1, as previously described by Lossin et al. 2002. Cells that expressed β1 and β2-subunits were identified with CD8 positive beads (Invitrogen, Oslo, Norway) and GFP epifluorescence, respectively. Cells that expressed both b-subunits were patched 48 to 72 hours after transfection. For electrophysiological measurements at least two different clones of either WT or mutant constructs were tested. The introduction of R859H (c.G2576A) and R865G (c.G2593G) mutations in the SCN1A plasmid DNA has previously been described (Volkers et al., 2011).

Electrophysiological measurements

Prior to patching, cells were incubated for at least 1 hour in cell culture medium containing 140 mM NMDG, 4 mM KCl, 1 mM $CaCl_2$, 1 mM $MgCl_2$, 14.3 mM Na_2HCO_3, 15.1 mM HEPES, 17.5 mM Glucose, 1X Amino Acids (Gibco, Paisley, UK), 1X Non Essential Amino Acids (NEAA) (Gibco, Paisley, UK) (pH 7.35) supplemented with 10% FCS (Biowhitakker, Vervier, Belgium), penicillin 100 U/ml (Biowhitakker, Vervier, Belgium), streptomycin 100 mg/ml (Biowhitakker, Vervier, Belgium) and 2 mM L-glutamine (Biowhitakker, Vervier, Belgium) a in humidified atmosphere at 37ºC, 5% CO_2. For patch experiments, cells were bathed in modified Tyrode's solution containing in mM: 140 NaCl, 5.4 KCl, 1.8 $CaCl_2$, 1 $MgCl_2$, 6 Glucose, 6 HEPES (pH 7.4). Na_v1.1 sodium currents were measured at 37ºC and 40ºC using the whole-cell patch clamp configuration with an Axopatch 200B amplifier (Axon instruments, Union City, CA, U.S.A.). In most cells electrophysiological parameters were measured at both 37ºC and 40ºC. Patch pipettes were pulled from borosilicate glass capillaries with a Sutter P2000 pipette puller (Sutter Instrument, Novato, CA, U.S.A.) and fire polished. Patch pipettes had a tip resistance between 1.3-2.2 MΩ when filled with the following internal solution (mM): 10 NaF, 110 CsF, 20 CsCl, 2 EGTA and 10 HEPES (pH 7.35). Cells were allowed to stabilize at room temperature (20-22ºC) for 10 minutes after whole cell configuration was established. Next, temperature was raised to 37ºC or 40ºC using a temperature controlled perfusion chamber (Cell MicroControls, Norfolk, VA, U.S.A) and cells were allowed to stabilize at each temperature for approximately seven minutes. Cells expressing sodium current < -600 pA at room temperature were excluded because of small endogenous sodium currents possibly interfering with the electrophysiological measurements. Cells exhibiting currents

> -6000 pA were excluded to avoid voltage clamp errors. Recordings were ≥90% compensated for pipette series resistance and capacitive transients. Leak currents were subtracted using a P/4 procedure. Sodium currents were filtered at 10 kHz and digitized at 100 kHz using a Digidata1322A (Axon instruments, Union City, CA, U.S.A.). For analysis, a 5 kHz low pass-filtering step was used. Voltage clamp protocols were generated and data acquisition was performed using pCLAMP9.2 (Axon instruments, Union City, CA, U.S.A.). Voltage clamp protocols are depicted in the figures where applicable. Steady-state activation was analyzed from consecutive measurements at 37ºC and 40ºC. Current densities were determined by normalizing peak current amplitudes to cell capacitance. Voltage dependence of activation and slow inactivation were determined by fitting the data with a single Boltzmann equation $I = I_{max} / (1+\exp((V-V½)/k))$ and the voltage dependence of fast inactivation with a double Boltzmann equation $I = I_1/(1+\exp(V-V_1½)/k_1)) + I_2/(1+\exp(V-V_2½)/k_2))$, where V is the variable test or conditioning potential, V½ the voltages of half maximum activation or inactivation, k are slope factors, I_1 and I_2 the fractional amplitudes of I_{max}, and I_{max} is the normalized maximum amplitude of the sodium current. The entry into and recovery from fast and slow inactivation was analyzed by fitting the data with a double exponential $I/I_{max} = A_1 * (1-\exp(-t/\tau_1)) + A_2 * (1-\exp(-t/\tau_2)) + C$, where τ_1 and τ_2 denote fast and slow time constants, A_1 and A_2 represent the fractional amplitude of each time constant and C the level of non-inactivating sodium current. Speed of inactivation was evaluated by fitting the decay phase of the sodium current with a double exponential function $I/I_{max} = A_1 * \exp(-t/\tau_1) + A_2 * \exp(-t/\tau_2) + C$, where the parameters are defined as above. Persistent sodium current was determined by applying a 100 ms depolarizing pulse at voltages -20 mV, -10 mV and 0 mV from a holding potential of -120 mV. Cells were recorded in the absence and presence of 10 μM TTX (Alomone, Jerusalem, Israel) and traces were digitally subtracted to obtain persistent current. Next, the average persistent current at the final 10 ms of the depolarizing pulse was normalized to the peak sodium current. Use-dependency was investigated by applying 100 depolarizing test pulses of 2 ms to +15 mV starting from a resting membrane potential of -65 mV at various frequencies (10, 20, 33, 40, 64, 80, 100, 125 and 143 Hz). The peak current of the last pulse was normalized to the peak current generated by the first pulse. The Q_{10} value of sodium current densities measured at -5 mV was calculated using the following formula; $Q_{10} = (I_{40ºC}/I_{37ºC})^{(10/(T2-T1))}$ in where $I_{37º}$ and $I_{40ºC}$ represent the sodium current densities at indicated temperatures and T1 and T2 are 37ºC and 40ºC respectively. Voltages are not corrected for liquid junction potentials of 9.9 mV (37ºC) and 10 mV (40ºC). Data analysis was performed using Clampfit 9.2 (Axon instruments, Union City, CA, U.S.A.), Excel 2008 (Microsoft, Seattle, WA, U.S.A.), Kaleidagraph 4.0 (Synergy Software, Reading, PA, U.S.A) and OriginPro 8.0 (Microcal, Northhamption MA, U.S.A.) software. Results are presented as mean ± S.E.M.. Statistical analysis was performed using an unpaired Student’s t-test. A value of $P<0.05$ was considered significant.

Results

The DS mutant R865G produces reduced peak sodium currents at physiologic and febrile temperatures $Na_v1.1$ WT, R859H and R865G sodium currents were obtained by applying test pulses ranging from -80 mV to +90 mV from a holding potential of -120 mV. Figure 1A-F shows sodium current densities for WT, R859H and R865G channels at room temperature (RT), 37ºC and 40ºC. When the temperature was raised from 37ºC to 40ºC, WT ion channels gained ~-50 pA/pF in peak current density and a similar increase in sodium current density at elevated temperature was also present in the R859H mutant (Figure 1A and B). In contrast, the R865G mutation caused no significant increase at 40ºC (Figure 1C). Compared to WT, R865G caused a reduction in sodium current density at physiological temperature and a significant reduction at voltages -10 mV to 30 mV at 40ºC (Figure 1E and F). This reduction was not detected at room temperature (Figure 1D). Thus, the R865G mutant shows a loss of function defect in current density at febrile temperature. We calculated the Q_{10} value of the temperature-dependent current density changes between 37ºC and 40ºC at -5 mV. The Q_{10} value of the R865G mutant (1.17 ± 0.14, t_{21}=2.58, P=0.017, n=10) was significantly lower than WT (2.38 ± 0.40, n=13) or R859H (2.13 ± 0.32, n=12) sodium channels, suggesting that the R865G mutant is less temperature dependent than WT.

Time to peak-current and speed of inactivation

To determine whether the speed of activation or inactivation plays a role in the reduced current density of the R865G mutant, we analyzed the activation time by measuring the time from the onset to the peak of sodium currents (time to peak-current). Fitting the decay phase of the sodium currents with a double exponential function to obtain fast and slow inactivation time constants determined the inactivation rate. Febrile temperatures increased the rate of activation (decreased time to peak current) of WT channels, while the speed of inactivation was unaffected (Figure 2A, D and I). The R859H mutants showed similar activation rates at both temperatures, a significant decrease in fast inactivation time constants at 40ºC at membrane potentials between -30 mV to -20 mV and a trend towards increased slow inactivation time constants at all voltage ranges (Figure 2B, E and J). The kinetics of the R865G mutant were unaffected by febrile temperature (Figure 2C, F and K) and were comparable to the activation rate and speed of inactivation of WT channels at 40ºC (Figure 2H and M), indicating that neither time to peak nor speed of inactivation contributes to the reduced current density of R865G at elevated temperatures.

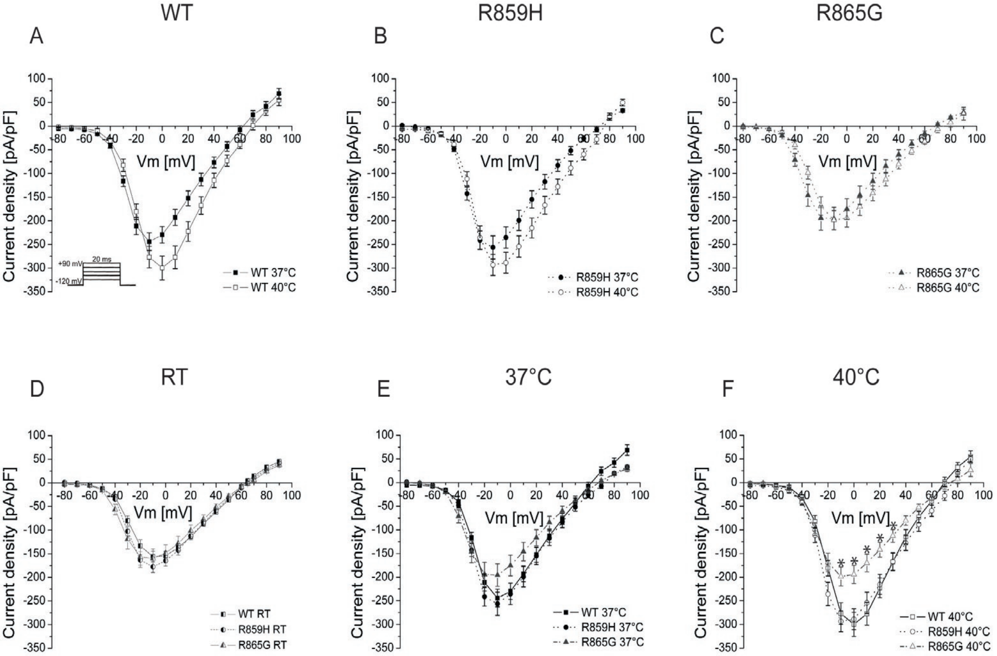

Figure 1.

I-V relationships and current densities of Na$_v$1.1 WT (37ºC, 40ºC), R859H (37ºC, 40ºC), and R865G (37ºC, 40ºC) ion channels co-expressed with β1 and β2-subunits in tsA201 cells. (A-C) Average voltage-current relationship for (A) Nav1.1 WT, (B) R859H and (C) R865G sodium currents consecutively measured at 37ºC and 40ºC, demonstrating decreased R865G current density at physiological and febrile temperatures. Current density was obtained by normalizing peak sodium currents to cell capacitance. (D-F) Average IV curve of WT, R859H, and R865G measured at (D) room temperature (RT), (E) 37ºC and (F) 40ºC showing a decrease in current density for the DS mutant R865G at 37ºC and 40ºC ($P<0.05$). Figure D, with subtle modification of the Y-axis and figure symbols and lines, is reproduced from Na$_v$1.1 Dysfunction in Genetic Epilepsy with Febrile Seizures Plus or Dravet Syndrome, Volkers et al., European Journal of Neuroscience 34(8), Copyright © 2011, Federation of European Neuroscience Societies and Blackwell publishing Ltd.*

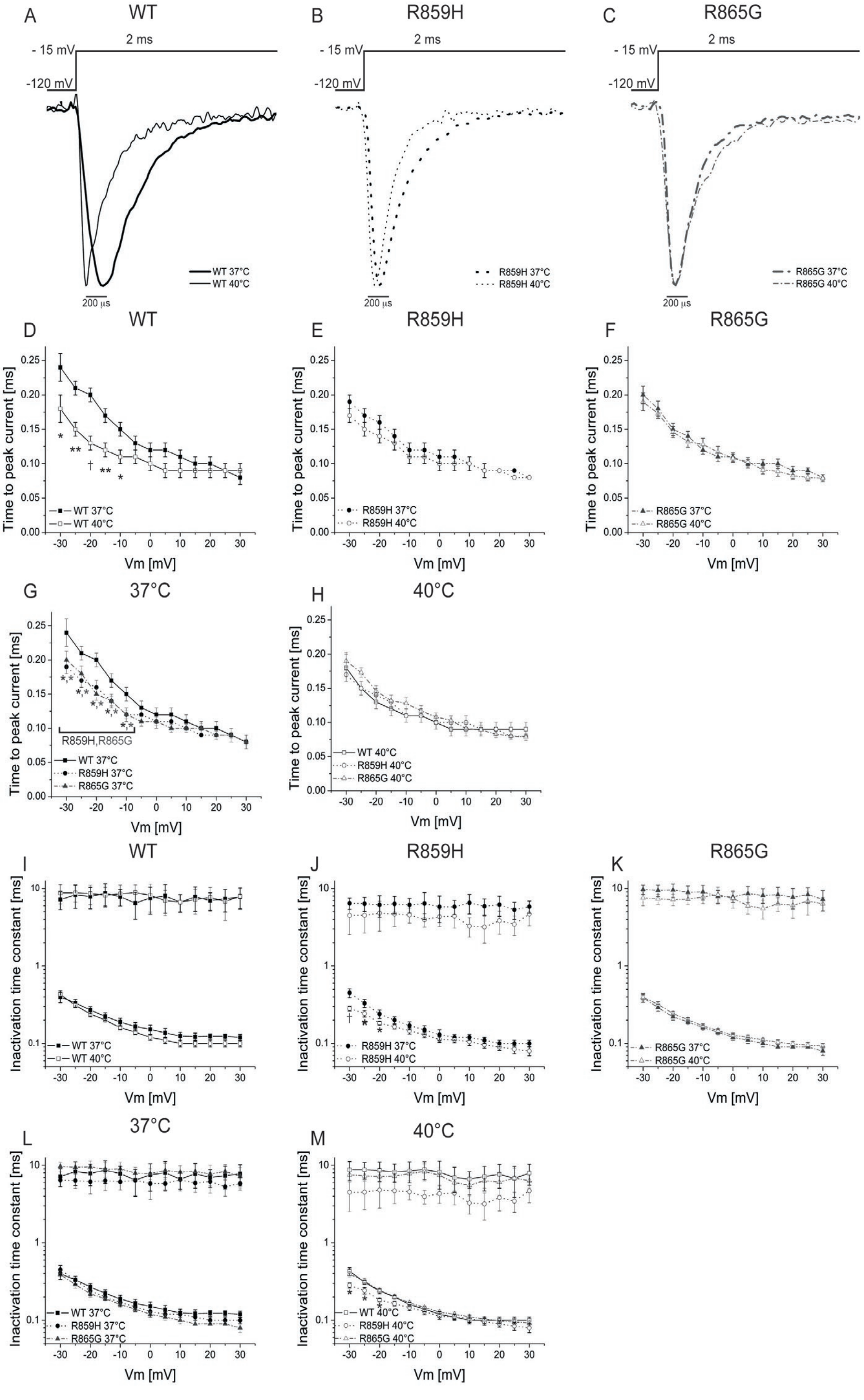
A
WT
- 15 mV
-120 mV
2 ms
WT 37°C
WT 40°C
200 µs
B
R859H
- 15 mV
-120 mV
2 ms
R859H 37°C
R859H 40°C
200 µs
C
R865G
- 15 mV
-120 mV
2 ms
R865G 37°C
R865G 40°C
200 µs
D
WT
Time to peak current [ms]
0.00
0.05
0.10
0.15
0.20
0.25
*
**
†
**
*
WT 37°C
WT 40°C
-30
-20
-10
0
10
20
30
Vm [mV]
E
R859H
Time to peak current [ms]
R859H 37°C
R859H 40°C
Vm [mV]
F
R865G
Time to peak current [ms]
R865G 37°C
R865G 40°C
Vm [mV]
G
37°C
Time to peak current [ms]
R859H,R865G
WT 37°C
R859H 37°C
R865G 37°C
Vm [mV]
H
40°C
Time to peak current [ms]
WT 40°C
R859H 40°C
R865G 40°C
Vm [mV]
I
WT
Inactivation time constant [ms]
0.1
1
10
WT 37°C
WT 40°C
Vm [mV]
J
R859H
Inactivation time constant [ms]
†
*
*
R859H 37°C
R859H 40°C
Vm [mV]
K
R865G
Inactivation time constant [ms]
R865G 37°C
R865G 40°C
Vm [mV]
L
37°C
Inactivation time constant [ms]
WT 37°C
R859H 37°C
R865G 37°C
Vm [mV]
M
40°C
Inactivation time constant [ms]
†
*
*
WT 40°C
R859H 40°C
R865G 40°C
Vm [mV]

Voltage dependence of activation is not temperature sensitive

Next, we analyzed the voltage dependence of activation. Febrile temperature caused a depolarizing shift in the voltage dependence of activation of WT ion channels (Figure 3A; Table 1). The half maximal activation (V½) at 40ºC of R859H was similar to 37ºC, while the R865G mutant showed a significant depolarizing shift in the voltage dependence of activation at 40ºC (Figure 3B and C; Table 1). Compared to WT, however, there was a significant hyperpolarized shift in the voltage dependence of activation of R859H (V½ 37ºC = -28.3 ± 1.0, t_{23}=2.45, P=0.02 n=12; V½ 40ºC = -28.1 ± 1.2 t_{23}= 3.41, P=0.002, n=12) and R865G (V½ 37ºC = -32.9 ± 0.6 t_{21}=8.02, P<0.0001, n=10; V½ 40ºC = -31.4 ± 0.6, t_{23}= 7.09, P<0.0001, n=10) at both temperatures, albeit more prominent for the DS mutation (Figure 3D-F). On the other hand, the V½ at 37ºC and 40ºC of WT, R859H and R865G are similar to the values obtained at room temperature ($Na_v1.1$ WT -23.1±1.1 mV; R859H -27.1±0.6 mV; R865G -31.2±1.1 mV; Volkers et al., 2011), indicating that increased temperatures do not affect the activation gating of the $Na_v1.1$ WT ion channel and mutants.

Figure 2.

*(A-C) Normalized whole-cell recordings at 37ºC and 40ºC of (A) $Na_v1.1$ WT, (B) R859H and (C) R865G currents evoked by a depolarizing test pulse to -15 mV from a holding potential of -120 mV. For comparison, recorded currents were normalized to the peak currents. (D-F) Speed of activation was assessed by measuring the time to peak current at voltages between -30 mV to +30 mV at 37°C and 40°C of (D) $Na_v1.1$ WT (37ºC, 40ºC), (E) R859H (37ºC, 40ºC) and (F) R865G (37ºC, 40ºC) ion channels. Only WT showed a significant decrease in time to peak-current at 40°C. (G-H) Comparison of the time to peak-current of $Na_v1.1$ WT, R859H, and R865G at (G) 37ºC and (H) 40ºC, showing a significant decrease in time to peak-current at 37ºC but not 40ºC. (I-K) The decay of the sodium currents was fitted by a double exponential to obtain fast and slow inactivation time constants of (I) $Na_v1.1$ WT, (J) R859H and (K) R865G at physiological and febrile temperatures. The R859H mutant showed a small but significant decrease in the fast time constant of inactivation at 40°C compared to 37ºC between -30 mV to -20 mV. (L-M) Comparison of fast and slow inactivation time constants of WT and mutant channels plotted against the membrane potential at (L) 37ºC and (M) 40ºC demonstrating decreased speed in fast inactivation time constants between -30 mV to -20 mV for R859H at 40ºC. Data points that significantly differ are indicated as * P<0.05; ** P<0.01; † P<0.001.*

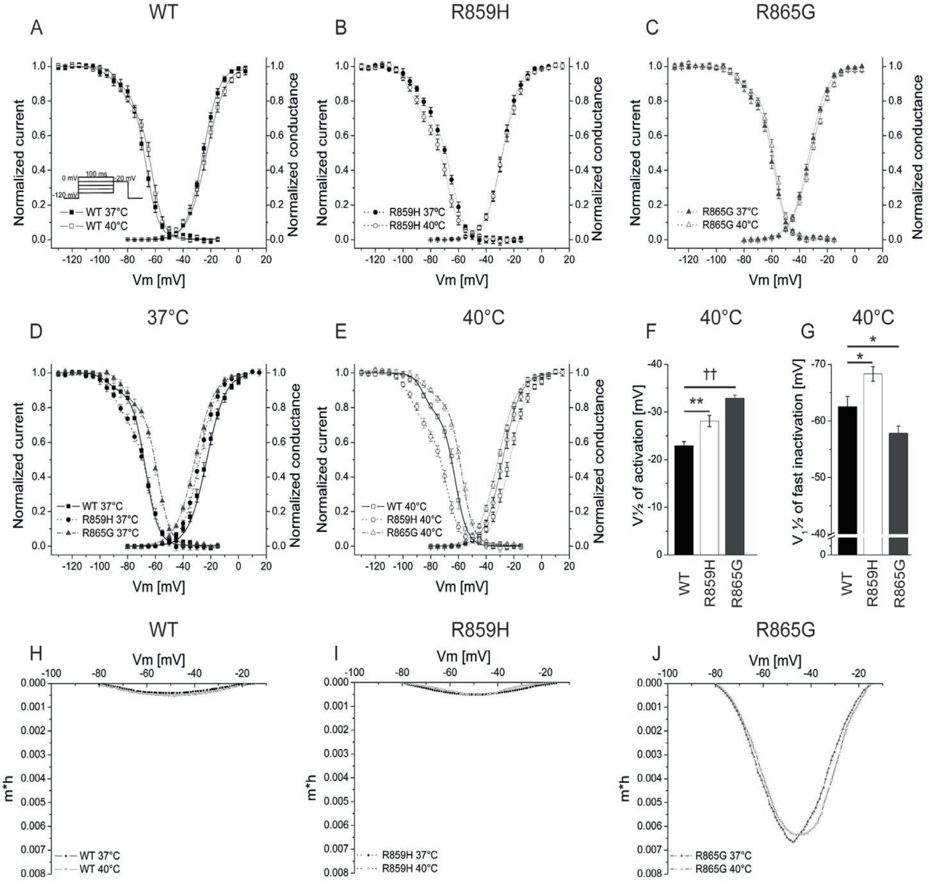

Figure 3.

*(A-C) The voltage dependence of activation and inactivation of (A) $Na_v1.1$ WT (37ºC, 40ºC), (B) R859H (37ºC, 40ºC), and (C) R865G (37ºC, 40ºC) sodium channels at 37ºC and 40ºC. (D-E) Comparison of the voltage dependence of activation and inactivation of WT and mutant channels at (D) 37ºC and (E) 40ºC and (F-G) the half maximal values of WT, R859H, and R865G channels of the voltage dependent of (F) activation and (G) fast inactivation at 40ºC. The voltage clamp protocol depicted in these figures applies to the voltage dependence of inactivation. The protocol used for determining activation can be found in Figure 1A. Compared to WT, both mutants showed a gain-of-function in the voltage dependence of activation at both temperatures. The negative shift in the voltage dependence of inactivation of the GEFS+ mutant indicated decreased channel availability at febrile temperatures, while the DS mutant showed a gain-of-function in the voltage dependence of inactivation at both temperatures. (H-J) Window-currents produced by (H) $Na_v1.1$ WT, (I) R859H and (J) R865G channels at 37ºC and 40ºC. The voltage dependence and amplitude of the window-current was estimated by plotting the product of the average fractional availability for steady-state activation (m) and inactivation (h) curves (obtained from A, B and C). The resultant values show the fraction of active WT, R859H or R865G sodium channels as a function of the membrane potential. The DS mutant R865G clearly shows an enlarged window-current compared to $Na_v1.1$ WT and R859H currents. * $P<0.05$; ** $P<0.01$; †† $P<0.0001$.*

Table 1. Biophysical parameters of Na$_v$1.1 WT, R859H, and R865G sodium ion channels measured at 37°C and 40°C

		Na$_v$1.1 WT 37°C	***Na$_v$1.1 WT 40°C***	***R859H 37°C***	***R859H 40°C***	***R865G 37°C***	***R865G 40°C***
Activation	V½ [mV]	-25.5 ± 0.6	22.9 ± 0.9*	-28.3 ± 1.0	-28.1 ± 1.2	-32.9 ± 0.6	-31.4 ± 0.6††
	k	5.9 ± 0.3	6.7 ± 0.3*	6.0 ± 0.3	6.3 ± 0.4	6.5 ± 0.2	7.0 ± 0.2
	n	13	13	12	12	10	10
Fast inactivation	V_1½ [mV]	-67.2 ± 1.0	-62.5 ± 1.8*	-64.7 ± 1.3	-68.3 ± 1.3*	-58.4 ± 1.4	-57.8 ± 1.3
	k_1	4.7 ± 0.3	4.4 ± 0.1	4.9 ± 0.3	4.9 ± 0.4	4.6 ± 0.5	4.3 ± 0.1
	A_1	0.72 ± 0.03	0.73 ± 0.01	0.64 ± 0.02	0.69 ± 0.02*	0.75 ± 0.03	0.74 ± 0.03
	V_2½ [mV]	-94.7 ± 2.2	-85.4 ± 2.3*	-87.8 ± 2.3	-94.3 ± 1.9	-82.9 ± 2.8	-83.9 ± 2.5
	k_2	4.4 ± 0.8	3.9 ± 0.7	5.8 ± 0.9	5.1 ± 0.9	3.5 ± 0.8	6.3 ± 1.3*
	A_2	0.28 ± 0.04	0.27 ± 0.01	0.35 ± 0.02	0.32 ± 0.02	0.25 ± 0.03	0.26 ± 0.03
	n	10	9	9	8	8	9
Recovery from inactivation	τ_1 [ms]	10.1 ± 2.10	8.80 ± 1.40	5.90 ± 1.20	23.8 ± 8.80†	26.8 ± 5.30	13.2 ± 3.36*
	A_1	0.32 ± 0.04	0.48 ± 0.07*	0.18 ± 0.03	0.33 ± 0.07*	0.48 ± 0.08	0.30 ± 0.05*
	τ_2 [ms]	46.3 ± 4.50	47.7 ± 6.30	175 ± 14.8	141 ± 13.9*	128 ± 20.8	53.1 ± 7.10**
	A_2	0.47 ± 0.04	0.33 ± 0.07*	0.68 ± 0.04	0.49 ± 0.07*	0.36 ± 0.07	0.57 ± 0.05*
	n	13	9	12	12	10	9

*Ion channel gating parameters of WT, R859H, or R865G at 40°C that significantly differ from the values obtained at 37°C are indicated as follows *$P<0.05$; **$P<0.01$; †$P<0.001$; ††$P<0.0001$*

The GEFS+ mutant R859H shows febrile temperature induced decrease in voltage dependent channel availability

Subsequently, we investigated steady state inactivation by applying series of depolarizing conditioning pulses in the voltage range of -140 mV to 0 mV starting from a holding potential of -120 mV, immediately followed by a depolarizing test pulse of -20 mV. Steady state channel inactivation was best fitted by a double Boltzmann equation. When temperature was raised to 40ºC, WT channels showed an increase in channel availability (Figure 3A; Table 1). Opposite results were obtained for the R859H mutant, which showed a significant hyperpolarized shift in the voltage dependence of inactivation at elevated temperatures (Figure 3B; Table 1). Furthermore, the contribution of the more negative portion of the Boltzmann curve (A_2) for R859H was significantly increased compared to WT channels at 37ºC (A_2 R859H = 0.35 ± 0.02, t_{17}=2.11, P=0.049, n=9) (Table 1). The temperature dependent negative shift in the steady state inactivation of sodium ion channels harboring the R859H mutation suggests that fever leads to a decrease in channel availability (Figure 3B, E and G). In contrast, elevated temperatures did not affect the voltage dependence of inactivation of the R865G mutant (Figure 3C; Table 1). However, the R865G mutant at 37ºC and 40ºC revealed an increase in the voltage dependence of channel availability compared to WT channels (V_1½ 37ºC = -58.4 ± 1.4, t_{16}=-5.45, P<0.0001, n=9; V_1½ 40ºC = -57.8 ± 1.3, t_{16}=-2.14, P<0.048, n=9) (Figure 3D, E and G), a feature that was not observed at room temperature (Volkers et al. 2011).

R865G exhibits increased window-current

The steady-state of activation and inactivation curves showed an overlap, indicating that a window-current was present. Compared to WT, the window-current of R865G was enlarged due to the shifts in the voltage dependence of activation and inactivation (Figure 3A, C, F and G). We have therefore analyzed changes in the window-current in more detail. The size of the window-current produced by WT, R859H and R865G channels was calculated as the product of the average steady-state of activation (m) and inactivation (h). These resultant products are a measure of the probability of incompletely inactivated sodium channels to open, and were plotted against the membrane potential. The size of the window-current of R865G was increased more than 10 fold at both 37ºC and 40ºC compared to WT (Figure 3H-J). This increased window-current results in an increase in channel function especially when the membrane potential is near firing threshold, which could lead to enhanced excitability.

Recovery from inactivation is delayed in both mutants.

Febrile temperatures accelerated the recovery from inactivation of both WT and mutant channels. However, this effect was less pronounced in both mutants (Figure 4A-E; Table 1). At 37ºC, cells expressing R859H had a significant smaller fraction of channels recovering from the fast inactivation component (A_1) and a larger population recovering from the slower inactivation (A_2) compared to WT ($A_1 = 0.48 \pm 0.07$, $t_{23}=2.82$, P=0.01, n=12; $A_2 = 0.68 \pm 0.04$, $t_{23}=-3.96$, P=0.0006, n=12) (Table 1). In addition, there was a significant slowing in recovery from inactivation, as was evident by a larger time constant (τ_2) of recovery ($\tau_2 = 128 \pm 20.8$ $t_{23}=-8.63$, P<0.0001, n=12). At 40ºC, the recovery from inactivation of R859H is accelerated but still significantly slower compared to WT channels (τ_1 R859H = 23.8 ± 8.80, $t_{19}=-3.23$, P=0.004, n=9) (Fig 4E). The R865G mutation also caused an overall slowing in recovery from inactivation at 37ºC and 40ºC, as shown by the larger time constants τ_1 (τ_1, $t_{17}=2.11$, P=0.049) (Table 1; Figure 4D). At 40ºC, a smaller R865G channel population was recovering from the fast inactivation component (A_1, $t_{17}=2.11$, P=0.049) and a significant larger ion channel population present in the second inactivation status (A_2, $t_{17}=3.24$, P=0.048) (Table 1). In summary, these results show that both mutants exhibited a slowing in recovery from inactivation at both temperatures, with the largest delay observed for R859H (Figure 4A-E).

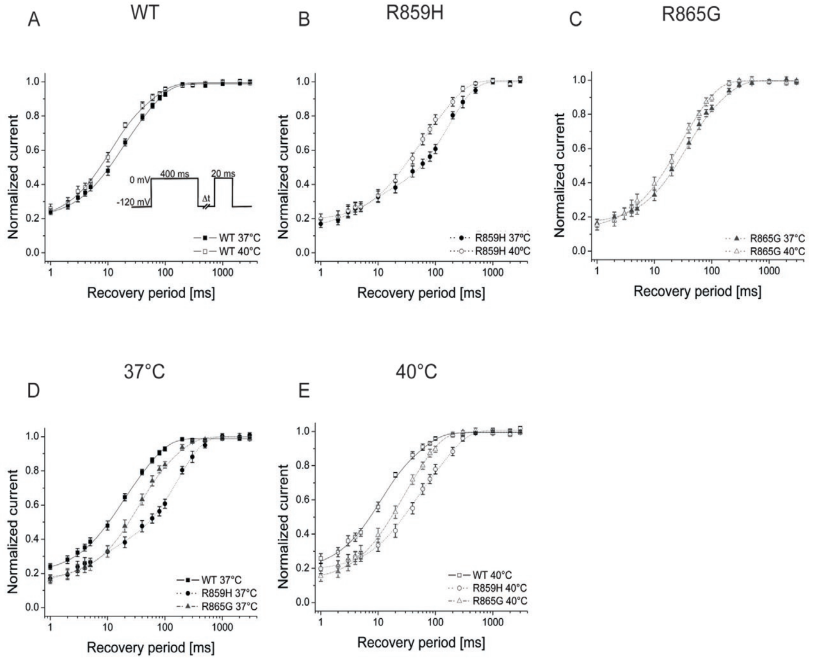

Figure 4.

Time dependent recovery from inactivation at 37ºC and 40ºC of (A) Na_v1.1 WT (37ºC, 40ºC), (B) R859H (37ºC, 40ºC) and (C) R865G (37ºC, 40ºC) sodium ion channels was assessed using the two pulse protocol shown as inset in panel A. Peak currents of the test pulse were normalized to the peak currents generated by the conditioning pulse and plotted against the recovery time. (D-E) Comparison of the recovery from inactivation of WT and mutant channels at (D) 37ºC and (E) 40ºC. Significant slowing in recovery from inactivation at 37ºC and 40ºC was observed for both mutants (see also Table 1).

R859H and R865G mutants have gating defects in slow inactivation

Slow inactivation is a process distinct from fast inactivation. This independent process is functionally relevant for setting the fractional availability of the sodium channel population at voltages around the resting membrane potential or in response to prolonged bursts of action potentials.

The entry into inactivation was analyzed by fitting the data to a double exponential function (Figure 5A-C). Increased temperatures accelerated the entry into inactivation of WT, R859H and R865G channels, which is evident by decreased time constants τ_2 (Table 2). Compared to WT ion channels, at 37ºC both mutants have a larger inactivating ion channel population in the first time fraction (A_1) (A_1 R859H = 0.29 ± 0.06, t_{15}=2.24, P=0.04, n=9; A_1 R865G = 0.32 ± 0.08, t_{15}=2.15, P=0.049, n=9) than WT ion channels (Figure 5A-C; Table 2). At both temperatures, R859H had a larger ion channel population that entered into a slow inactivation state compared to WT, as evident by the smaller value of the residual current ($I_{residual}$ 37ºC = 14 ± 3, t_{15}=2.89, P=0.01, n=9; $I_{residual}$ 40ºC = 14 ± 3, t_{15}=2.10 P=0.048, n=12) (Figure 5A and B; Table 2). At 40ºC, the $I_{residual}$ of R865G is similar to WT (t_{18}=0.57, P=0.57, n=10) (Table 2). Compared to WT, the R865G mutant showed an acceleration of entry into steady state inactivation (τ_2) at both temperatures (τ_2 37ºC, t_{15}=2.69, P=0.02, n=9; τ_2 40ºC, t_{18}=4.34, P=0.0004, n=10).

At 40ºC both WT and R859H channels showed a hyperpolarized shift in the voltage dependence of steady-state slow inactivation (Figure 5D-E). The steady-state slow inactivation of R859H channels at both temperatures was comparable to WT, while the R865G mutation caused a hyperpolarized shift in the V½ of -10 mV and -7.7 mV at 37ºC and 40ºC, respectively (V½ 37ºC = -64.3 ± 0.9, t_{16}=6.96, P<0.0001, n=7; V½ 40ºC = -65.6 ± 0.8, t_{15}=5.26 P<0.0001, n=10) (Figure 5D-I; Table 2).

Figure 5J-L shows the recovery from slow inactivation for WT, R859H and R865G. Compared to WT, both mutations caused a significant slowing in recovery from slow inactivation at both temperatures (Figure 5J-L; Table 2), albeit more prominent for R859H.

Table 2. Biophysical parameters of slow inactivation Na$_v$1.1 WT, R859H, and R865G sodium ion channels

		Na$_v$1.1 WT 37°C	***Na$_v$1.1 WT 40°C***	***R859H 37°C***	***R859H 40°C***	***R865G 37°C***	***R865G 40°C***
Entry into inactivation	t_1 [ms]	35.8 ± 9.30	42.6 ± 9.80	64.3 ± 16.2	69.3 ± 14.3	50.2 ± 10.8	36.4 ± 9.00
	A_1	0.14 ± 0.03	0.16 ± 0.04	0.29 ± 0.06	0.24 ± 0.06	0.32 ± 0.08	0.25 ± 0.08
	t_2 [ms]	290 ± 26.3	217 ± 19.8*	302 ± 28.3	216 ± 26.5*	196 ± 23.1	122 ± 9.50*
	A_2	0.61 ± 0.05	0.61 ± 0.04	0.58 ± 0.08	0.62 ± 0.06	0.55 ± 0.09	0.56 ± 0.07
	$I_{residual}$ [%]	26 ± 4	22 ± 2	14 ± 3	14 ± 3	13 ± 4	19 ± 4
	n	8	10	9	12	9	10
Slow inactivation	V½ [mV]	-54.3 ± 1.0	-57.9 ± 1.1*	-56.3 ± 1.2	-59.3 ± 0.7*	-64.3 ± 0.9	-65.6 ± 0.8
	k	6.9 ± 0.4	6.9 ± 0.5	7.5 ± 0.3	7.6 ± 0.4	6.6 ± 0.3	6.3 ± 0.5
	n	11	10	10	7	7	7
Recovery from slow inactivation	t_1 [ms]	11.2 ± 1.80	11.8 ± 1.90	18.7 ± 7.70	25.4 ± 5.10	22.5 ± 2.80	21.3 ± 3.9
	A_1	0.57 ± 0.06	0.65 ± 0.07	0.23 ± 0.03	0.31 ± 0.07	0.52 ± 0.07	0.59 ± 0.07
	t_2 [ms]	90.7 ± 8.80	86.0 ± 14.6	178 ± 29.2	131 ± 13.8*	124 ± 8.00	111 ± 17.8
	A_2	0.49 ± 0.05	0.41 ± 0.07	0.79 ± 0.02	0.68 ± 0.08	0.48 ± 0.06	0.40 ± 0.07
	n	10	10	8	9	7	10

*Ion channel gating parameters of WT, R859H, or R865G at 40°C that significantly differ from the values obtained at 37°C are indicated as follows *P<0.05; **P<0.01; †P<0.001; ††P<0.0001*

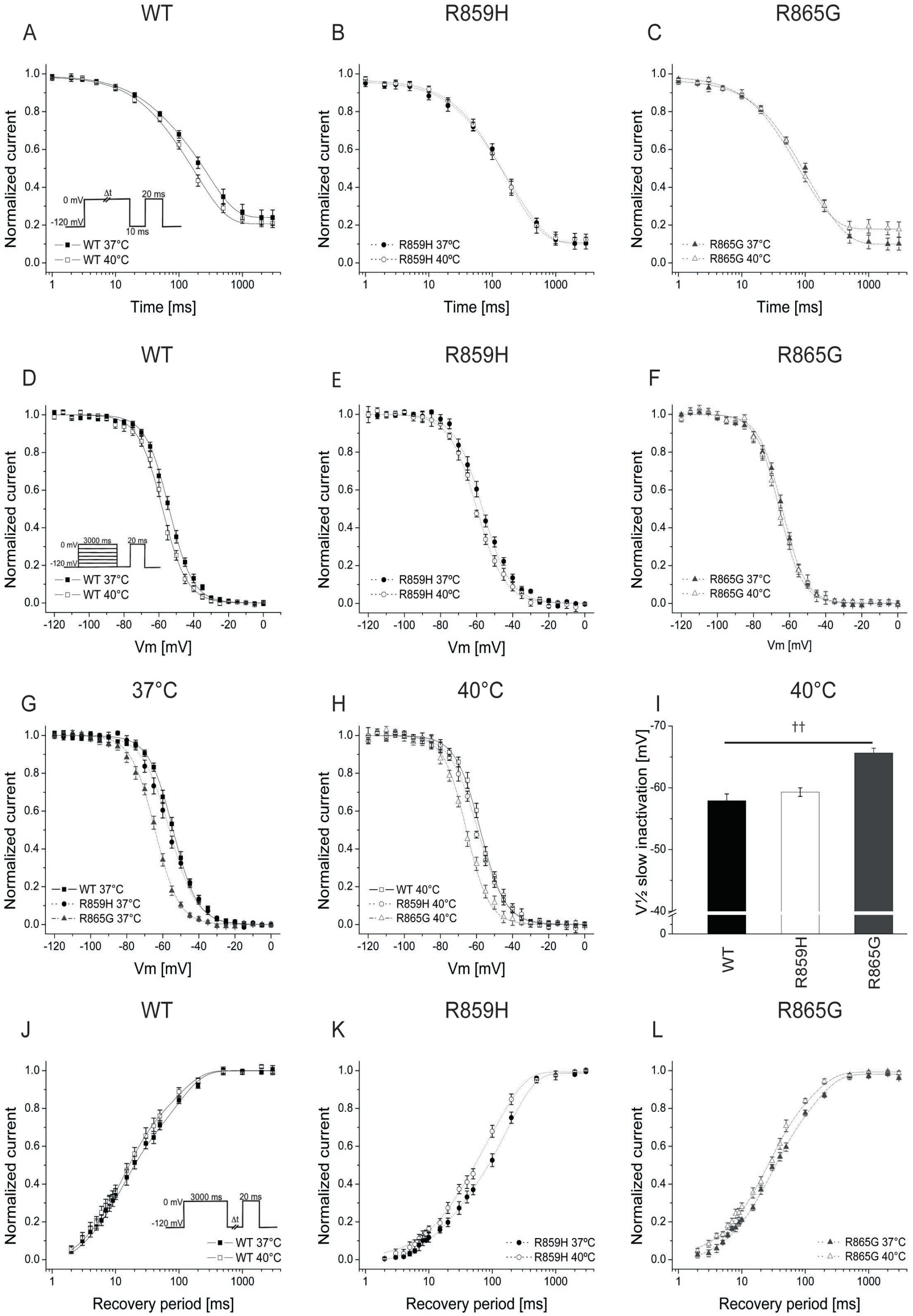
A
WT
Normalized current
Time [ms]
0 mV
Δt
20 ms
-120 mV
10 ms
WT 37°C
WT 40°C
B
R859H
R859H 37ºC
R859H 40ºC
C
R865G
R865G 37°C
R865G 40°C
D
WT
Vm [mV]
0 mV
3000 ms
20 ms
-120 mV
WT 37°C
WT 40°C
E
R859H
R859H 37ºC
R859H 40ºC
F
R865G
R865G 37°C
R865G 40°C
G
37°C
WT 37°C
R859H 37°C
R865G 37°C
H
40°C
WT 40°C
R859H 40°C
R865G 40°C
I
40°C
V½ slow inactivation [mV]
††
WT
R859H
R865G
J
WT
Recovery period [ms]
0 mV
3000 ms
20 ms
-120 mV
Δt
WT 37°C
WT 40°C
K
R859H
R859H 37ºC
R859H 40ºC
L
R865G
R865G 37°C
R865G 40°C

R859H and R865G exhibit divergent use-dependency at elevated temperatures

We tested the use-dependent behaviour of WT and mutant ion channels by applying a train of 2 ms depolarizing test pulses at various frequencies to mimic repetitive action potential firing. The use-dependency was analyzed by normalizing the peak sodium currents at the last test pulse with the currents generated at the first pulse (Figure 6). When temperature was increased to 40ºC, WT ion channels showed a trend toward decreased use-dependent decay in sodium currents (Figure 6A). In contrast, the R859H mutation caused a significant increase in use-dependence in the frequency range of 64Hz-143Hz (Figure 6B), while R865G showed a similar use-dependent behaviour at both temperatures (Figure 6C). At 37ºC, the use-dependency of R859H was significantly less use-dependent than WT and R865G, whereas R865G was similar as WT (Figure 6D). At 40ºC, R859H channels showed similar use-dependency as WT channels. The R865G mutation caused an increase in use-dependent behaviour at frequencies 20Hz to 40 Hz, and 80Hz to 143Hz compared to WT sodium channels (Figure 6E).

Figure 5.

Biophysical slow gating characteristics of $Na_v1.1$ WT, R859H, and R865G channels. (A-C) Time dependent entry into inactivation of (A) $Na_v1.1$ WT (37ºC, 40ºC), (B) R859H (37ºC, 40ºC) and (C) R865G (37ºC, 40ºC). Sodium channels were inactivated by a depolarizing pulse to 0 mV with varying duration between 1 to 3000 ms, allowed to recover from fast inactivation for 10 ms, followed by a depolarizing test pulse to 0 mV. (D-F) Steady-state voltage dependence of slow inactivation of (D) $Na_v1.1$ WT, (E) R859H and (F) R865G at 37ºC and 40ºC was assessed by applying depolarizing conditioning pulses of 3 seconds, starting from -120 mV, to 0 mV with increments of 5 mV. Cells were allowed to recover from fast inactivation for 10 ms before applying a 20 ms depolarizing test pulse to 0 mV. Peak currents of the test pulse were normalized to the peak currents obtained from the conditioning pulse and plotted against the duration of the conditioning pulse. (G-H) Comparison of the voltage the dependence of slow inactivation of WT and mutant channels at (G) 37ºC and (H) 40ºC. (I) The half maximal values of the voltage dependence of slow inactivation of WT, R859H, and R865G channels at 40ºC show a significant hyperpolarized shift for the R865G mutant (†† $P<0.0001$). WT and the R859H mutant showed a significant hyperpolarized shift in voltage dependence of slow inactivation at 40ºC (see also table 2). (J-L) Recovery from slow inactivation of (J) $Na_v1.1$ WT, (K) R859H and (L) R865G measured at 37ºC and 40ºC. Sodium channels were inactivated by a 3000 ms depolarizing pulse to 0 mV and allowed to recover for increasing time periods at -120 mV, before giving a 20 ms test pulse at 0 mV. Peak currents obtained from the test pulses were normalized to the peak currents obtained from the conditioning pulse and plotted against the recovery time.

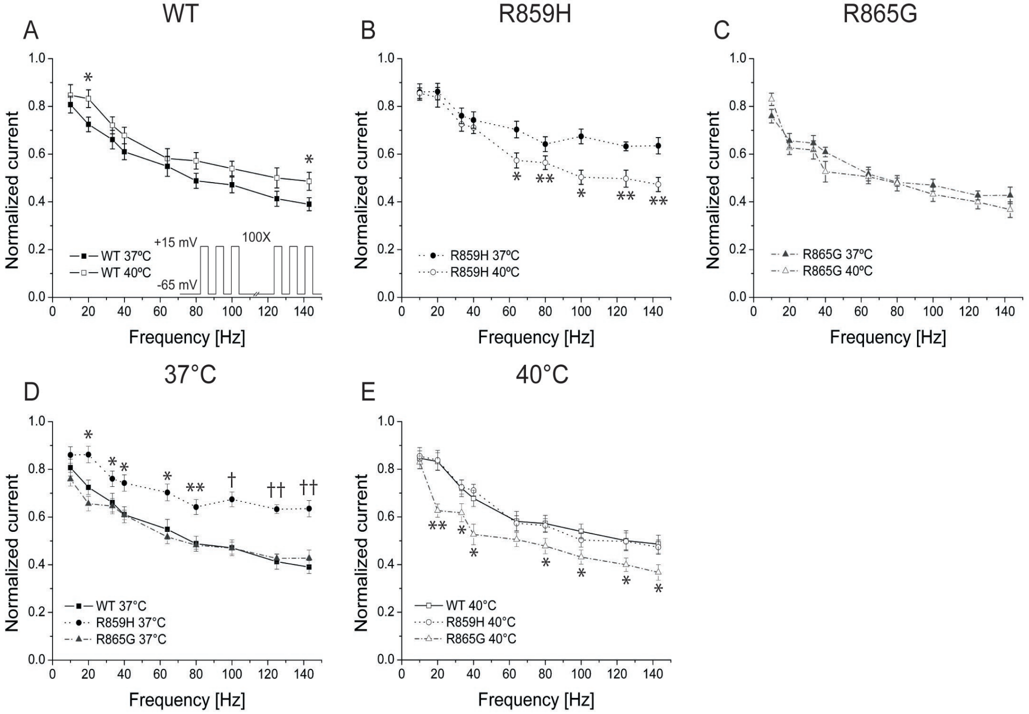

Figure 6.

*Use-dependent channel availability of (A) $\mathrm{Na_v}$1.1 WT (37ºC n=10; 40ºC n=7), (B) R859H (37ºC n=7; 40ºC n=6), and (C) R865G (37ºC n=7; 40ºC n=8) channels at 37ºC and 40ºC. Cells were given a train of 100 depolarizing pulses of 2 ms from a holding membrane potential of -65 mV to +15 mV at various frequencies. Peak sodium currents of the last pulse (100th) were normalized to the peak currents generated at the first pulse. WT channels showed a slight decreased use-dependency at 40ºC. In contrast, the GEFS+ mutant R859H showed a significant increase in use-dependency at frequency range 64Hz-143Hz, while the use-dependency of R865G was unaffected by febrile temperatures. (D-E) Comparison of the use-dependency of $\mathrm{Na_v}$1.1 WT, R859H, and R865G at (D) 37ºC and (E) 40ºC. At 37ºC, WT and R865G showed similar use-dependencies, while the use-dependency of R859H was decreased. At 40ºC, WT and R859H channels had similar use-dependencies, and the use-dependency of the R865G mutant at most frequencies was significantly increased. Values significantly different between WT and mutant ion channels (D and E) or between measurements at 37°C and 40°C (A-C) are indicated as follows *P<0.05; **P<0.01; †P<0.001; ††P<0.0001.*

Absence of increased persistent current in R859H and R865G mutants

In our previous characterization at room temperature, both mutants exhibited a significant increase in persistent current (Volkers et al. 2011). Since persistent current is rather common in GEFS+ and DS mutant channels at room temperature (Lossin et al., 2002; Rhodes et al., 2004), we examined the persistent current of these mutant channels at physiological and febrile temperatures. In contrast to our previous findings, both mutants had comparable small persistent currents as WT channels at elevated temperatures (Figure 7A-C).

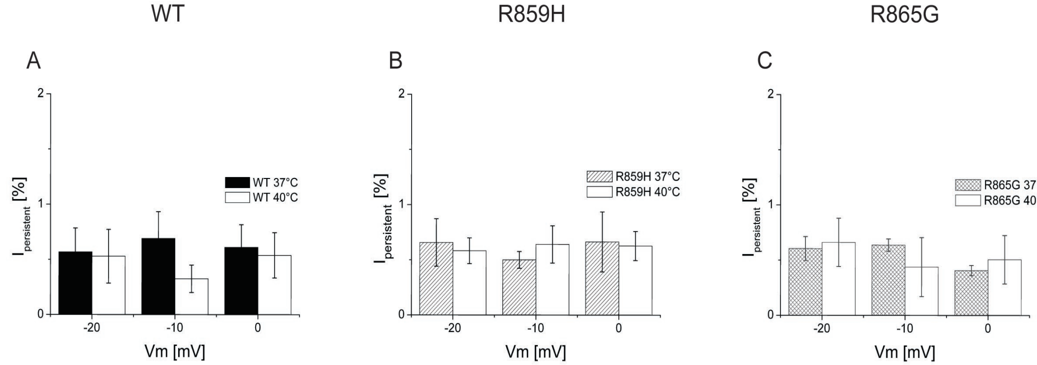

Figure 7.

Persistent current of (A) Na$_v$1.1 WT (37ºC and 40ºC n=4), (B) R859H (37ºC and 40ºC n=4), and (C) R865G (37ºC and 40ºC n=5) ion channels measured at 37°C and 40°C. Cells were given 100 ms depolarizing test pulses to -20 mV, -10 mV and 0 mV from a holding potential of -120 mV with and without TTX in the bath solution. Sodium currents recorded in the absence of TTX were digitally subtracted from currents obtained in the presence of TTX. The amplitude of the persistent current was measured at the last 10 ms of the 100 ms depolarizing pulse and normalized to the peak sodium current. No significant differences between Na$_v$1.1 WT and R859H or R865G mutants were found.

Discussion

Molecular defects in $Na_v1.X$ ion channels have been reported in association with temperature-sensitive disorders such as heat induced myotonia and cold induced paramyotonia linked to $Na_v1.4$ mutations; Brugada syndrome associated with $Na_v1.5$ mutations; and erythromelalgia, a disabling chronic pain disorder associated with mutations in the $Na_v1.7$ ion channel. $Na_v1.4$, $Na_v1.5$ and $Na_v1.7$ sodium ion channels are thermosensitive and mutations in these ion channel proteins can alter the temperature dependent gating of the channel (Dumaine et al., 1999; Han et al. 2007; Webb and Cannon, 2008; Carle et al. 2009; Samani et al. 2009).

Fever induced seizures are common in GEFS+ and DS subjects, and GEFS+ and DS mouse models showed increased seizure susceptibility at elevated body temperatures (Oakley et al., 2009; Martin et al., 2010). The physiological mechanisms behind the temperature dependent reduced seizure threshold are unclear. Reversible temperature-dependent trafficking defects in the $GABA_A$ γ2-subunit receptor - associated with GEFS+ - have been reported, which suggest that accelerated endocytosis could be caused by an abnormal folding of the receptor protein at elevated temperatures (Kang et al., 2006). Abnormal folding of the $Na_v1.1$ ion channel has also been shown for two SCN1A mutations at room temperature (Rusconi et al., 2007; Rusconi et al., 2009). This suggests that a lowered inhibition by GABAergic interneurons at febrile temperatures is a contributing factor to febrile seizures in individuals harboring a $Na_v1.1$ mutation. DS Scn1a mouse models already show drastically reduced sodium currents in GABAergic interneurons that cause action potential attenuation during repetitive firing (Yu et al., 2006; Ogiwara et al., 2007). In addition, Scn1a heterozygote animals also show markedly different effects depending on the genetic background, with one strain having a more severe phenotype compared to other strains (Yu et al., 2006). Also, truncation mutations in SCN1A in patients can lead to febrile seizures or GEFS+ instead of DS (Gennaro et al., 2003; Yu et al., 2010). These observations reflect the role of genetic background or modifier genes in the phenotypic outcome of DS patients. Additionally, the role of acute fever in triggering the seizure remains to be clarified.

Previous work on the R859H (GEFS+) and R865G (DS) mutant channels studied at room temperature demonstrated a gain-of-function in the voltage dependence of activation and a loss-of-function in recovery of fast inactivation for both mutants (Volkers et al., 2011). In addition, the R859H mutant also showed a loss-of-function in the voltage dependence and speed of inactivation. The current densities of I_{Na} carried by both mutated channels were comparable to WT. Although the slow inactivation behaviour of these channels was not investigated, the data recorded at room temperature suggest only small gating defects for the

R865G mutant that are insufficient to explain the severe phenotype of this patient. Therefore, in this study, we characterized the biophysical behaviour of these two mutants, R859H and R865G, at physiological and febrile temperature to mimic the pathophysiological condition at which these epileptic seizures are triggered.

Physiological and febrile temperatures (37ºC and 40ºC) unmasked a depolarized shift in the voltage dependence of inactivation (gain-of-function) of the R865G channel and a significant decrease in current density compared to WT channels, which was previously not detected at room temperature (Volkers et al., 2011). Opposite results were obtained for R859H channels, in where loss-of-function in voltage dependent channel availability found at room temperature was virtually abolished at 37ºC but unmasked again at 40ºC. In addition, the reduced speed of inactivation detected at room temperature was abolished at 37ºC and increased at 40ºC at -30 mV to -20 mV range. These results emphasize that caution should be used when extrapolating ion channel gating properties obtained at room temperature to 37ºC or 40ºC using a single scale factor. Moreover, our results underline the need of electrophysiological measurements at physiological and febrile temperatures to gather a better insight in the biophysical behaviour of $Na_v1.1$ WT and mutated ion channels.

At room temperature, the R859H and R865G mutations caused an enlarged persistent current (Volkers et al., 2011). Interestingly, this increase in persistent current was abolished completely at 37ºC and 40ºC. This suggests that the time dependent stabilization of the inactivation gate of $Na_v1.1$ channels is highly temperature sensitive and that these mutations hamper complete channel inactivation at lower temperatures. Whether the increased persistent sodium currents measured in other mutants associated with GEFS+ and DS (Lossin et al., 2002; Rhodes et al., 2004) can still be relevant at physiological and febrile temperatures remains to be determined.

Compared to WT and R859H channels, R865G show a more than 10 fold increase in window-current at both temperatures. The window-current occurs at a small range of voltages were sodium ion channels activate and inactivate incompletely. This activity can play an important role in the excitability of a neuron and an increase in window-current is predicted to increase channel function. After correction of liquid junction potentials of the patch pipettes (37ºC = 9.9 mV; 40ºC = 10 mV) the maximal window-current is in range of the resting membrane potential of a neuron (~-60 mV) and could reduce the threshold for initiating action potential firing in an inhibitory neuron that expresses R865G mutant sodium channels.

The voltage dependence of fast inactivation at 37ºC revealed two distinct gating processes in Na_v1.1 WT and mutant ion channels. The inactivation process present at a more negative voltage range is maybe not very significant, because of the hyperpolarized range it occurs at (Table 1; see V_2½). Interestingly, the voltage dependence of fast inactivation of WT Na_v1.4, Na_v1.5 and Na_v1.7 sodium channels at elevated temperatures show only one inactivation process (Han et al., 2007; Carle et al., 2009; Samani et al., 2009). This could indicate that the temperature dependent gating characteristics of Na_v1.1 WT ion channels differ between sodium ion channel isoforms.

A DS-like phenotype can be caused by decreased sodium currents in GABAergic inhibitory interneurons, as shown in Scn1a$^{+/-}$ DS mouse models (Yu et al., 2006; Ogiwara et al., 2007). In our experiments, the DS mutant R865G also showed an acute reduction in current density at a febrile temperature although the I_{Na} reduction is not as complete compared to the knock-out models. Nevertheless, the reduced neuronal inhibition could contribute to the epileptic severity in DS subjects harbouring an R865G mutation. In contrast, at febrile temperatures the WT sodium currents increase in magnitude and channel availability increases in parallel during repetitive stimulation (gain-of-function), both of which predict increased GABAergic inhibition and seizure suppression. This divergence in the inhibitory drive of the GABAergic network for WT versus R865G could inform as to the susceptibility of DS patients to febrile convulsions.l

In summary, our study indicates that febrile temperatures differentially change the gating of WT and mutated Na_v1.1 channels. For the GEFS+ mutant (R859H), we found a temperature dependent loss-of-function in the voltage dependence of inactivation and a use-dependent increase in channel availability during repetitive firing at 40ºC. We hypothesize that the decreased voltage dependent channel availability in combination with an increased use-dependency contributes to the development of febrile seizures in GEFS+ patients harbouring a R859H mutation. In the DS mutant R865G, despite the gain-of-function in the voltage dependence of activation and inactivation at 37ºC and 40ºC, febrile temperatures reduced peak sodium currents and decreased use-dependency compared to WT. This data suggests that fever-induced gating defects in combination with the biophysical ion channel alterations at elevated temperatures could contribute to the phenotypic outcome in DS patients with a R865G mutation. In addition, the faster entry into the slow inactivation state in combination with a loss-of-function in the voltage dependence of the slow inactivation of R865G at febrile temperatures suggests that prolonged membrane depolarization can ultimately lead to membrane inexcitability in GABAergic inhibitory neurons expressing this mutant and could explain the severe outcome in this DS subject.

References

Amin AS, Herfst LJ, Delisle BP, Klemens CA, Rook MB, Bezzina CR, Underkofler HA, Holzem KM, Ruijter JM, Tan HL, January CT, Wilde AA (2008) Fever-induced QTc prolongation and ventricular arrhythmias in individuals with type 2 congenital long QT syndrome. J Clin Invest 118, 2552-61

Carle T, Fournier E, Sternberg D, Fontaine B, Tabti N (2009) Cold-induced disruption of Na+ channel slow inactivation underlies paralysis in highly thermosensitive paramyotonia. J Physiol 587, 1705-714

Catterall WA, Kalume F, Oakley JC (2010) Nav1.1 channels and epilepsy. J Physiol 588,1 849-1859

Claes LR, Ceulemans B, Audenaert D, Smets K, Löfgren A, Del-Favero J, Ala-Mello S, Basel-Vanagaite L, Plecko B, Raskin S, thiry P, Wolf NI, Van Broeckhoven C (2003) De novo SCN1A mutations are a major cause of severe myoclonic epilepsy of infancy. Hum Mutat 21, 615-621

Claes LR, Deprez L, Suls A, Baets J, Smets K, van Dyck T, Deconinck T, Jordanova A, De Jonghe P (2009) The SCN1A variant database: a novel research and diagnostic tool. Hum Mutat 30, E904-920

Deprez L, Jansen A, De Jonghe P (2009) Genetics of epilepsy syndromes starting in the first year of life. Neurology 72,273-81

Dumaine R, Towbin JA, Brugada P, Vatta M, Nesterenko DV, Nesterenko VV, Brugada J, Brugada R, Antzelevitch (1999) Ionic Mechanisms Responsible for the Electrocardiographic Phenotype of the Brugada Syndrome Are Temperature Dependent. Circ Res 85, 803-809

Escayg A, MacDonald BT, Meisler MH, Baulac S, Huberfeld G, An-Gourfinkel I, Brice A, Leguern E, Moulard B, Chaigne D, Buresi C, Malafosse A (2000) Mutations of SCN1A, encoding a neuronal sodium channel, in two families with GEFS+. Nat Genet 24, 343-345

Gennaro E, Veggiotti P, Malacarne M, Madia F, Cecconi M, Cardinalli S, Cassetti A, Cecconi I, Bertini E, Bianchi A, Gobbi G, Zara F (2003) Familial severe myoclonic epilepsy of infancy: truncation of Nav1.1 and genetic heterogeneity. Epileptic Disord 5, 21-25

Han C, Lampert A, Rush AM, Dib-Hajj SD, Wang X, Yang Y, Waxman SG (2007) Temperature dependence of erythhromelalgia mutation L858F in sodium channel Nav1.7. Mol Pain 3:3

Kang JQ, Shen W, MacDonald RL (2006) Why does fever trigger febrile seizures? GABAA receptor 2 subunit mutations associated with Idiopathic Generalized Epilepsies have temperature dependent trafficking deficiencies. J Neurosci 26, 2590-2597

Lossin C (2009) A catalog of SCN1A variants. Brain Dev 31, 114-130

Lossin C, Wang DW, Rhodes TH, Vanoye CG, George AL Jr (2002) Molecular basis of an inherited epilepsy. Neuron 34, 877-884

Lossin C, Rhodes TH, Desai RR, Vanoye CG, Wang D, Carniciu S, Devinsky O, George AL Jr (2003) Epilepsy-Associated Dysfunction in the Voltage-Gated Neuronal Sodium Channel SCN1A. J Neurosci 23, 11289-11295

Martin MS, Dutt K, Papale LA, Dubé CM, Dutton SB, de Haan G, Shankar A, Tufik S, Meisler MH, Baram TZ, Goldin AL, Escayg A (2010) Altered function of the SCN1A voltage-gated sodium channel leads to gamma-aminobutyric acid-ergic (GABA-ergic) interneuron abnormalities. J Biol Chem 285, 9823-9834

Oakley JC, Kalume F, Yu FH, Scheuer T, Catterall WA (2009) Temperature-and age-dependent seizures in a mouse model of severe myoclonic epilepsy in infancy. Proc Natl Acad Sci USA 106, 3994-3999

Ogiwara I, Miyamoto H, Morita N, Atapour N, Mazaki E, Inoue I, Takeuchi T, Itohara S, Yanagawa Y, Obata K, Furuichi T, Hensch TK, Yamakawa K (2007) Nav1.1 localized to axons of parvalbumin-positive inhibitory interneurons: a circuit basis for epileptic seizures in mice carrying an Scn1a gene mutation. J Neurosci 27, 5903-5914

Ohmori I, Kahlig KM, Rhodes TH, Wang DW, George AL Jr (2006) Nonfunctional SCN1A is common in severe myoclonic epilepsy of infancy. Epilepsia 47, 1636-1642

Rhodes TH, Lossin C, Vanoye CG, Wang DW, George AL Jr (2004) Noninactivating voltage-gated sodium channels in severe myoclonic epilepsy of infancy. Proc Natl Acad Sci USA 101, 11147-11152

Rhodes TH Vanoye CG, Ohmori I, Ogiwara I, Yamakawa K, George AL Jr (2005) Sodium channel dysfunction in intractable childhood epilepsy with generalized tonic-clonic seizures. J Physiol 569, 433-445

Rusconi R, Combi R, Cestèle S, Grioni D, Franceschetti S, Dalprà L, Mantegazza M (2009) A rescuable folding defective Nav1.1 (SCN1A) sodium channel mutant causes GEFS+: common mechanism in Nav1.1 related epilepsies? Hum Mutat 30, E747-760

Rusconi R, Scalmani P, Cassulini RR, Giunti G, Gambardella A, Franceschetti S, Annesi G, Wanke E, Mantegazza M (2007) Modulatory proteins can rescue a trafficking defective epileptogenic Nav1.1 Na+ channel mutant. J Neurosci 27, 11037-11046

Samani K, Wu G, Ai T, Shuraih M, Mathuria NS, Li Z, Sohma Y, Purevjav E, Xi Y, Towbin JA, Cheng J, Vatta M (2009) A novel SCN5A mutation V1340I in Brugada syndrome augmenting arrhythmias during febrile illness. Hearth Rhythm 6, 318-326

Spampanato J, Escayg A, Meisler MH, Goldin AL (2001) Functional effect of two voltage-gated sodium channel mutations that cause generalized epilepsy with febrile seizures plus type 2. J Neurosci 21, 7481-7490

Spampanato J, Esacyg A, Meisler MH, Goldin AL (2003) Generalized epilepsy with febrile seizures plus type 2 mutations W1204R alters voltage-dependent gating of Na_v1.1 sodium channels. Neuroscience 116, 37-48

Spampanato J, Kearney JA, de Haan G, McEwen DP, Escayg A, Aradi I, MacDonald BT, Levin SI, Soltesz I, Benna P, Montalenti E, Isom LL, Goldin AL, Meisler MH (2004) A novel epilepsy mutation in the sodium channel SCN1A identifies a cytoplasmic domain for beta subunit interaction. J Neurosci 24, 10022-10034

Volkers L, Kahlig KM, Verbeek NE, Das, JHG, van Kempen MJA, Stroink H, Augustijn P, van Nieuwenhuizen O, Lindhout D, George AL Jr., Koeleman BPC, Rook MB (2011) Na_v1.1 Dysfunction in Genetic Epilepsy with Febrile Seizures Plus or Dravet Syndrome. Eur J Neurosci 34, 1268-1275

Webb J, Cannon SC (2008) Cold-induced defects of sodium channel gating in atypical periodic paralysis plus myotonia. Neurology 70, 755-761

Yu FH, Mantegazza M, Westenbroek RE, Robbins CA, Kalume F, Burton KA, Spain WJ, McKnight GS, Scheuer T, Catterall WA (2006) Reduced sodium current in GABAergic interneurons in a mousemodel of severe myoclonic epilepsy in infancy. Nat Neurosci 9, 1142-1149

Yu MJ, Shi YW, Gao MM, Liu XR, Chen L, Long YS, Yi YH, Liao WP (2010) Milder phenotype with SCN1A truncation mutation other than SMEI. Seizure 19, 443-445

General discussion

6

Different experimental methods are nowadays used to validate single gene mutations found in subjects diagnosed with epilepsy. These single genes of major effect are convenient in determining which critical pathways are involved in monogenic epilepsies and could help to determine what type of neurons and sort of gene mutations could play a role in complex epilepsies. In this chapter we aim to bridge the genotype phenotype gap in our current knowledge on the etiology of certain epilepsy types by 1) using our own results acquired from the functional studies described in CHAPTER 2-5, 2) highlighting recent pathophysiological findings and 3) discussing the use of different physiological tests in the epilepsy field.

Pathomechanism of KCNQ2 mutations in BFNE

In chapter 2 we studied the electrophysiological and biochemical properties of three mutated KCNQ2 ion channels associated with BFNE in a nonneuronal cell line. All three mutant channels showed decreased potassium currents. The V589X and T359K mutations are are expressed at the cell surface and compatible with loss of function defects while the P410fs12X mutation causes virtually complete impairment in trafficking to the cell surface (CHAPTER 3). Notably, since these mutants have not been tested in a neuronal assay, caution in interpreting the trafficking behavior of these ion channels is needed. Recently Chung and colleagues reported that several KCNQ2 mutations previously tested in non-neuronal cells also led to a reduced axonal surface expression due to mistargeting. Since axonal mistargeting of KCNQ2 ion channels could contribute to hyperexcitability in neurons leading to BFNE in neonates, further research on the trafficking, localization and integration of these three and other mutants in neurons is warranted.

The effect of temperature on channel gating

Molecular defects in Nav1.X ion channels have been reported in association with temperature-sensitive disorders such as heat induced myotonia and cold induced paramyotonia linked to $Na_v1.4$ mutations; Brugada syndrome associated with $Na_v1.5$ mutations; and erythromelalgia, a disabling chronic pain disorder associated with mutations in the $Na_v1.7$ ion channel. $Na_v1.4$, $Na_v1.5$ and $Na_v1.7$ sodium ion channels are thermosensitive and mutations in these ion channel proteins can alter the temperature dependent gating of the channel (Carle et al. 2009, Webb et al. 2008, Dumaine et al. 1999, Samani et al. 2009, Han et al. 2007).

It is likely that the influence of both genetic and environmental factors generate febrile seizures in the developing brain of infants. Febrile seizures can be triggered by fever, although other factors such as infection and cytokines may also be involved (Dubé et al. 2005, Heida JG. and Pittman QJ. 2005). Hyperthermia alone provokes seizures in young rodent pups (Holtzman et al. 1981, Bender et al. 2004, Tsai ML. and Leung LS. 2006) and children (Fukuda et al. 1997). Moreover, Dubé et al. demonstrated that different mouse strains exhibited different seizure susceptibility thresholds, suggesting that genetic factors are not necessary to cause febrile seizures but can greatly influence the severity (Dubé et al. 2005). In addition, temperature studies on invitro brain slices revealed widely varying effects of temperature on membrane properties, single spikes and spike bursts as well as excitatory and inhibitory postsynaptic potentials (Volgushev et al. 2000) supporting this hypothesis.

In CHAPTER 4 we described an electrophysiological characterization of one GEFS+ and three DS mutants performed at room temperature. The two DS mutants, R946C and R946H, produced nonfunctional channels, which is in concordance with the current DS mouse models (Yu et al. 2006, Ogiwara et al. 2007). The GEFS+ mutant showed mixed biophysical gating defects, i.e. a reduction in voltagedependent steadystate channel availability (loss of function), a delayed recovery from fast inactivation (loss of function), increased persistent current (gain of function), and a slower inactivation rate constant (gain of function). Interestingly, the third DS mutant (R865G) appeared to produce functional channels that exhibited predominantly gain-of-functions defects i.e. hyperpolarized shift in the voltage dependence of activation (gain of function) and an increased persistent current (gain of function), which cannot explain the severity observed in this DS subject.

Since the gating of the $Na_v1.1$ ion channel is probably temperature dependent, we sought to investigate the gating behavior of wildtype, R859H (GEFS+), and R865G (DS) at elevated temperatures. This study is described in CHAPTER 5.

Fever induced seizures are common in GEFS+ and DS subjects. Seizures at elevated body temperatures are also common in GEFS+ and DS mouse models. Compared to WT mice (44ºC), GEFS+ mice experienced seizures at an average increased body temperature of 43ºC and DS mice had temperatureinduced seizures at 39.5ºC (Martin et al. 2010, Oakley et al. 2009). The physiological mechanisms behind the temperature dependent reduced seizure threshold are unclear. In CHAPTER 5 we describe a detailed electrophysiological study of $Na_v1.1$ WT and GEFS+ (R859H) and DS (R865G) mutants at physiological and febrile temperatures. Our study indicates that febrile temperatures change the gating of WT and mutated $Na_v1.1$ channels in a temperature dependent manner. For the GEFS+ mutant (R859H), we found a temperature dependent loss-of-function in the voltage dependence of inactivation and an increased use-dependency during at 40ºC. We hypothesize that the decreased voltage dependent channel availability in combination with an increased use-dependency contributes to the development of febrile seizures in GEFS+ patients harboring a R859H mutation. In the DS mutant R865G, despite the gain-of-function in the voltage dependence of activation and inactivation at 37ºC and 40ºC, febrile temperatures reduced peak sodium currents and increased usedependency compared to WT. This data suggests that fever-induced gating defects in combination with biophysical ion channel alterations at elevated temperatures could contribute to the phenotypic outcome in the DS patient with a R865G mutation. In addition, the faster entry into the slow inactivation state in combination with a lossoffunction in the voltage dependence of the slow inactivation of R865G at febrile temperatures suggests that prolonged membrane depolarization can ultimately lead to membrane inexcitability in GABAergic inhibitory neurons expressing this mutant and could explain the severe outcome in this DS subject. Whether these gating defects are common in GEFS+ and DS patients at elevated temperatures needs to be determined in the nearby future by functionally testing more GEFS+ and DS mutants at these elevated temperatures.

Alternative splicing and sodium channel diversity

Sodium channel transcripts undergo alternative mRNA splicing, which is a cellular process that can be relevant to disease severity outcome, but complicates functional testing of SCN1A mutations. Alternative splicing of SCN1A leads to the incorporation of either exon 5N (‘neonatal’) or exon 5A (‘adult’). Exon 5N and 5A encode Na_v1.1 channels which are nearly identical (~67%) and only have a three amino acid difference in the DI S3-S4 region (Copley et al. 2004). This splicing event is conserved among neuronal ion channels Na_v1.2, Na_v1.3, Na_v1.6, and Na_v1.7, and the cardiac sodium channel Na_v1.5 (Plummer et al. 1997, Onkal et al. 2008, Gazina et al. 2010). Studies on the gating of Na_v1.1, Na_v1.2, and Na_v1.7 neonatal and adult isoforms revealed subtle gating differences (Jarecki et al. 2009, Liao et al. 2010, Thompson et al. 2011); gating differences between neonatal and adult isoforms harboring the same mutation were observed apart from the defects caused from the mutation. This implies that changes in neuronal excitability can be altered by alternative splicing, but gating differences are predominantly caused by individual mutations.

In the mouse Scn1a gene, the region corresponding to human exon 5N contains several stop codons and is not flanked by a splice site sequence at the 3′ end, making the adult $Na_v1.1$ isoform the only expressed transcript in mice (Gazina et al. 2010). Consequently, since the $Scn1a^{+/-}$ and $Scn1a^{R1648H/+}$ mouse models correctly represent DS and GEFS+ phenotypes respectively, the physiological relevance of human $Na_v1.1$ 5N in relation to epilepsy can be debated. However, Scn1a expression in rodents is detectable at embryonic day 10 (E10) and strongly upregulated during the first week of birth, peaking at postnatal day 15 (P15) (Beckh et al. 1989, Gazina et al. 2010), highlighting the importance of $Na_v1.1$ channel expression in the developing brain.

Another SCN1A alternative splicing event occurring in exon 11 produces either the full length isoform of 2009 amino acids or two shortened versions $Na_v1.1$[-33] and $Na_v1.1$[-84] that either lack 33 or 84 nucleotides respectively. These two isoforms have a shortened DIDII intracellular loop. $Na_v1.1$[-33] appears to be the dominant isoform highly expressed in the brain (Lossin et al. 2002), although scientific reports of this observation are lacking. Moreover, the D674G mutation in exon 11 is only present in the full length isoform and gives rise to a DS phenotype (Lossin C 2009, Claes et al. 2009), which suggests that a pathogenic mutation in only the full-length isoform is sufficient to develop DS. In summary, full length $Na_v1.1$ harboring exon 5A, appears to fully represent DS and GEFS+, and is therefore the most appropriate isoform to use for testing pathogenicity of SCN1A variants in mutation carriers and has therefore been used throughout CHAPTERS 4 and 5 of this thesis.

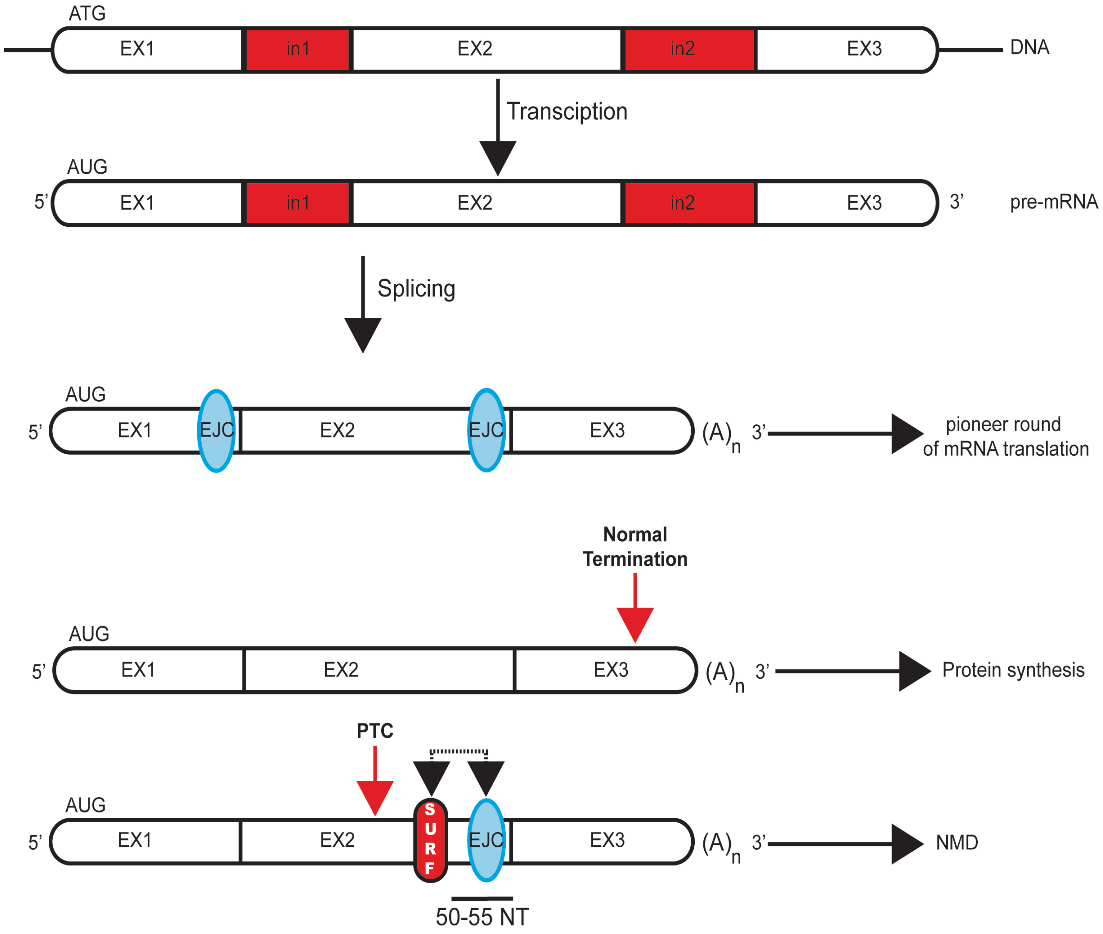
ATG
EX1
in1
EX2
in2
EX3
DNA
Transciption
AUG
5'
3'
pre-mRNA
Splicing
EJC
(A)n
pioneer round of mRNA translation
Normal Termination
Protein synthesis
PTC
SURF
NMD
50-55 NT

Figure 1.

Nonsense mediated mRNA decay (NMD). Premature termination codons (PTCs) located more than 50-55 nucleotides upstream of an exon exon junction within mRNA generally elicit NMD. Pre mRNA processing consists of co and post translational steps. The splicing of introns and ligation of the resulting exons results in the deposition of an exon junction complex (EJC) ~20-25 nucleotides upstream of each exon exon junction. Most mRNA undergo the first pioneer round of translation. If a PTC resides more than 50 55 nucleotides upstream of an exon exon junction, the UPF1, a component of the SURF complex, interacts with UPF2 (protein of EJC), which activates NMD. A transcript that does not contain a PTC or a PTC located less than 50-55 nucleotides of an exon exon junction, NMD will not occur, and the mRNA is stably being translated.

Nonsense mutations in coding sequences

Nonsense and frameshift mutations leading to a premature translationtermination codon (PTC) are commonly found in BFNE and DS subjects. In our current functional assays where mammalian cells are transfected with cDNA constructs, a protein harboring a PTC will express a truncated protein. Invivo, however, most of these mutated mRNAs are subjected to mRNA degradation through activation of the nonsensemediated mRNA decay (NMD) pathway (Tian M and Macdonald RL 2012, Figure 1). NMD is a quality control mechanism that activates the degradation of mRNAs harboring a PTC located more than 50-55 nucleotides upstream of the intron-exon splicing site (Figure 1) thereby reducing the protein synthesis of the mutated allele.

During pre-mRNA splicing and subsequent ligation of the resulting exons, a set of proteins known as the exon junction complexes (EJCs) are deposited 20-24 nucleotides upstream of exonexon junctions. Newly synthesized mRNAs undergo a first pioneer round of translation, wherein no protein is translated. In mammals, PTC recognition occurs during this pioneer translational round, in which the ribosome scans the mRNA strain for the presence of PTCs. mRNAs containing a PTC located more than 50-55 nucleotides upstream of an exon-exon junction will be subjected to mRNA decay. Two important protein complexes are involved during NMD, the SURF and EJC complex, containing the core proteins upf1, upf2 and upf3 of the NMD pathway. The SURF complex is composed of several proteins including upf1. The EJC consist of mRNA decay factors including upf2 and upf3, and act as a bridge to link upf1 and the EJC to activate the mRNA degradation pathway. The essence of EJC is highlighted by mRNAs harboring PTCs in the last exon of the transcript that have been shown to be immune to NMD (Nicholson et al. 2010). This has also been shown for intronless pre-mRNAs containing a PTC (Maquat LE 2004).

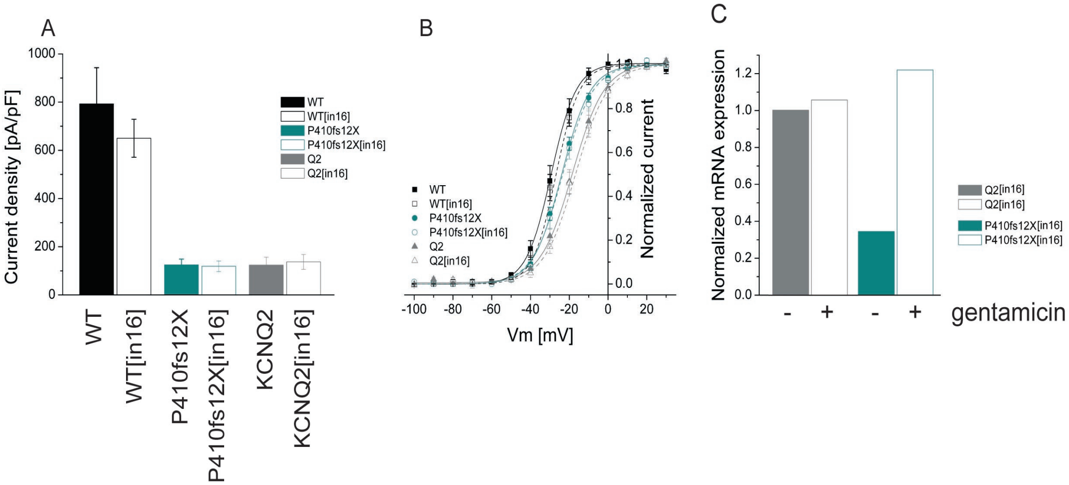

Figure 2.

Preliminary results of our in vitro NMD assay. The intron containing cDNA constructs in combination with either KCNQ2 or KCNQ2 and KCNQ3 were transfected in HEK293 cells and analyzed three days later. A) Current density measured in cells expressing WT (ratio KCNQ2:KCNQ3 2:2), WT[in16] (ratio KCNQ2[in16]:KCNQ3 2:2), P410fs12X (ratio P410fs12X:KCNQ2:KCNQ3 1:1:2), P410fs12X[in16] (ratio P410fs12X[in16]:KCNQ2:KCNQ3 1:1:2), and KCNQ2 and KCNQ2[in16] monomeres. Cells expressing WT, KCNQ2 and P410fs12X in combination with KCNQ2 harboring intron 16 showed similar current densities as WT, KCNQ2 and P410fs12X channels, which were previously characterized and described in CHAPTER 3. B) The voltage dependence of activation was analyzed from the same cells analyzed in figure A. The voltage dependence of activation of WT (V1/2=-28.4±1.9 mV, k=6.1±0.3, n=8), KCNQ2 (V1/2=-18.0±2.0 mV, k=8.5±0.5, n=7) and P410fs12X (V1/2=-23.9±1.5 mV, k=6.4±0.2, n=6) was comparable to their intron 16 containing cDNA counterparts WT[in16] (V1/2=-26.8±2.0 mV, k=6.1±0.2, n=6), KCNQ2[in16] (V1/2=-14.1±1.5 mV, k=6.4±0.2, n=6), and P410fs12X[in16] (V1/2=-23.4±0.8 mV, k=7.4±0.3, n=8). C) HEK293 cells were overexpressed with KCNQ2[in16] and P410fs12X[in16] in the presence or absence of 50 µg/ml gentamicin. mRNA was isolated three days after transfection and quantified using the 7900HT Fast Real-Time PCR System (Applied Biosystems, Nieuwerkerk a/d IJssel, the Netherlands). KCNQ2 mRNA levels were quantified with Taqman assay Hs01548342_m1 and each sample was standardized to mRNA level expression of the housekeeping gene Glucuronidase beta (GUSB; Hs99999908_m1). Furthermore, mRNA levels were normalized to KCNQ2[in16] mRNA expression in cells untreated with gentamicin. KCNQ2 mRNA expression in cells treated with or without gentamicin were comparable, while cells expressing P410fs12X[in16] showed a huge decrease in mRNA expression that could be restored with the addition of gentamicin. This indicates that P410fs12X transcripts are subjected to NMD and patients harboring the P410fs12X mutation would develop BFNC due to allelic haploinsufficiency. Notably, the data presented in figure C are preliminary results (n=1) and needs to be interpreted with cautiousness.

NMD cannot be detected in our current functional assays used to characterize the pathogenicity of a gene mutation, since the cDNA constructs do not contain intronic sequences necessary to generate premRNA and to create EJCs for the induction of NMD. We have investigated mRNA decay in our current KCNQ2 invitro assay by introducing intron 16 of KCNQ2 in our cDNA construct. Q2[in16] and P41012fsX[in16] were cotransfected with KCNQ3 in HEK293 cells and measured three days after transfection. Preliminary results (Figure 2A) showed a drastic reduction in total Mcurrent, which was comparable to the reduction seen in our previous functional cDNA invitro assay (CHAPTER 2). The voltage dependence of activation between WT and WT[in16], Q2 and Q2[in16], and P410fs12X and P410fs12X[in16] (Figure 2B) was comparable to our previous findings in chapter 3, indicating that intron containing cDNA constructs are functionally transcribed and translated and do not influence the gating of the potassium channels. To determine whether the reduced potassium current was caused by NMD, WT[in16] and P41012fsX[in16] were overexpressed in HEK293 cells with and without the antibiotic gentamicin and mRNA expression levels were quantified. Gentamicin is an aminoglycoside that prevents NMD suppressing PTC recognition by the ribosome during translation of mRNA, by selectively inducing ribosomal readthrough of premature but not normal termination codons (Howard et al. 1996). Our preliminary results confirmed that KCNQ2 mRNA levels were reduced in the P410fs12X PTC mutant, and could be restored by the application of 50 μg/ml gentamicin (Figure 2C). This indicates that this specific KCNQ2 transcript harboring the P410fs12X mutation could be subjected to NMD, thereby reducing the expression of the mutated allele.

GABA in neuronal network maturation and seizure susceptibility

Hippocampal sharp waves (SPWs) are the first patterned type of network activity generated by the hippocampus in-vivo during development. Spontaneous network events known as ‘giant depolarizing potentials’ (GDPs) are the in-vitro brainslice counterparts of early SPWs in rat and are generated by the synergistic excitatory action of GABA and glutamate on $GABA_A$ and AMPA receptors (Bolea et al. 1999, Lamsa et al. 2000).

Patchclamp recordings of CA1 hippocampal slices using selective glutamate and GABA receptor antagonists showed that GABAergic receptors and synapses are active before glutamatergic synapses (Walton et al. 1993, Chen et al. 1995, Köller et al. 1990). Moreover, during the maturation of GABA and glutamate synapses, the formation of glutamate synapses occurs in more developed neurons. In other words, in the developing brain $GABA_A$ synapses are formed first in the entire population of neurons before pyramidal neurons, providing a crucial role to interneurons in the control of network-driven patterns at an early developmental stage (Tyzio et al. 1999, Hennou et al. 2002).

Early in the postnatal brain, GABA acts as an excitatory instead of inhibitory neurotransmitter, which causes the spontaneous generation of GDPs (Figure 3). This polarity of GABA responses depends upon the intracellular chloride concentration in a neuron, which is mainly controlled by the action of NKCC1 and KCC2 chloride cotransporters. In the immature brain, NKCC1 expression determines a high intracellular chloride concentration, promoting depolarizing GABA responses. GABA acquires its hyperpolarizing (inhibitory) action via the progressive reduction of NKCC1 expression in parallel to a progressive enhanced action of KCC2 chloride exporter (Blaesse et al. 2009), leading to the disappearance of GDPs by the end of the first postnatal weeks. Several groups have shown the importance of NKCC1 and KCC2 expression in proper synapse formation and connectivity during the maturation of the brain and in seizure susceptibility.

Inhibition of Nkcc1 in-utero blocks early SPWs in neonatal rats. In particular, Nkcc1 is required for the depolarizing action of GABA in immature CA3 pyramidal neurons, and thereby promotes the spontaneous burst activity of individual immature CA3 pyramids (Sipilä et al. 2006). Moreover, in Nkcc1$^{-/-}$ mice this early spontaneous electrical activity is severely affected and showed a transiently delayed maturation of glutamatergic and GABAergic synapses in CA1 neurons, without leading to morphological defects (Pfeffer et al. 2009). In addition, Nkcc1 knockout mice showed an increased threshold to thermal stimulation (Sung et al. 2000), indicating that decreased intracellular chloride accumulation increase thermal response thresholds.

Rodent Kcc2 is expressed in both cortical pyramidal neurons and interneurons (Blaesse et al. 2009) and extrudes chloride from a neuron to establish adult concentration of intracellular chloride. Neonatal Kcc2$^{-/-}$ hippocampal slices have a higher density of GABAergic and glutamatergic synapses and generate spontaneous and evoked epileptiform activities (Khalilov et al. 2011). In addition, KCC2 is down regulated in tissue from human adults with epilepsy (Cohen et al. 2002). Moreover, Kcc2 hypomorphic mice, a mouse model that expresses ~17% of the potassium chloride transporter Kcc2, showed reduced sensitivity to thermal stimuli (Tornberg, et al. 2005, Sung et al. 2000). In general, the above observations on NKCC1 and KCC2 confirm the importance of chloride transporters in chloride homeostasis during neuronal maturation in the developing brain and suggest the formation of a seizure susceptibility window during the developmental switch.

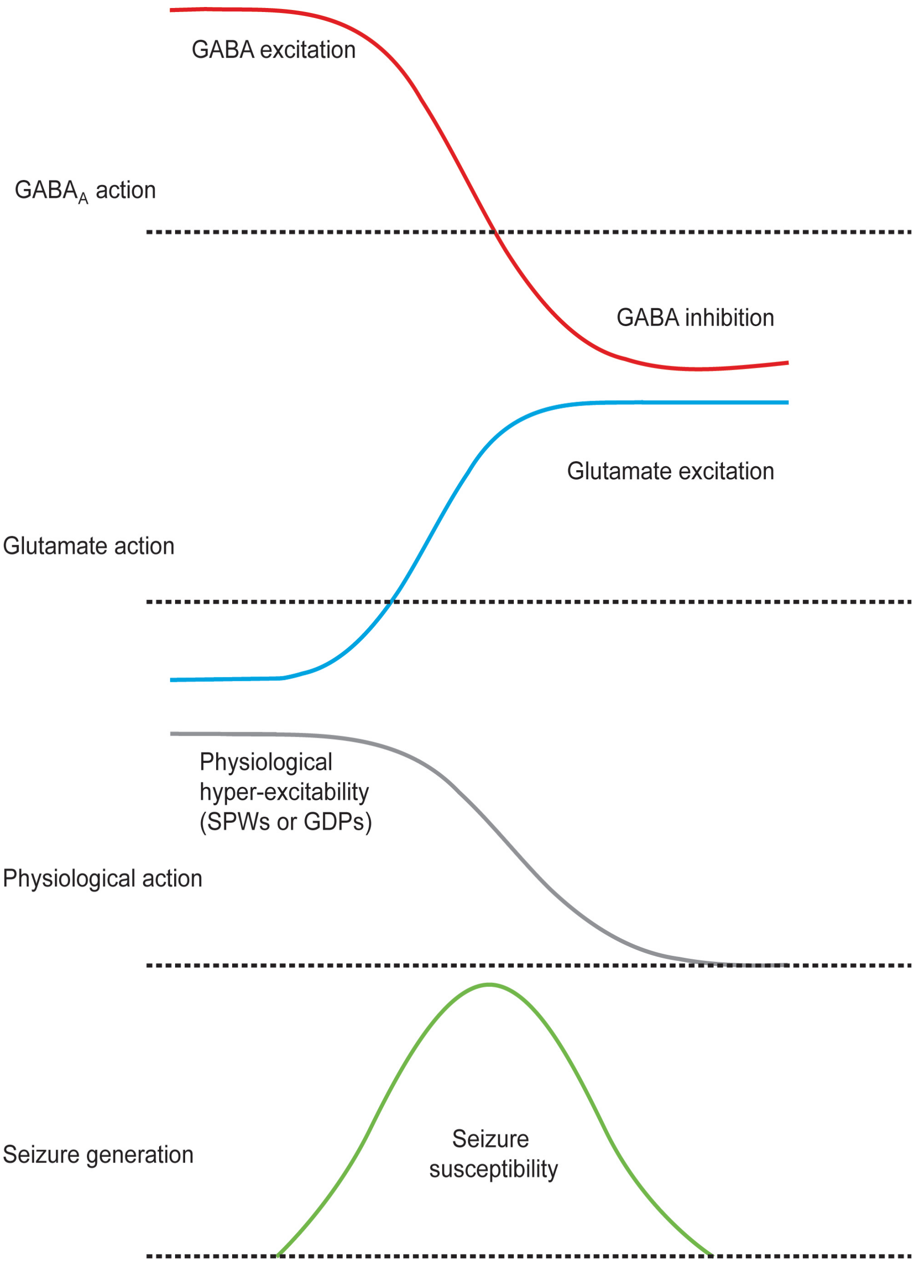
GABA excitation
GABA$_A$ action
GABA inhibition
Glutamate excitation
Glutamate action
Physiological hyper-excitability (SPWs or GDPs)
Physiological action
Seizure susceptibility
Seizure generation

Figure 3.

Developmental polarity shift of the GABAergic response during maturation of the rat brain in hippocampal slices. Seizure susceptibility (green) is highest when GABA actions (red) are less excitatory but not yet inhibitory, while the glutamatergic synapse density (aquamarine) is close to that of adults. Thus, seizures will be readily generated and propagated as a result of a relatively dense glutamatergic network.

Apart from NKCC1 and KCC2, the developmental polarity switch of the GABAergic response in the immature brain also appears to be regulated by GABA itself, since the developmental switch can be prevented by blocking $GABA_A$ receptors or accelerated by increasing $GABA_A$ receptor activity (Ganguly et al. 2001). Furthermore, depolarization by GABA activates sodium channels that generate GDPs that are important in synapse strengthening and neuronal network connectivity (Thompson et al. 1979, Shatz et al. 1990, BenAri Y. and Spitzer NC. 2004, BenAri Y. 2001), suggesting a prominent role for GABA signaling during postnatal brain development (Owens DF. and Kriegstein AR. 2002). Moreover, as $GABA_A$ signaling is critical for brain development and early synaptogenesis (Cancedda et al. 2007, Nakanishi et al. 2007, Wang et al. 2011), a dysfunctional GABA receptor mediated pathway may cause miswiring that could predispose subjects to epileptic seizures. This has already been demonstrated in the Scn1a$^{+/-}$ DS mouse model; reduced sodium current densities in GABAergic inhibitory neurons caused reduced frequency in action potentials that would lead to a reduced GABA release and thereby impair inhibitory neurotransmission (Yu et al. 2006).

As previously mentioned, increased thermal susceptibility for seizures is common in the immature brain (Schuchmann et al. 2009). This susceptibility is caused by a reduction in inhibitory postsynaptic currents (IPSC) in neonatal CA1 neurons (Qu et al. 2007). The reduced IPSCs produce an age-dependent depression of GABAergic synaptic transmission, which leads to a loss of inhibition in the immature hippocampus (Qu et al. 2009). Whether GABAergic depression in the hippocampus causes the increased thermal seizure susceptibility observed in Scn1a$^{+/-}$ (DS) (Oakley et al. 2009) and Scn1a$^{R1648H/+}$ (GEFS+) (Martin et al. 2010) mouse models needs to be determined. Nevertheless, thermally induced myoclonic and generalized tonicclonic seizures in Scn1a knockout mice can be suppressed by the administration of stiripentol (enhancing GABAergic transmission) in one-month-old mice (Coa et al. 2012), which suggests that febrile seizure susceptibility could be generated by decreased GABA concentrations in the synaptic cleft.

The decreased GABAergic neurotransmission hypothesis can be further extrapolated to other epilepsy mouse models. In the Scn1a$^{+/}$- mouse models, recording of isolated hippocampal and cortical neurons showed drastically reduced sodium currents in GABAergic interneurons causing action potential attenuation during repetitive firing (Ogiwara et al. 2007, Yu et al. 2006), while the R1648H knockin mouse model showed increased use-dependent channel inactivation that would lead to decreased GABAergic inhibition (Martin et al. 2010). The Scn1a$^{R1648H/+}$ model only shows a mild GEFS+ phenotype, which can be exacerbated by crossbreeding this model with the transgenic Scn2a^{Q54} mice that have a gain-of-function in $Na_v1.2$. These Scn1a$^{R1648H/+}$/Scn2a^{Q54} double mutants exhibit early onset severe epilepsy and juvenile lethality. This phenotypic outcome may be caused by the combination of increased excitability of pyramidal neurons due to the gain of function in SCN2A and decreased GABAergic inhibition in the Scn1a$^{R1648H/+}$ mice, that will lead to decreased GDPs in neonates causing decreased synaptic connectivity and thus decreased synaptic transmission. Similarly, it has been shown that loss of Mcurrent in Kcnq2$^{V182M/+}$ mice results in hyperexcitability of hippocampal pyramidal CA1 neurons (Singh et al. 2008). The mild phenotype observed in these mice, possibly caused by reduced dampening of GDPs during the developmental stage, parallels the benign epileptic phenotype of most of the BFNC patients. Moreover, introducing a larger defect in synaptogenesis during brain maturation by crossbreeding the Kcnq2$^{V182M/+}$ mice with Scn1a$^{R1648H/+}$ mice that have reduced GABAergic neurotransmission resulted in spontaneous generalized seizures and decreased lifespan significantly (Hawkins et al. 2011).

In summary, these double mouse model mutants highlight the importance of a balanced excitation/inhibition activity during postnatal development and hint towards disturbed synaptogenesis as part of the pathogenic mechanism of epilepsy. Nevertheless, future studies are warranted to establish the precise pathogenic mechanisms in these animal models.

Phenotypic spectrum of epilepsy and genetic background

For SCN1A mutations, DS is sometimes observed in GEFS+ families, while identical KCNQ2 mutations can give rise to the very mild BFNE as well as neonatal or infantile encephalopathy (Marini et al. 2010, Weckhuysen et al. 2012). Animals heterozygous for Scn1a mutations also show markedly different effects depending on the genetic background, with some strains having a more severe phenotype and sporadic death compared to other strains (Yu et al. 2006, Ogiwara et al. 2007). These observations reflect the role of genetic background or modifier genes in the phenotypic outcome of DS patients. Previous studies have shown that mice carrying a loss of function mutation in Scn8a could counteract the reduced seizure threshold and premature lethality of heterozygous Scn1a knock-out mice (Martin et al. 2007). In contrast, concomitant loss of function of either Scn2a or Kcnq2 ion channels can exacerbate the clinical manifestation of GEFS+ in the Scn1a$^{R1648H/+}$ mouse model (Hawkins et al. 2011). An increased disease severity has also been observed for transgenic Scn2a^{Q54} mice crossbred with mice that have a loss of Kv7.2 channel function; the epileptic phenotype changed from a mild lateonset epilepsy to a severe generalized epilepsy with early onset and lethality (Kearney et al. 2006). Also some DS cases have been described in which the mutation was inherited by an asymptomatic or mildly affected parent, suggesting that the expression of the mutated gene was modified due to environmental and/or genetic factors. In some exceptional cases this resulted from germline or somatic SCN1A mosaicism (Depienne et al. 2006, Gennaro et al. 2006, Marini et al. 2006, Morimoto et al. 2006). In addition, SCN9A variants are found in a few DS subjects harboring a SCN1A mutation suggesting SCN9A as a modifier gene that could influence the severity outcome in epilepsy patients (Singh et al. 2009). Another possible explanation for the differences in disease severity in this epileptic spectrum is that genetic alterations in regulatory sites outside the coding region of a gene can enhance or suppress the expression of the normal or affected allele, yielding more or less mutant proteins which could lead to a benign or severe disease outcome (Emison et al. 2010, Musunuru et al. 2010, Lee et al. 2012, Figure 4).

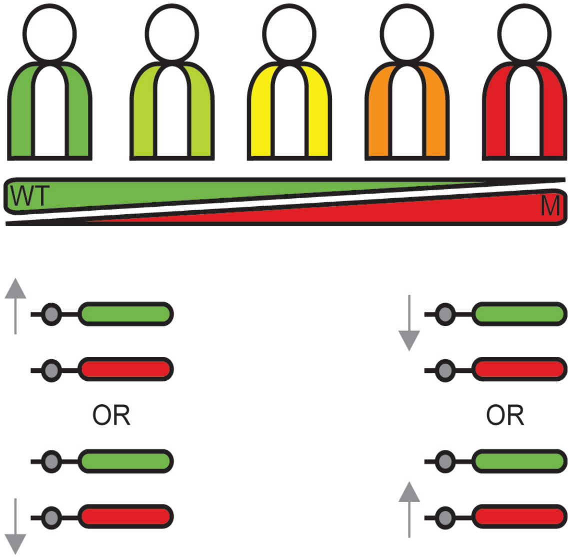

Figure 4.
Allelic expression of wildtype (WT) and mutant (M) alleles can differ in subjects, which can create a spectrum of epileptic phenotypes ranging from mild to severe within an epileptic syndrome. A rare variation or common polymorphism in regulatory elements, indicated as gray circles located upstream of the start codon, can influence the expression of wildtype or mutant alleles. The higher the expression of the mutant allele is, the more severe the disease outcome will be.

Functional in-vitro assays

Animal models of epilepsy can be used to model the complexity of epilepsy and can be used to study the functional effects of a specific gene mutation in a neuronal network, in cell type specific neurons and on molecular levels. Despite all the advantages in-vivo experiments have, in-vitro expression systems do permit a faster analysis of mutants and thus faster screening and functional analysis of several mutations. However, the functional properties of voltage-gated channels depend on the cell type in which they are studied, complicating the interpretation of defects in heterologous systems. For example, in Xenopus oocytes, some type of cloned neuronal α-units form functional channels that inactivate and recover from inactivation an order of magnitude slower than sodium channels in neurons (Krafte et al. 1990). In mammalian cell lines, α-units form fast-inactivating channels, even in the absence of β-subunits, although the gating of the channels still depends on cell background. For example, co-expression of β-subunits shift the voltage dependence of steady state $Na_v1.2$ channel inactivation to more negative potentials in CHO cells (Isom et al. 1995), but to more positive potentials in tsa201 cells (Qu et al. 2001). This is also true for the $Na_v1.3$ persistent current measured in HEK293 cells, which is completely abolished in CHO cells (Cheng et al. 2000). Moreover, a mutated $Na_v1.7$ transfected in neurons produced hyperexcitability in sensory neurons and hypoexcitability in sympathetic neurons. These differences are due to the selective presence of $Na_v1.8$ in sensory neurons that is sequentially activated after activation of $Na_v1.7$ (Rush et al. 2006). Similar to Xenopus oocytes, cell lines are single-cell expression systems that do not form synapses and do not allow the direct study of the effect that the mutations have on synaptic transmission. A solution could be the use of induced neuronal (iN) cells from patients. These iN cells have been generated by expressing neuron specific transcription factors in mouse fibroblasts and showed that in culture they form functional synapses and generate action potentials (Vierbuchen et al. 2010). Another method to generate iN cells is the microRNA-mediated conversion of human fibroblasts to neurons (Yoo et al. 2011). These in-vitro models are already used to study the disease mechanisms behind genetic diseases such as amyotrophic lateral sclerosis (ALS) and are promising techniques to study the functional consequences of mutations in neuronal genes in a neuronal background in combination with the genetic signature of the patient. Of note, these iN cells possess a rather immature transcription pattern instead of a mature background. On the other hand, BFNE as well as febrile seizures predominantly occur in the immature brain (Hauser et al. 1993, Kotsopoulos et al. 2002) making the use of iN cells a promising functional assay. Thus, in addition to being a promising in-vitro assay, iN cells may also become a potent research tool for elucidating the underlying etiology of epilepsy, including the determination of seizure susceptibility and synaptogenesis under normal and hyperthermic conditions, and in determining the putative positive pharmacological effects of novel anti-epileptic drugs.

References

Beckh S, Noda M, Lübbert H, Numa S. (1989) Differential regulation of three sodium channel messenger RNAs in the rat central nervous system during development. EMBO J. 8:36113616

BenAri Y. (2001) Developing networks play a similar melody. Trends Neurosci. 24:353360

BenAri Y, Spitzer NC. (2004) Nature and nurture in brain development. Trends Neurosci 27:361

Bender RA, Dube C, Baram TZ. (2004) Febrile seizures and mechanisms of epileptogenesis: insights from an animal model. Adv Exp Med Biol. 548:213225

Blaesse P, Airaksinen MS, Rivera C, Kaila K. (2009) Cationchloride cotransporters and neuronal function. Neuron 61:820838

Bolea S, Avignone E, Berretta N, SanchezAndres JV, Cherubini E. (1999) Glutamate controls the induction of GABA-mediated giant depolarizing potentials through AMPA receptors in neonatal rat hippocampal slices. J Neurophysiol. 81:2095-2102

Cao D, Ohtani H, Ogiwara I, Ohtani S, Takahashi Y, Yamakawa K, Inoue Y. (2012) Efficacy of stiripentol in hyperthermiainduced seizures in a mouse model of Dravet syndrome. Epilepsia doi: 10.1111/j.1528-1167.2012.03497.x.

Cancedda L, Fiumelli H, Chen K, Poo MM. (2007) Excitatory GABA action is essential for morphological maturation of cortical neurons in vivo. J Neurosci. 27:52245235

Carle T, Fournier E, Sternberg D, Fontaine B, Tabti N (2009) Cold-induced disruption of Na+ channel slow inactivation underlies paralysis in highly thermosensitive paramyotonia. J Physiol 587: 1705714

Chen G, Trombley PQ, van den Pol AN. (1995) GABA receptors precede glutamate receptors in hypothalamic developments; differential regulation by astrocytes. J Neurophysiol. 74:14731484

Chen YH, Dale TJ, Romanos MA, Whitaker WR, Xie XM, Clare JJ. (2000) Cloning, distribution and functional analysis of the type III sodium channel from human brain. Eur J Neurosci. 12:42814289

Chung HJ, Jan YN, Jan LY. (2006) Polarized axonal surface expression of neuronal KCNQ channels is mediated by multiple signals in the KCNQ2 and KCNQ3 Cterminal domain. Proc Natl Acad Sci. U.S.A. 103:88708875

Claes LR, Deprez L, Suls A, Baets J, Smets K, Van Dyck T, Deconinck T, Jordanova A, De Jonghe P. (2009) 10:E904920

Cohen I, Navarro V, Clemenceau S, Baulac M, Miles R. (2002) On the origin of interictal activity in human temporal lobe epilepsy in vitro. Science 298:14181421

Copley RR. (2004) Evolutionary convergence of alternative splcing in ion channels. Trends Genet. 20:171176

Depienne C, Arzimanoglou A, Trouillard O, Fedirko E, Baulac C, SaintMartin C, Ruberg M, Dravet C, Nabbout R, Baulac M, GourfinkelAn I, LeGeurn E. (2006) Parental mosaicism can cause recurrent transmission of SCN1A mutations associated with Severe Myoclonic Epilepsy of Infancy. Hum Mutat. 27:389

Dubé C, Vezzani A, Behrens M, Bartfai T, Baram TZ. (2005) Interleukin1beta contributes to the generation of experimental febrile seizures. Ann Neurol. 57:152155

Dumaine R, Towbin JA, Brugada P, Vatta M, Nesterenko DV, Nesterenko VV, Brugada J, Brugada R, Antzelevitch (1999) Ionic Mechanisms Responsible for the Electrocardiographic Phenotype of the Brugada Syndrome Are Temperature Dependent. Circ Res. 85:803809

Emison ES, GarciaBarcelo M, Grice EA, Lantieri F, Amiel J, Burzynski G, Fernandez RM, Hao L, Kashuk C, West K, Miao X, Tam PK, Griseri P, Ceccherini I, Pelet A, Jannot AS, de Pontual L, HenrionCaude A, Lyonnet S, Verheij JB, Hofstra RM, Antiñolo G, Borrego S, McCallion AS, Chakravarti A. (2010) Differential contributions of rare and common, coding and noncoding Ret mutations to multifactorial Hirschsprung disease liability. Am J Hum Genet. 87:6074

Fukuda M, Morimoto T, Nagao H, Kida K. (1997) Clinical study of epilepsy with severe febrile seizures and seizures induced by hot water bath. Brain Dev. 19:212216

Ganguly K, Schinder AF, Wong ST, Poo M. (2001) GABA itself promotes the developmental switch of neuronal GABAergic responses from excitation to inhibition. Cell 105:521532

Gazina EV, Richards KL, Mokhtar MB, Thomas EA, Reid CA, Petrou S. (2010) Differential expression of exon 5 splice variants of sodium channel alpha subunit mRNAs in the developing mouse brain. Neuroscience 166:195200

Gennaro E, Santorelli FM, Bertini E, Buti D, Gaggero R, Gobbi G, Lini M, Granata T, Freri E, Parmeggiani A, Striano P, Veggiotti P, Cardinali S, Bricarelli FD, Minetti C, Zara F. (2006) Somatic and germline mosaicisms in severe myoclonic epilepsy of infancy. Biochem Biophys Res Commun 341:489493

Han C, Lampert A, Rush AM, Dib-Hajj SD, Wang X, Yang Y, Waxman SG (2007) Temperature dependence of erythhromelalgia mutation L858F in sodium channel Nav1.7. Mol Pain 3:3

Hauser WA, Annegers JF, Kurland LT. (1993) Incidence of epilepsy and unprovoked seizures in Rochester, Minnesota. Epilepsia 3:453468

Hawkins NA, Martin MS, Frankel WN, Kearney JA, Escayg A. (2011) Neuronal voltagegated channels are genetic modifiers of generalized epilepsy with febrile seizures plus. Neurobiol Dis. 41:655660

Heida JG, Pittman QJ. (2005) Causal links between brain cytokines and experimental febrile convulsions in the rat. Epilepsia 46:19061913

Hennou S, Khalilov I, Diabira D, BenAri Y, Gozlan H. (2002) Early sequential formation of functional GABA(A) and glutamatergic synapses on CA1 interneurons of the rat foetal hippocampus. Eur J Neurosci. 16:197208

Holtzman D, Obana K, Olson J. (1981) Hyperthermiainduced seizures in the rat pup: a model for febrile convulsions in children. Science 213:10341936

Howard M, Frizzell RA, Bedwell DM. Aminoglycoside antibiotics restore CFTR function by overcoming premature stop mutations. Nat Med. 2:467469

Isom LL, Scheuer T, Brownstein AB, Ragsdale DS, Murphy BJ, Catterall WA. (1995) Functional coexpression of the beta 1 and type IIA alpha subunits of sodium channels in a mammalian cell line. J Biol Chem. 270:33063312

Jarecki BW, Sheets PL, Xiao Y, Jackson JO, Cummins TR. (2009) Alternative splicing of Nav1.7 exon 5 increases the impact of the painful PEPD mutant channel I1461T. Channels 3:259267

Kearney JA, Yang Y, Beyer B, Bergren SK, Claes L, Dejonghe P, Frankel WN. (2006) Severe epilepsy resulting from genetic interaction between Scn2a and Kcnq2. Hum Mol Genet. 15:1043:1048

Khalilov I, Chazal G, Chudotvorova I, Pellegrino C, Corby S, Ferrand N, Gubkina O, Nardou R, Tyzio R, Yamamoto S, Jentsch TJ, Hübner CA, Gaiarsa JL, BenAri Y, Medina I. (2011) Enhanced synaptic activity and epileptiform events in the embryonic KCC2 deficient hippocampus. Front Cell Neurosci. 5:23

Köller H, Siebler M, Schmalenbach C, Müller HW. (1990) GABA and glutamate receptor development of cultured neurons from rat hippocampus, septal region, and neocortex. Synapse 5:5964

Kotsopoulos IA, van Merode T, Kessels FG, de Krom MC, Knottnerus JA. (2002) Systemic review and metaanalysis of incidence studies of epilepsy and unprovoked seizures. Epilepsia 43:14021409

Krafte DS, Goldin AL, Auls VJ, Dunn Rj, Davidson N, Lester HA. (1990) Inactivation of cloned Na channels expressed in Xenopus oocytes. J Gen Physiol 96:689706

Lamsa K, Palva JM, Ruusuvuori E, Kaila K, Taira T. (2000) Synaptic GABAA activation inhibits AMPAkainate receptor-mediated bursting in the newborn (P0-P2) rat hippocampus. J Neurophysiol 83:359-366 (2000)

Lee JH, Silhavy JL, Lee JE, AlGazali L, Thomas S, Davis EE, Bielas SL, Hill KJ, Iannicelli M, Brancati F, Gabriel SB, Russ C, Logan CV, Sharif SM, Bennettt CP, Abe M, Hildebrandt F, Diplas BH, AttiéBitach T, Katsanis N, Rajab A, Koul R, Sztriha L, Water ER, GerroNovick S, Woods CG, Johnson CA, Valente EM, Zaki MS, Gleeson JG. (2012) Evolutionarily assembled cisregulatory module at a human ciliopathy locus. Science 335:966969

Liao X, Deprez L, Maljevic S, Pitsch J. Claes L, Hristova D, Jordanova A, AlaMello S, BellanKoch A, Blazevic D, Schubert S, Thomas EA, Petrou S, Becker AJ, De Jonghe P, Lerche H. (2010) Molecular correlates of agedependent seizures in an inherited neonatalinfantile epilepsy. Brain 133:1403141

Lossin C, Wang DW, Rhodes TH, Vanoye CG, George AL Jr. (2002) Molecular basis of an inherited epilepsy. Neuron 34:877884

Lossin C. (2009) A catalog of SCN1A variants. Brain Dev. 31:114130

Maquat LE. (2004) Nonsensemediated mRNA decay: splicing, translation and mRNP dynamics. Nat Rev Mol Cell Biol. 5:8999

Marini C, Mei D, Cross JH, Geurrini R. (2006) Mosaic SCN1A mutation in familial Severe Myoclonic Epilepsy of Infancy. Epilepsia 47:17371740

Marini C, Mantegazza M. (2010) Na+ channelopahties and epilepsy: recent advances and new perspectives. 3:371384

Martin MS, Tang B, Papale LA, Yu FH, Catterall WA, Escayg A. (2007) The voltagegated sodium channel Scn8a is a genetic modifier of severe myoclonic epilepsy of infancy. Hum Mol Genet 16:28922899

Martin MS, Dutt K, Papale LA, Dubé CM, Dutton SB, de Haan G, Shankar A, Tufik S, Meisler MH, Baram TZ, Goldin AL, Escayg A. (2010) Altered function of the SCN1A voltagegated sodium channel leads to gammaaminobutyric acidergic (GABAergic) interneuron abnormalities. J Biol Chem. 285:98239834

Morimoto M, Mazaki E, Nishimura A, Chiyonobu T, Sawai Y, Murakami A, Nakamura K, Inoue I, Ogiwara I, Sugimoto T, Yamakawa K. (2006) SCN1A mutation mosaicism in a family with Severe Myoclonic Epilepsy in Infancy. Epilepsia 47:17321736

Musunuru K, Strong A, FrankKamenetsky M, Lee NE, Ahfeldt T, Sachs KV, Li X, Li H, Kuperwasser N, Ruda VM, Pirruccello JP, Muchmore B, ProkuninaOlsson L, Hall JL, Schadt EE, Morales CR, LundKatz S, Phillips MC, Wong J, Cantley W, Racie T, Ejebe KG, OrhoMelander M, Melander O, Koetliansky V, Fitzgerald K, Krauss RM, Cowan CA, Kathiresan S, Rader DJ. (2010) From noncoding variant to phenotype via SORT1 at the 1p13 cholesterol locus. Nature 466:714719

Nakanishi K, Yamada J, Takayama C, Oohira A, Fukuda A. (2007) NKCC1 activity modulates formation of functional inhibitory synapses in cultured neocortical neurons. Synapse 61:138149

Nicholson P, Yepiskoposyan H, Metze S, Zamudio Orozco R, Kleinschmidt N, Muhlemann O. (2010) Nonsensemediated mRNA decay in human cells: mechanistic insights, functions beyond quality control and the doublelife of NMD factors. Cell Mol Life Sci. 67:677700

Oakley JC, Kalume F, Yu FH, Scheuer T, Catterall WA. (2009) Temperature and agedependent seizures in a mouse model of severe myoclonic epilepsy in infancy. Proc Natl Acad Sci U.S.A. 106:39943999

Ogiwara I, Miyamoto H, Morita N, Atapour N, Mazaki E, Inoue I, Takeuchi T, Itohara S, Yanagawa Y, Obata K, Furuichi T, Hensch TK, Yamakawa K. (2007) Nav1.1 localizes to axons of parvalbuminpositiv inhibitory interneurons: a circuit basis for epileptic seizures in mice carrying an Scn1a gene mutation. J Neurosci. 27:59025914

Onkal R, Mattis JH, Fraser SP, Diss JK, Shao D, Okuse K, Djamgoz MB. (2008) Alternative splicing of Nav1.5: an electrophysiological comparison of ‘neonatal’ and ‘adult’ isoforms and critical involvement of a lysine residue. J Cell Physiol. 216:716726

Owens DF, Kriegstein AR. (2002) Is there more to GABA than synaptic inhibition? Nat Rev Neurosci. 3:715727

Pfeffer CK, Stein V, Keating DJ, Maier H, Rinke I, Rudhard Y, Hentschke M, Rune GM, Jentsch TJ, Hübner CA. (2009) NKCC1dependent GABAergic excitation drives synaptic network maturation during early hippocampal development. J Neurosci. 29:34193430

Plummer NW, McBurney MW, Meisler MH. (1997) Alternative splicing of the sodium channel SCN8A predicts a truncated twodomain protein in fetal brain and nonneuronal cells. J Biol Chem 272:2400824015

Qu L, Liu X, Wu C, Leung LS. (2007) Hyperthermia decreases GABAergic synaptic transmission in hippocampal neurons of immature rats. Neurobiol Dis. 27:320327

Qu L, Leung LS. (2009) Effects of temperature elevation on neuronal inhibition in hippocampal neurons of immature and mature rats. J Neurosci Res. 87:27732785

Qu Y, Curtis R, Lawson D, Gilbride K, Ge P, DiStedano PS, SilosSantiago I, Catterall WA, Scheuer T. (2001) 18:570580

Rush AM, DibHajj SD, Liu S, Cummins TR, Black JA, Waxman SG. (2006) A single sodium channel mutation produces hyper of hypoexcitability in different types of neurons. Proc Natl Acad Sci. U.S.A. 103:82458250

Samani K, Wu G, Ai T, Shuraih M, Mathuria NS, Li Z, Sohma Y, Purevjav E, Xi Y, Towbin JA, Cheng J, Vatta M (2009) A novel SCN5A mutation V1340I in Brugada syndrome augmenting arrhythmias during febrile illness. Hearth Rhythm 2009; 6: 318326

Schuchmann S, Vanhatalo S, Kaila K. (2009) Neurobiological and physiological mechanism of feverrelated epileptoform syndromes. Brain Dev. 31:378382

Shatz CJ. (1990) Impulse activity and the patterning of connections during CNS development. Neuron 5:745756

Singh NA, Otto JF, Dahle EJ, Pappas C, Leslie JD, Vilaythong A, Noebels JL, White HS, Wilcox KS, Leppert MF. (2008) Mouse models of humand KCNQ2 and KCNQ3 mutations for benign familial neonatal convulsions show seizures and neuronal plasticity without synaptic reorganization. J Physiol. 586:34053423

Singh NA, Pappas, C, Dahle EJ, Claes LR, Pruess TH, De Jonghe P, Thompson J, Dixon M, Pfeiffer A, White HS, Filloux F, Leppert MF. (2009) A role of SCN9A in human epilepsies, as a cause of febrile seizures and as a potential modifier in Dravet syndrome. PLoS Genet. 5: e1000649. doi:10.1371/journal.pgen.1000649

Sipilä AT, Schuchmann S, Voipo J, Yamada J, Kaila K. (2006) The cationchloride cotransporter NKCC1 promotes sharp waves in the neonatal rat hippocampus. J Physiol. 573:765773

Sung KW, Kirby M, McDonald MP, Lovinger DM, Delpire E. (2000) Abnormal GABAA receptormediated currents in dorsal root ganglion neurons isolated from NaK2Cl cotransporter. J Neurosci. 20:75317538

Thompson W, Kuffler DP, Jansen JK. (1979) The effect of prolonged, reversible block of nerve impulses on the elimination of polyneuronal innervation of newborn rat skeletal muscle fibers. Neuroscience 4:271281

Thompson CH, Kahlig KM, George AL Jr. (2011) SCN1A splice variants exhibit divergent sensitivity to commonly used antiepileptic drugs. Epilepsia 52:10001009

Tian M, Macdonald RL. (2012) The intronic GABRG2 mutations, IVS6+2T□G, associated with childhood absence epilepsy altered subunit mRNA intron splicing, activated Nonsensemediated decay, and produced a stable truncated g2 subunit. J Neurosci. 32:59375952

Tornberg J, Voikar V, Savilahti H, Rauvala H, Airaksinen MS. (2005) Behavioural phenotypes of hypomorphic KCC2deficient mice. Eur J Neurosci. 21:13271337

Tsai ML, Leung LS. (2006) Decrease of hippocampal GABA B receptormediated inhibition after hyperthermiainduced seizures in immature rat. Epilepsia 47:277287

Tyzio R, Represa A, Jorquera I, BenAri Y, Gozlan H, Aniksztejn L. (1999) The establishment of GABAergic and glutamatergic synapases on CA1 pyramidal neurons is sequential and correlates with the development of the apical dendrite. J Neurosci. 19:1037210282

Vierbuchen T, Ostermeier A, Pang ZP, Kokubu Y, Sudhof TC, Wernig M. (2010) Direct conversion of fribroblasts to functional neurons by defined factors. Nature 463:1035:1041

Volgusehv M, Vidyasagar TR, Chistiakova M, Eysel UT. (2000) Synaptic transmission in the neocortex during reversible cooling. Neuroscience 98:922

Walton MK, Schaffner AE, Barker JL. (1993) Sodium channels, GABAA receptors, and glutamate receptors develop sequentially on embryonic rat spinal cord cells. J Neurosci. 13:20682084

Wang DD, Kriegstein AR. (2011) Blocking early GABA depolarization with bumetanide results in permanent alterations in cortical circuits and sensorimotor gating deficits. Cereb Cortex 21:574578

Webb J, Cannon SC (2008) Cold-induced defects of sodium channel gating in atypical periodic paralysis plus myotonia. Neurology 70:755761

Weckhuysen S, Mandelstam S, Suls A, Audenaert D, Deconinck T, Claes LRF, Deprez L, Smets K, Hristova D, Yordanova I, Jordanova A, Ceulemans B, Jansen A, Hasaerts D, Roelens F, Lagae L, Yendle S, Stanley T, Heron SE, Mulley JC, Berkovic SF, Scheffer IE, de Jonghe P. (2012) KCNQ2 encephalopathy: emerging phenotype of a neonatal epileptic encephalopathy. Ann Neurol. 71:1525

Yoo AS, Sun AX, Li L, Shcheglovitov A, Portmann T, Li Y, LeeMesser C, Dolmetsch RE, Tsien RW, Crabtree GR. (2011) MicroRNAmediated conversion of human fibroblasts to neurons. Nature 476:228:231

Yu FH, Mantegazza M, Westenbroek RE, Robbins CA, Kalume F, Burton KA, Spain WJ, McKnight GS, Scheuer T, Catterall WA. (2006) Reduced sodium current in GABAergic interneurons in a mouse model of severe myoclonic epilepsy in infancy. Nat. Neurosci. 9:11421149

Summary

7

Epilepsy

Epilepsy is a chronic neurological disorder characterized by spontaneous, repeatable attacks or seizures and in more severe cases patients will lose consciousness. The familial component in epilepsy has been recognized since the time of Hippocrates. However, epilepsy can also occur via specific neurological events during life, or a combination of these two causes. The identification of the first gene linked to idiopathic epilepsy in 1995, has led to a series of discoveries that gradually reveal the molecular basis of epilepsy. Most gene mutations in epilepsy are found in genes that code for ion channels and receptors. These are protein structures that are incorporated into the cell membrane and are responsible for ion transport and selective passage of specific ions such as sodium, potassium, calcium, or chloride. The ion channel activity is determined by changes in membrane voltages or by the binding of an agonist to a nearby receptor. The combination of multiple and different ion channels determine the neuronal action potential. Mutations in these ion channels can disturb the excitability of neurons and may cause epilepsy. Remarkably, a single ion channel gene mutation can lead to different types of epilepsies via abnormal ion channel functioning. Chapter 1 in this thesis addresses the structure and function of different ion channels in combination with the role ion channels can play in epilepsy.

There are a variety of epilepsy syndromes, categorized according to age of onset, seizure type and other clinical data, such as electroencephalogram (EEG) and imaging (MRI and CT scan). The epileptic features are genetically determined, but environmental factors can also play a role in the development of epilepsy.

The most prevalent epilepsy syndrome is febrile seizures, with a prevalence of approximately 3% in young children. Febrile seizures is a selflimiting disorder, age of onset < 5 years, and is triggered by an elevated body temperature. Children, after the age of 6 years, that develop epileptic seizures without fever are diagnosed with genetic epilepsy with febrile seizures plus (GEFS+). Epileptic syndromes that occur during the first year of life are more difficult to categorize into local and generalized epilepsies, due to the immaturity of the young brain. A few epileptic syndromes with a first year onset are: benign familial neonatal epilepsy (BFNE), benign familial neonatalinfantile seizures (BFNIS), and benign familial infantile seizures (BFIS). The names refer to the age of onset. A severe infantile form of epilepsy, which starts around the 6th month of life, is Dravet syndrome and is considered to be a severe form of GEFS+. Dravet syndrome is characterized by prolonged febrile convulsions at a very young age, followed by a heterogenous pattern of epileptic seizures and severe developmental regression later in life.

Chapter 2-5 in this thesis describe fundamental research of novel gene mutations found in subjects diagnosed with BFNE, or GEFS+ and Dravet syndrome to gain more insight in the etiology and treatment of these epileptic disorders.

BFNE and KCNQ2

The genes KCNQ2 and KCNQ3 encode for $K_v7.2$ $K_v7.3$ asubunits of voltage dependent potassium channels. Homomeric ($K_v7.2$ or Kv7.3) and heteromeric ($K_v7.2$ and $K_v7.3$) potassium channels have the electrophysiological characteristics of M-channels. The M-current is a noninactivating potassium current, mediated via muscarinic receptors, that activates during prolonged membrane depolarizations, and plays an important role in dampening action potential firing of a neuron. Mutations in KCNQ2 and KCNQ3 were found in BFNE families; most mutations were reported in KCNQ2.

Most mutations in KCNQ2 are localized in the C-terminus. The C-terminus harbors several domains that are involved in asubunit assembly. Chapter 2 describes an electrophysiological and molecular study of novel $K_v7.2$ Cterminal mutations found in BFNE patients. The most consistent result of these mutated asubunits is a complete lossoffunction, which is caused by either a biophysical loss of function or a trafficking defect to the cell membrane. Besides these two mechanisms, chapter 6 (general discussion) provides a third, namely that KCNQ2 transcripts harboring a premature stop codon could be subjected to mRNA degradation.

Chapter 3 describes a short study of the importance of the assembly domain in the C-terminus of homomeric $K_v7.2$ α-subunits.

SCN1A in GEFS+ and Dravet syndroom

The primary role of voltage gated sodium ion channels is the initiation and propagation of action potentials. This points to Na+ sodium channels as crucial determinants of neuronal excitability. The sodium channel family consists of nine sodium channel genes (SCN1A-SCN11A) that encode for sodium α-subunits ($Na_v1.1$-$Na_v1.9$). Mutations in SCN1A cause a spectrum of epileptic phenotypes, ranging from mild GEFS+ to severe Dravet syndrome. Mutations that give rise to GEFS+ result in changes in the voltage dependency and/or kinetics of the $Na_v1.1$ ion channel, while a complete loss of channel function in inhibitory interneurons is common in Dravet syndrome.

Chapter 4 describes a clinical and electrophysiological study of novel SCN1A missense mutants, R859H (GEFS+), and the Dravet syndrome mutations R865G, R946C, R946H. The GEFS+ mutant shows divergent gating defects, including gain and loss of Nav1.1 channel function. The Dravet syndrome mutants R946C and R946H produce nonfunctional channels, which is in concordance with current literature. The R865G mutant, on the other hand, produces functional channels. R865G shows differences in the voltage dependence and kinetics of the channel. Both mutants, R859H and R865G, also exhibited a slowing in the recovery of fast inactivation. These two mutants clearly show that a mutation in the sodium ion channel can either cause gain or loss of channel function. Nevertheless, the changes in channel kinetics and voltage dependency do not explain the differences between the mild phenotype of the GEFS+ patients and the severe epileptic outcome in the patient with Dravet syndrome.

Fever plays a crucial role in the onset of GEFS+ and Dravet syndrome. Since the above-mentioned functional research was conducted at room temperature, chapter 5 describes an electrophysiological characterization of the two Nav1.1 mutants R859H and R865G at 37°C and 40°C. When temperature is raised to 40°C, both mutants as well as wildtype channel show differences in the voltage dependency and channel kinetics. Interestingly, compared to 37°C, R859H and R865G show different changes in channel gating compared to wildtype at febrile temperatures. R859H channels have decreased voltage dependent channel availability and an increased usedependency of channel availability at 40°C, which in combination with the other gating defects could lead to GEFS+. The R865G mutant shows a significant reduction in sodium current density and decreased use-dependency of channel availability. These channel defects, together with the other channel defects could lead to a nonexcitable neuron after long depolarizations, which cause Dravet syndrome.

Future perspectives

Chapter 6, general discussion, discusses the advantages and disadvantages of the common invitro asssay used throughout this thesis. The research conducted in chapter 2-5 was done with easy to transfect mammalian kidney cells. These cell lines are single cell expression systems that do not posses a neuronal background and are unable to generate action potentials. In-vivo, neurons function in a network that consists of excitatory and inhibitory cells. Also, when using mammalian cell lines as a functional assay, the influences of the genetic background on the epileptic outcome in patients are not been taken into account. To overcome these limitations of nonneuronal in-vitro assays, one could use neuronal cells derived from induced pluripotent stemcells (iPS); these cells are obtained from fibroblasts of epilepsy patients that are subsequently transduced with reprogramming factors.

Conclusion

Most genetically determined epilepsies are caused by gene mutations in genes that encode for ion channels and receptors. Functional analysis of these protein mutants shows changes in voltage dependency and/or kinetics or a complete loss of channel function via different mechanisms. Nevertheless, the severity of the epileptic seizures is not only determined by a specific gene mutation, but genetic background, modifying genes and genetic compensatory factors are playing a crucial role in the phenotypic outcome of patients.

8

Samenvatting

Epilepsie

Epilepsie is een chronische neurologische aandoening die gekarakteriseerd wordt door spontane, herhaalde aanvallen van stuiptrekkingen die al dan niet met bewustzijnsverlies gepaard kunnen gaan. Sinds de tijd van Hippocrates is een erfelijke component van epilepsie al erkend. Epilepsie kan ook ontstaan na een specifieke neurologische gebeurtenis gedurende het leven, of door een combinatie van deze twee oorzaken. De identificatie van het eerste gen voor idiopathische epilepsie in 1995 heeft geleid tot een serie van ontdekkingen die geleidelijk helpt om de moleculaire basis van epilepsie te ontrafelen. De meeste mutaties die geassocieerd zijn met epilepsie zijn tot nu toe gevonden in genen die coderen voor ionkanalen en receptoren voor signaalstoffen tussen zenuwcellen. Ionkanalen zijn eiwitstructuren in de celmembraan die verantwoordelijk zijn voor transport van ionen over de celmembraan, en meestal selectief doorgankelijk zijn voor één bepaald ion, zoals natrium, kalium, calcium, of chloor. De activiteit van het ionkanaal of de receptor wordt bepaald door onder andere de membraanspanning of door binding van een agonist aan een nabijgelegen receptor. Deze ionkanalen en receptoren zorgen samen voor de totstandkoming van de neuronale actiepotentiaal. Wanneer één van deze eiwitten gemuteerd is, kan dat leiden tot een abnormale kanaalfunctie wat kan leiden tot bepaalde epilepsiesyndromen. Hoofdstuk 1 van dit proefschrift geeft een algemene inleiding over de functies en structuren van verschillende ionkanalen, evenals de rol van deze gemuteerde ionkanalen bij het ontstaan van epilepsie.

Epilepsiesyndromen worden onderverdeeld in subcategorieën bepaald door onder meer de leeftijd waarop de eerste aanval zich manifesteert, het aanvalspatroon en andere klinische kenmerken zoals het electroencefalogram (EEG) en beeldvorming van de hersenen (MRI and CTscan) kenmerken. Deze kenmerken worden veroorzaakt door genetische of verkregen factoren. Bij veel patiënten spelen ook bekende en naar vermoed wordt nog onbekende milieufactoren een rol bij het ontwikkelen van epilepsie.

Met een frequentie van ongeveer 3% in de algemene bevolking vormen koortsstuipen een meest voorkomende vorm van epileptische aanvallen. Koortsstuipen worden overigens in de meeste classificaties van epilepsie als een aparte categorie, niet als ene vorm van epilepsie, benoemd. Koortsstuipen zijn doorgaans een zelflimiterende afwijking, waarbij alleen kinderen jonger dan 5 jaar stuipen krijgen na een verhoogde lichaamstemperatuur. Wanneer deze kinderen op latere leeftijd aanvallen krijgen zonder een stijging in lichaamstemperatuur, in het bijzonder ook wanneer koortsstuipen en of epilepsie ook in de naaste familie voorkomen, is er vaak sprake van een gegeneraliseerde epilepsie met koortsstuipen (Generalised Epilepsy with Febrile Seizures plus other seizures, GEFS+). Epilepsiesyndromen die in het eerste levensjaar beginnen zijn lastiger onder te verdelen in gelokaliseerde en generaliseerde epilepsie; hierbij speelt de immaturiteit van het jonge brein een rol. Een groep epilepsiesyndromen die in het eerste levensjaar voorkomen zijn: Benign Familial Neonatal Epilepsy (BFNE), Benign Familial NeonatalInfantile Seizures (BFNIS), en Benign Familial Infantile Seizures (BFIS) waarbij de naamgeving equivalent is aan de periode in het eerste levensjaar wanneer de eerste aanval plaats vond. Een ernstige infantiele vorm van epilepsie, waarbij de eerste aanvallen gemiddeld rond de 6de maand beginnen bij koorts, al dan niet na een vaccinatie, is Dravet syndroom. Dravet syndroom kan gezien worden als een zeer ernstige vorm van GEFS+ en wordt gekarakteriseerd door langdurige koortsstuipen op zeer jonge leeftijd, gevolgd door een heterogeen patroon van epileptische aanvallen en een ernstige achterstand in de ontwikkeling. HOOFDSTUKKEN 2-5 in dit proefschrift beschrijven functioneel fundamenteel onderzoek van genmutaties gevonden in patiënten gediagnosticeerd met BFNE, GEFS+ en Dravet syndroom om meer inzicht te krijgen in het ontstaan en de behandeling van deze epilepsie syndromen.

BFNE en KCNQ2

KCNQ2 en KCNQ3 coderen voor de K_v7.2 en K_v7.3 asubunits van spanningsafhankelijke kalium ionkanalen. Homomere (K_v7.2 of K_v7.3) en heteromere (K_v7.2 en K_v7.3) ionkanalen hebben de electrofysiologische karakteristieken van Mkanalen. De Mstroom is een door muscarine receptoren gemedieerde niet inactiverende kalium stroom, die geactiveerd wordt tijdens langdurige depolarisaties, en speelt een belangrijke rol bij het dempen van een vurend neuron. Mutaties in KCNQ2 en KCNQ3 zijn geïdentificeerd in aangedane BFNEfamilies, met het merendeel van de gerapporteerd mutaties in KCNQ2.

De meeste mutaties in KCNQ2 zijn gelokaliseerd in de C-staart van het gen. De C-staart herbergt verschillende domeinen en is betrokken bij asubunit assemblage van het K_v7.2 eiwit. Hoofdstuk 2 beschrijft een functionele studie van nieuw ontdekte Kv7.2 C-staart mutaties gevonden in BFNS patiënten. Het meest consistente resultaat bij het testen van deze eiwitmutaties is een volledig verlies van kanaalfunctie. Dit kanaalverlies wordt veroorzaakt door een volledig biofysisch functieverlies of door een verstoord transport van gemuteerde ionkanaaleiwitten naar het celmembraan. Naast deze twee mechanismes wordt in HOOFDSTUK 6 (algemene discussie) een derde beschreven, namelijk dat gemuteerde KCNQ2 transcripten met een prematuur stopcodon ook blootgesteld kunnen worden aan mRNA afbraak.

In HOOFDSTUK 3 wordt een korte studie aan de C-staart van de K_v7.2 α-subunit beschreven. Daarbij is gekeken naar het belang van het assemblagedomein met betrekking tot het vormen van K_v7.2 homomeren.

SCN1A in GEFS+ en Dravet syndroom

De primaire rol van spanningsafhankelijke natrium ionkanalen is de initiatie en voortgeleiding van actiepotentialen. Hierdoor zijn Na+ ionkanalen cruciale determinanten van neuronale prikkelbaarheid. Er zijn in totaal negen natrium ionkanaal genen (SCN1A-SCN11A) die coderen voor natrium asubunits ($Na_v1.1$-$Na_v1.9$). Mutaties in SCN1A veroorzaken een spectrum van epileptische fenotypes, gaande van de milde epileptische aandoening GEFS+ tot aan het zeer ernstige Dravet syndroom. De GEFS+ mutanten laten voornamelijk kleine verschuivingen in de spanningsafhankelijkheid en/of kinetiek van het ionkanaal zien, terwijl een volledig verlies kanaalfunctie bij Dravet syndroom veel voorkomend is.

Hoofdstuk 4 is een klinische en electrofysiologische studie van nieuwe SCN1A missense mutanten, R859H (GEFS+), en de Dravet syndroom mutaties R865G, R946C, R946H. De GEFS+ mutant laat verschillende kanaaldefecten zien die, zowel een verlies als een toename in kanaalfunctie omvatten. De Dravet syndroom mutanten R946C en R946H produceren nietfunctionele kanalen, wat overeenkomt met de huidige literatuur. Daarentegen produceert de R865G mutant wel functionele kanalen. De R865G mutant laat verschuivingen zien in de spanningsafhankelijkheid en kinetiek van het kanaal. Bovendien vertonen beide mutanten, R859H en R865G, een vertraging in het herstel van kanaal inactivatie. Deze twee mutanten laten duidelijk zien dat een mutatie in het natrium ionkanaal zowel verlies als een toename in kanaalfunctie veroorzaakt. Toch kunnen de gemeten verschillen in kanaalkinetiek en spanningsafhankelijkheid niet het verschil verklaren tussen het milde fenotype van de GEFS+ patiënt en het ernstige ziektebeeld van de patiënt met Dravet syndroom.

Koorts speelt een zeer belangrijke rol bij zowel GEFS+ als Dravet syndroom. Aangezien het bovenstaande onderzoek van de R859H en R865G kanaal mutanten bij kamertemperatuur was uitgevoerd, zijn deze twee mutanten in hoofdstuk 5 opnieuw gekarakteriseerd, maar ditmaal werden de metingen gedaan bij 37°C en 40°C in plaats van kamertemperatuur. Wanneer de temperatuur wordt verhoogd naar 40°C, vertonen zowel wildtype kanalen en de twee mutanten veranderingen in de spanningsafhankelijkheid en kinetiek van het ionkanaal. Opvallend genoeg zijn er bij de mutanten veranderingen in kanaalfunctie te zien bij verhoogde temperatuur overeenkomend met koorts. R859H heeft bij negatieve membraanpotentialen een verlaagde kanaalbeschikbaarheid en een gebruiksafhankelijke toename in kanaalbeschikbaarheid tijdens het constant vuren van een neuron, welke in combinatie met de andere gevonden kanaaldefecten samen GEFS+ veroorzaken. De R865G mutant laat een significante reductie in natrium stroom zien en verlaging van de gebruiksafhankelijkheid van het kanaal bij 40°C, wat samen met andere veranderde kanaalfuncties kan leiden tot een niet-exciteerbaar neuron na langdurige stimulatie van een neuron. Deze reductie in natriumstroom en de verlaagde exciteerbaarheid van een neuron kan dus leiden tot Dravet syndroom

Toekomst perspectief

In Hoofdstuk 6, algemene discussie, worden de voor- en nadelen van de technieken die gebruikt zijn in dit proefschrift kritisch besproken. In HOOFDSTUK 2-5 hebben we kanaalfuncties bestudeerd in makkelijk te transfecteren niercellen in isolatie. Deze cellen hebben geen neuronale achtergrond en zijn niet in staat om actiepotentialen te generen. Bovendien functioneren neuronen in ingewikkelde en complexe netwerken, bestaande uit veel verschillende gespecialiseerde excitatoire en inhibitoire zenuwcellen omringd door gliacellen. Met het gebruik van getransfecteerde cellen wordt ook geen rekening gehouden met de invloed van de genetische achtergrond variatie in patiënten op het uiteindelijke epileptische fenotype. Om deze nadelen te ondervangen zou men in de nabije toekomst gebruik kunnen gaan maken van neuronale cellen afkomstig van geïnduceerde pluripotente stemcellen (iPS) van epilepsie patiënten welke sinds kort verkregen kunnen worden uit fibroblasten van epilepsie patiënten.

Conclusie

De meeste thans bekende genetische vormen van epilepsie worden veroorzaakt door genmutaties in genen die coderen voor ionkanalen of receptoren. Functionele studies van deze eiwitmutanten laten of een verschil in spanningsafhankelijkheid en/of kinetiek zien of een volledig verlies van kanaalfunctie via verschillende mechanismen. Toch moet er rekening mee worden gehouden dat de ernst van de epileptische aanvallen niet alleen wordt bepaald door de genmutatie, maar ook door de genetische achtergrond, modificerende genen en genetische compensatie factoren, die tesamen een belangrijke bijdrage leveren aan het klinisch beeld van patiënten.

Acknowledgements

Malin
Teun
Lukas
Hiroki
Magda
Tonny
Pascal
Mo
MARTIN
Harold
John
Marc
Mera
Sanne
Tobias
Roel
Toon
Marien
Maria
Tamara
Wendy
Thom
Bart
Siddarth
Leonie
Shirley
Jet
Maartje
Vincent
Hamid
Christian
Marti
Marcel
Rosanne
Peter
Sofieke

Florianne

Clara

Lude

Maciej

Dalila

Behrooz

Alfons

Sasha

Karen

Jelena

Esther

BOBBY

Frederieke

Flip

Cisca

DICK

Eric

Jacobine

Martin

JOOST

Simone

Ruben

Kristel

Albertien

Marjan

Carolien

Gosia

Jackie

Kris

Al

Jennifer

Melissa

Thom

Deborah

Douwe

Leffert

Wendy

Linda

Marieke

AREND-JAN

Margriet

Mama

Henny

Truus

Sander

Novi

Aagje

Buuf

Joop

Floris

Papa

Buum

Curriculum Vitae

Linda Volkers werd op 2 Juni 1978 geboren in Coevorden. In 1997 behaalde zij haar HAVO diploma aan scholengemeenschap ‘De Nieuwe Veste’ in Coevorden. Dit zelfde jaar ging zij de laboratoriumopleiding volgen aan de Hogeschool van Utrecht. In Februari 2002 behaalde zij haar diploma, en ging vervolgens Biomedische wetenschappen studeren aan de Vrije Universiteit in Amsterdam. In het kader van deze studie deed zij twee onderzoeksstages. Haar eerste stage was bij de afdeling Medische Genetica, Universitair Medisch Centrum Utrecht onder begeleiding van Dr. B.P.C. Koeleman. Haar tweede stage werd uitgevoerd bij de afdeling Fysiologische Chemie, Universitair Medisch Centrum Utrecht, onder begeleiding van Dr. F. Zwartkruis. In September 2004 behaalde zij haar Master in Science. In November 2004 begon ze als junior onderzoeker bij de afdeling Medische Genetica om vervolgens in November 2005 als assistent in opleiding te beginnen bij de afdeling Medische Genetica onder begeleiding van Dr. D. Lindhout en Dr. B.P.C. Koeleman en de afdeling Medische Fysiologie onder begeleiding van Dr. M.B. Rook. De resultaten van dat onderzoek staan beschreven in dit proefschrift.